On-Surface Magnetochemistry

Inauguraldissertation

zur

Erlangung der Würde eines Doktors der Philosophie

vorgelegt der

Philosophisch-Naturwissenschaftlichen Fakultät

der Universität Basel

von

Christian Wäckerlin

aus Siblingen (Schaffhausen)

Villigen PSI, 2013

Genehmigt von der Philosophisch-Naturwissenschaftlichen Fakultät auf Antrag von:

Prof. Dr. Thomas Jung

Prof. Dr. Ernst Meyer

Basel, den 26. März 2013
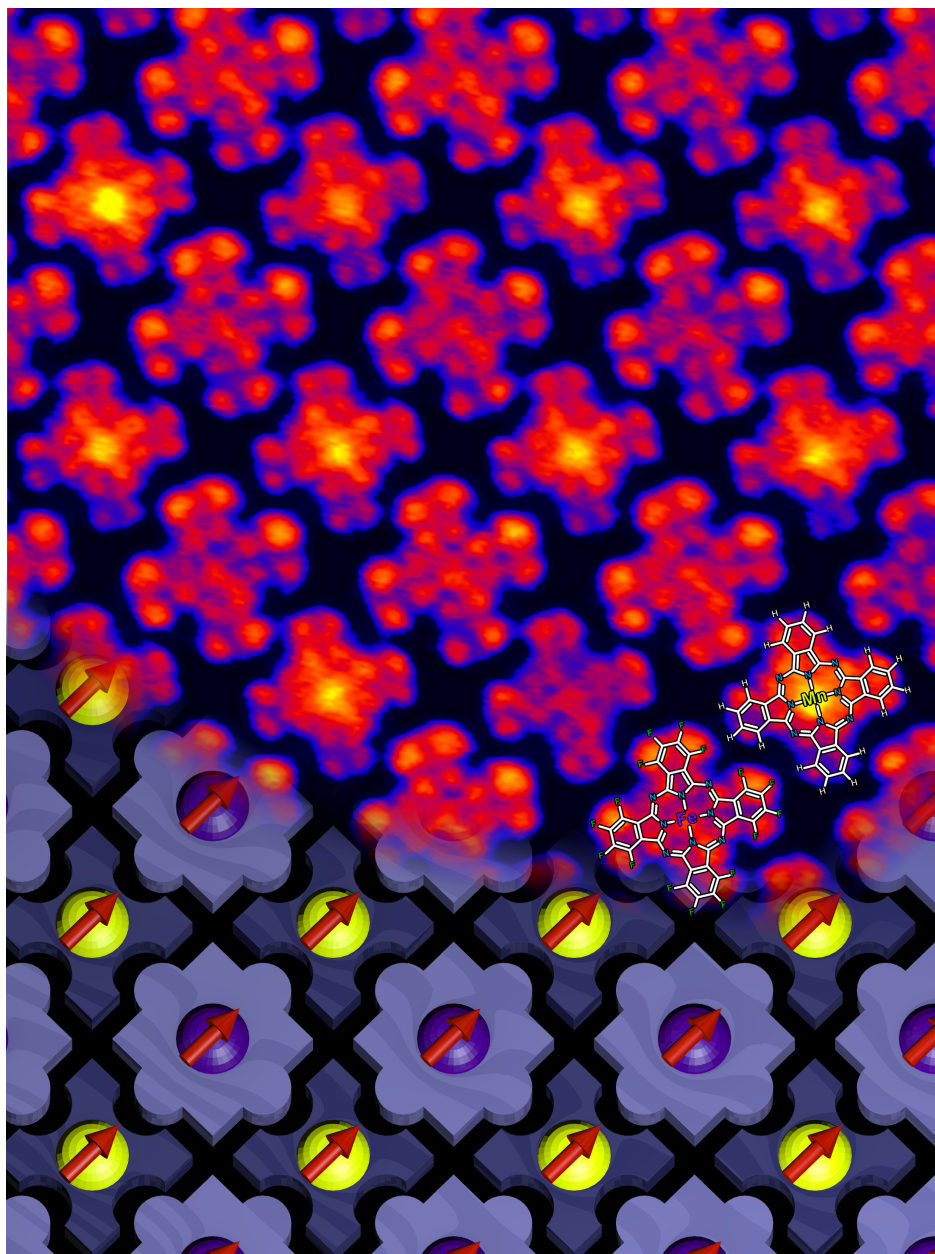
Prof. Dr. Jörg Schibler

Dekan

"The game of science is, in principle, without end. He who decides one day that scientific statements do not call for any further test, and that they can be regarded as finally verified, retires from the game."

Karl Popper

Abstract

This thesis reports on the on-surface magnetochemistry of square-planar transition-metal complexes adsorbed on ferromagnetic substrates. Specifically, the magnetochemistry of the transition-metal ions (Mn / Fe / Co / Ni) coordinated in square-planar porphyrin / phthalocyanine ligands arranged on native and oxygen-reconstructed ferromagnetic Ni(001) / Co(001) thin-films is studied. The metal-centers in the surface-adsorbed complexes are five-fold coordinated: four coordination-bonds with the square-planar ligand and one bond with the "surface-ligand". This arrangement leaves the sixth site on-top of the complex open for an additional ligand to bind with the transition-metal center and give the possibility to control the magnetic properties of the on-surface complex. Specifically, nitric oxide (NO) or ammonia (NH_3) gas is used to serve as the sixth ligand. The experiments were performed in ultra-high vacuum and the samples were studied by X-ray absorption spectroscopy (XAS), X-ray magnetic circular dichroism (XMCD), X-ray photoemission spectroscopy (XPS) and scanning tunneling microscopy (STM).

This work is based on the induced magnetic ordering in a monolayer of transition-metal porphyrins adsorbed on ferromagnetic substrates. The effect allows to study the magnetochemistry at ambient / near-ambient temperature in the remanent magnetization of the substrate. The experimental results are complemented by density functional theory with additional Hubbard interactions taken into account (DFT+U) conducted by Kartick Tarafder and Peter Oppeneer from Uppsala (Sweden).

Within the scope of this thesis, mechanisms for *switching off*, *tuning* and *switching on* the magnetic moments in the adsorbed complexes are demonstrated and explained. Furthermore, we show that apart from controlling the magnetic moment, the axial-ligand can also be used to *control the exchange-interaction* with the ferromagnetic substrate. Specifically, we observe that the strength and sign of the exchange-interaction can be controlled. These results clearly illustrate that the coordination-chemistry and magnetochemistry on-surface extends the framework of

classical coordination-chemistry, since the interaction with the "surface-ligand" has to be included into the considerations.

Furthermore, we show that highly-ordered two-dimensional arrays of molecular spin-systems can be fabricated by chemically directed self-assembly. Specifically, we produce *chessboard-like Fe – Mn – Fe spin-arrays* by mere co-evaporation of the functionalized molecular building-blocks. In a second step, the magnetic properties of this spin-array can be controlled by ammonia exposure and one half of the chessboard-like spin-array can be *selectively and reversibly switched*.

Also, the on-surface charge-transfer between the strong electron-acceptor TCNQ and alkali-*halides* (e.g. Na^+Cl^-) is discussed. The experiments show that the 2D metal-organic layers can be produced by the on-surface reaction of alkali-halides (instead of alkali-metals) and sufficiently strong electron acceptors.

List of Publications

This thesis is based on the following publications, which are referred to in the main text by double square brackets:

[[1]] C. WÄCKERLIN, D. CHYLARECKA, A. KLEIBERT, K. MÜLLER, C. IACOVITA, F. NOLTING, T. A. JUNG and N. BALLAV. Controlling spins in adsorbed molecules by a chemical switch. *Nat. Commun.*, **1**, 61 (2010). DOI:10.1038/ncomms1057.

[[2]] C. WÄCKERLIN, K. TARAFDER, D. SIEWERT, J. GIROVSKY, T. HÄHLEN, C. IACOVITA, A. KLEIBERT, F. NOLTING, T. A. JUNG, P. M. OPPENEER and N. BALLAV. On-surface coordination chemistry of planar molecular spin systems: novel magnetochemical effects induced by axial ligands. *Chem. Sci.*, **3**, 3154–3160 (2012). DOI:10.1039/c2sc20828h.

[[3]] C. WÄCKERLIN, J. NOWAKOWSKI, S.-X. LIU, M. JAGGI, D. SIEWERT, J. GIROVSKY, A. SHCHYRBA, T. HÄHLEN, A. KLEIBERT, P. M. OPPENEER, F. NOLTING, S. DECURTINS, T. A. JUNG and N. BALLAV. Two-Dimensional Supramolecular Electron Spin Arrays. *Adv. Mater.*, **25**, 17, 2404–2408 (2013). DOI:10.1002/adma.201204274.

[[4]] C. WÄCKERLIN, T. KARTICK, J. GIROVSKY, J. NOWAKOWSKI, T. HÄHLEN, A. SHCHYRBA, D. SIEWERT, A. KLEIBERT, F. NOLTING, P. M. OPPENEER, T. A. JUNG and N. BALLAV. Ammonia Coordination Introducing a Magnetic Moment in On-Surface Low-Spin Porphyrin. *Angew. Chem. Int. Ed.*, **52**, 4568–4571 (2013). DOI:10.1002/anie.201208028.

[[5]] C. WÄCKERLIN, C. IACOVITA, D. CHYLARECKA, P. FESSER, T. A. JUNG and N. BALLAV. Assembly of 2D ionic layers by reaction of alkali halides with the organic electrophile 7,7,8,8-tetracyano-p-quinodimethane (TCNQ). *Chem. Commun.*, **47**, 32, 9146 (2011). DOI:10.1039/c1cc12519b.

Contents

List of Abbreviations

General acronyms

CF   crystal field

MO   molecular orbital

UV   ultra-violet

Methods

DFT   density functional theory

DFT+U   DFT with additional Hubbard interactions

LEED   low energy electron diffraction

STM   scanning tunneling microscopy

UPS   UV photoelectron spectroscopy

XAS   X-ray absorption spectroscopy

XMCD   X-ray magnetic circular dichroism

XPS   X-ray photoelectron spectroscopy

Chemical compounds

M   metal

MTPP   5,10,15,20-tetraphenyl-21H,23H-porphine M

MOEP   2,3,7,8,12,13,17,18-octaethyl-21H,23H-porphine M

MPc   M phthalocyanine

$MF_{16}Pc$ M 1,2,3,4,8,9,10,11,15,16,17,18,22,23,24,25-hexadecafluoro-29H,31H-Pc

NH_3 ammonia

NO   nitric oxide

TCNQ   7,7,8,8-tetracyanoquinodimethane

CHAPTER 1

Introduction

1.1 Motivation

We live in the so-called "information age".[1, 2] Today's societies rely more than ever before on the availability of information, e.g. written text, spoken words, displayed images. It was Shannon and Weaver who developed a theory of information in 1949 [3] which uses the concept of entropy as a measure of information content. This description was the basis for the development of information technology in its modern sense. Today's information technologies are based on *top-down* fabrication of *inorganic solid-state devices* and rely on the *electron-charge* to store / retrieve, transmit and manipulate information.[1]

Nowadays, new technologies emerge, which do not rely on some of the above mentioned aspects. For example *organic-electronics* [4] which relies on carbon-based materials and *spintronics* [5] which uses the electron-spin as a tool to store / receive, transmit and manipulate information. More and more often *bottom-up* [6] fabrication, employing the self-assembly of building-blocks, is used to engineer structures / devices. Some terms like *molecular spintronics* [7] refer to a combination of novel technologies.

Storing / retrieving, transmitting and manipulating of information is not only important for computers. Information is also a central part in biological systems. Vast amounts of information are encoded in the sequence of linear macromolecules (deoxyribonucleic acids). This information encodes the sequence of polypeptides (proteins) which form real molecular nanomachines via intra-molecular and inter-molecular self-assembly. The actual "logic" in biology is mainly based on inter-molecular and inter-cellular chemical interactions / messaging.[8, 9] Biological

---

[1]Not exclusively: information is stored in the collective arrangement of electron-spins and transmitted via photons.

systems give examples for the great potential of molecular nanotechnology. A beautiful, recent demonstration how biology can be mimicked is given in ref. [10].

Metal-organic complexes, in particular natural porphyrins and their close derivatives, which are of interest in this thesis, are important in many vital processes: photosynthesis, O_2 / CO_2-transport, catalysis and redox-chemistry.[8, 9, 11] The O_2-transport via hemoglobin is a good example of the possible complexity in magnetochemical reaction. Hemoglobin consists of four natural Fe-porphyrins (heme b's) embedded in the globulin proteins. The 4-fold coordinated Fe in free heme b has two axial open-sides where it can by ligated. In hemoglobin, one of the two axial sides on the Fe is occupied by a histidine-ligand from the protein.[8, 9] The remaining open-side is free to be coordinated by O_2. Note that the magnetochemistry of heme b in hemoglobin is a complex process[2] and is distinct from the magnetochemistry of free heme b: for example, free Fe(II)-porphyrin is in its intermediate-spin (S = 1) state, but the interaction with the histidine-ligand of the protein results a high-spin (S = 2) state.[13]

This thesis is concerned with the on-surface magnetochemistry of synthetic porphyrins and phthalocyanines.[11] The ferromagnetic substrate blocks one of the two remaining axial sites of the transition-metal ions in the square-planar porphyrin / phthalocyanine ligands. Since the experiments are conducted in ultra-high vacuum (UHV), the availability of chemical agents binding to the on-top open-site of the on-surface transition-metal complex can be precisely controlled. The induced magnetic moment [14] in the on-surface transition-metal complexes allows the use of X-ray magnetic circular dichroism (XMCD) method to study its magnetic moment at ambient / near ambient temperatures on the remanently magnetized ferromagnetic substrate. We studied the influence of the *on-surface coordination* caused by gaseous ligands (nitric oxide and ammonia) onto the *induced magnetic moment and its exchange-interaction with the ferromagnetic substrate* (cf. figure 1.1). We have chosen the two gaseous ligands because of their complementary electronic structures and chemical properties. NO is a strong-field ligand (i.e. it results in a stronger splitting of the d orbitals), it is spin-bearing (S = 1/2) with its unpaired electron in the π^* orbital and it exhibits non-innocence (i.e. the ligand can change its oxidation-state).[15, 16] NH_3 is an innocent ligand with intermediate strength, it is not spin-bearing (S=0) and its chemistry is shaped by its lone-pair (non-bonding pair of electrons). The symmetry of ammonia's lone-pair (σ type) and of NO's π^* orbital defines the possible orbital-overlap in case of axial ligation to a square-planar metal complex: NO can form a σ and / or a π bond with the d_{z^2} (σ symmetry) and / or d_{xz} and d_{yz} (π symmetry) orbitals of the metal center (depending its d-occupation), while the symmetry of NH_3 only allows for orbital-overlap with the d_{z^2} orbital.[15, 17] For the symmetries of the d-orbitals, c.f. figure 1.2.

We were able to demonstrate that: i) coordination-chemistry can be used to control the magnetic moment of the adsorbed complexes (quenching, tuning and inducing a magnetic moment), ii) the magnetic response of the on-surface central metal ion towards an axial ligand

---

[2]The Fe(II) ion is found to change its oxidation-state and its spin-state,[12] but this finding has been debated for a long time.
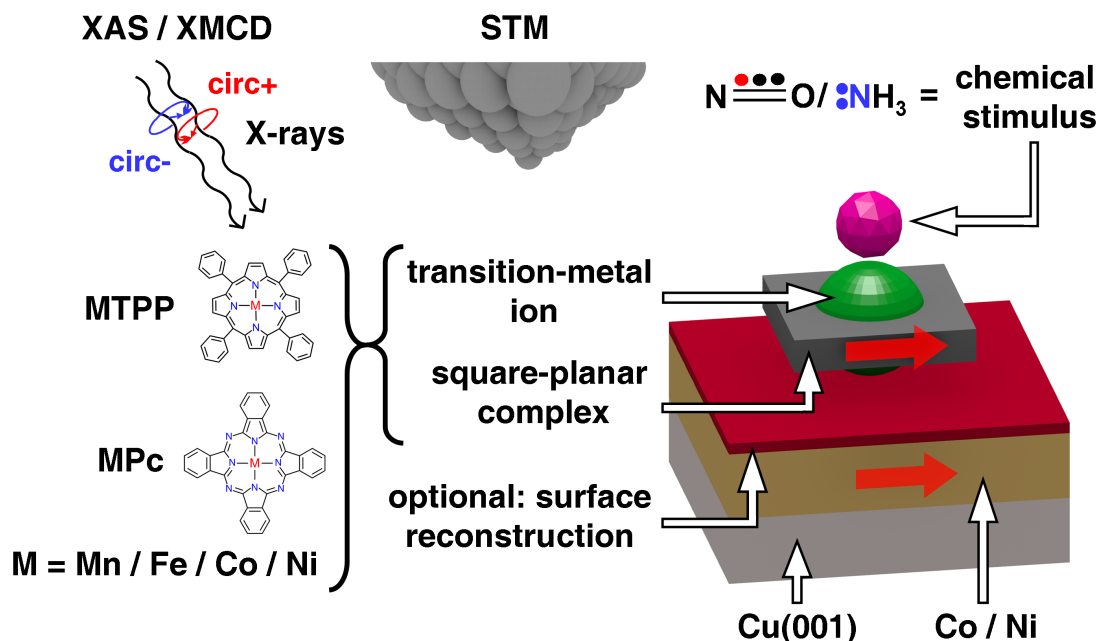
Figure 1.1: A sketch of the research-design used for the magnetochemistry studies in this thesis. Transition-metal ions (Mn / Fe / Co / Ni) embedded in four-dented porphyrin / phthalocyanine-ligands are studied on ferromagnetic Co / Ni thin films grown on Cu(001). The ferromagnetic thin-films can be modified by an (optional) oxygen-reconstruction. Depending on the substrate, a ferromagnetically / antiferromagnetically aligned magnetic moment is expected to appear in the transition metal complexes.[14, 18–22] The induced magnetic moment in the ad-complexes and its specific response towards axial ligation with a chemical stimulus (nitric oxide / ammonia) is studied by X-ray absorption spectroscopy (XAS) / X-ray magnetic circular dichroism (XMCD). The data from these element-specific techniques are complemented by scanning tunneling microscopy (STM) experiments and density functional theory + U (DFT+U) calculations.

differs decisively from the well studied response in bulk / solution and iii) competitive chemical bonding (i.e. the *trans effect* [23]) can be used to control the exchange-interaction with the ferromagnetic surface.

1.2 Methods and Concepts

This section provides a brief introduction into the key methods and concepts, which are essential in the investigation of magnetochemical properties of organic monolayers. For an in depth description of the methods the reader is advised to refer to the cited textbooks / review articles. Note that XPS / UPS / XAS / XMCD / LEED give spatially averaged information, XPS / XAS / XMCD provide element specific information which is complementary to STM which is a local probe.

Photoelectron spectroscopy, also known as photoemission spectroscopy, is based on electron emission from a substance caused by photon excitation (the photoelectric effect [24, 25]). In an

experiment the kinetic energy of the excited photoelectrons is measured and recalculated into their binding energy.[26, 27] The energy levels of electrons in matter discussed in two domains: i) levels with high binding energies - they are highly localized and are of atomic character (core-levels) and ii) levels / bands / molecular orbitals close to the Fermi-level (valence band). The core-level spectra (i) are conventionally obtained by excitation with X-rays, whereas valence band (ii) is approached by UV-light. Due to the very low inelastic mean free path of low-energy photoelectrons, photoelectron spectroscopy is a highly surface sensitive technique.[27]

X-ray photoelectron spectroscopy (XPS) refers to photoelectron spectroscopy based on excitation with X-rays. Since the core-levels can be assigned to certain elements, the method allows to determine the elemental composition of the samples. Furthermore, the binding energy E_B of a core-level varies depending on the chemical environment of the atom. This chemical shifts ΔE_B is roughly proportional to the charge on the atom (cf. Figure 3.3 in ref. [27]). The complementary information about composition and chemical identity makes XPS valuable tool for the quality control of the many component systems shown in this thesis. During the photoemission process, the core-hole can interact with the spin in valence levels. This interaction results in multiplet splitting, i.e. an increased line-width of a core-level.[28] This effect can be used to conclude on the presence / absence of unpaired electrons, e.g. in a paramagnetic compound like Co(II)-porphyrin (cf. section 2.1 and refs. [29–31]).

UV photoelectron spectroscopy (UPS) is based on electron excitation with UV-light and gives access to the occupied states in the valence region, where chemical bonding occurs. Furthermore, From the UP spectrum the sample work function which gives insight into e.g. charge-transfer between the ad-molecule and the substrate (cf. section 2.5) can be extracted. A review on UPS is given in ref. [32].

X-ray absorption spectroscopy (XAS) is based on a similar physical effect as photoemission spectroscopy, i.e. excitation of electrons by photons. In the XAS experiment the absorption is measured as a function of the photon energy, [33, 34], that is why the method requires a tunable source of X-rays (e.g. a synchrotron). The most intense features in a XA spectrum are dipole-allowed ($\Delta l = \pm 1$) transitions into *unoccupied states*, e.g. 2p → 3d or 1s → 2p. XAS is element-specific and can be measured in transmission, fluorescence and in partial / total electron yield mode. The total electron yield measurement is performed by measuring the sample current. The very low inelastic mean free path of the low-energy electrons in matter makes XAS in total electron yield mode highly surface sensitive. All data presented in this thesis were acquired in this mode.

XAS is very sensitive to the chemical environment of the excited atom and has a fine-structure which arises from the excitations into unoccupied orbitals. A great advantage of XAS is that various polarization effects can be observed when using linearly and circularly polarized X-rays : i) X-ray natural linear dichroism (XNLD),[35] ii) X-ray magnetic linear dichroism (XMLD),[36] iii) X-ray natural circular dichroism (XNCD),[37] iv) X-ray magnetic circular dichroism (XMCD)

[38] and more.[39] These effects allow the use of XAS to study the orientation of molecular orbitals (i), chirality (iii) and magnetism (ii and iv). In this thesis we use XMCD at the $L_{3;2}$ edges ($2p \rightarrow 3d$ transitions) to investigate the induced magnetic moments in the transition-metal complexes.

X-ray magnetic circular dichroism (XMCD) is the difference between two X-ray absorption spectra obtained with circularly polarized X-rays of opposite polarization. In case of XAS at the L_3 ($2p_{3/2} \rightarrow 3d$) and L_2 ($2p_{1/2} \rightarrow 3d$) edge, the simple picture of the XMCD effect is as follows: a photon transfers its angular momentum to a core electron (in $2p_{3/2}$ or $2p_{1/2}$) which is excited to an unoccupied state in the 3d shell. If the states are spin-polarized due to the presence of a magnetic moment, the unequal occupation of 3d spin$\uparrow$ and 3d spin$\downarrow$ results in differential absorption for circular+ and circular- polarized X-rays. Due to the spin-orbit interaction a spin magnetic moment will result in an opposite XMCD signals at the L_3 and L_2 edges.[39]

Low energy electron diffraction (LEED) is a highly surface sensitive, spatially averaging method which allows to measure the diffraction pattern of a surface.[40, 41] It allows the determination of the reciprocal unit-cells of single-crystalline substrates and of molecular ad-layers.

Scanning tunneling microscopy (STM) is a local method which allows to directly probe and visualize local electronic density of states of a surface of an electrically conductive material with atomic / submolecular resolution.[42, 43] The method is based on the tunnel-effect [44] and works by scanning a metallic tip over the surface. An electric potential is applied to the tip or the surface and the tunneling current is recorded. In the most commonly used imaging-mode which is also used in this thesis (constant current), a feedback-loop regulates the tip-sample distance to maintain a desired current-setpoint. The recorded height-data over the surface should in general not be considered as simple topography information, since the tunneling process depends crucially on the density of states of the surface and of the tip and on the applied electric potential over the tunneling gap. An example is bias dependent imaging given in section 2.3. It should be noted that spectroscopy modes which give access to the density of states (via elastic tunneling) and to vibrational / magnetic transitions (via inelastic tunneling) as well as imaging-modes based on spin-polarized tips become increasingly relevant, in particular for spin-bearing complexes studied such as the ones studied in this thesis.[45]

Epitaxy refers to the growth of a crystalline overlayer onto a crystalline substrate, if the overlayer is in atomic registry with the substrate.[41] For the work shown in this thesis, the overlayers (metals / molecules / salts) were deposited in ultra-high-vacuum by sublimation from resistively / electron-beam heated sources onto well defined, clean single-crystalline metal-substrates. Both the self-assembled monolayers (cf. sections 2.3 and 2.5) as well as the ferromagnetic Co and Ni thin films on Cu(001) are examples of epitaxial systems.

Ligand field theory is an application of molecular orbital theory to transition metal complexes.[15] Its predecessor, crystal-field theory is based on point charges in space which lift the degeneracy

of e.g. 3d states. For example, an octahedral crystal-field splits the initially fivefold degenerate d orbitals into a doubly-degenerate e_g level at increased energy and triply-degenerate t_{2g} level at reduced energy. However, the crystal field theory is based exclusively on electrostatic effects and neglects any covalent character.

An example for ligand field theory: the DFT+U calculations in section 2.2 reproduce the well known 180° / 120° metal-NO bond angle in NO-Mn-porphyrin and NO-Co-porphyrin. This finding can be well rationalized by ligand field theory / molecular orbital theory, considering the orbital symmetries of the respective 3d orbitals and of the π^* orbital of NO, cf. [[1, 2]] in sections 2.1 and 2.2.

Figure 1.2 shows a comparison of molecular orbital (MO) theory, DFT+U and crystal field theory, applied to Co(II)-porphyrin. It is apparent that the very simple assumptions used in the molecular orbital model give a quite good agreement with the DFT+U model.[[2]] Thus, MO theory can give us a quite deep qualitative insight and can help to explain and verbalize the density of states seen in the DFT+U calculations (which are a better approximation to reality and is needed to understand, for example, the molecule-surface interactions).

1.3 Prior Art

Molecules which show long magnetic relaxation times, i.e. hysteresis can be observed, are called single molecule magnets.[48] Mannini et al. demonstrated a magnetic hysteresis in such a molecule on surface.[49] The square-planar porphyrin / phthalocyanine complexes studied in this thesis are, in this regard, simpler as they do not exhibit intrinsic magnetic remanence. However, they can be magnetized on-surface i) in strong external magnetic fields at low temperatures [50] and ii) by coupling them to ferromagnetic substrates.[14, 18–21] Moreover, it was shown that the Mn and Fe based ad-complexes couple ferromagnetically on native (clean) ferromagnetic substrates [14, 18, 19] and antiferromagnetically [20, 21] on oxygen-reconstructed substrates. Furthermore, Iacovita et al. investigated the magnetic properties of Co-phthalocyanine adsorbed on Co(111) nanoislands and observed a spin-polarized conductance signal above the phthalocyanine molecule.[51] Gambardella et al. showed that the *magnetic anisotropy* in a monolayer of a metal-organic framework can be controlled by coordination chemistry.[52] One remarkable, early example of on-surface magnetochemistry is the study on the Kondo-effect[3] of $Co_x(CO)_y$ complexes on Cu(001) with low-temperature STM. Distinct variations in the Kondo-temperature for different on-surface $Co_x(CO)_y$ complexes were observed. However, the use of porphyrins / phthalocyanines as well defined ligands allows for identical ligand-fields acting on the central metal ions on the surface. This enables spatially averaging measurements (e.g. XPS, XAS, XMCD) to study the consequences of the interactions with the "surface-ligand" and the axial gaseous ligand.

---
[3]The scattering of conduction electrons due to magnetic impurities.[53]
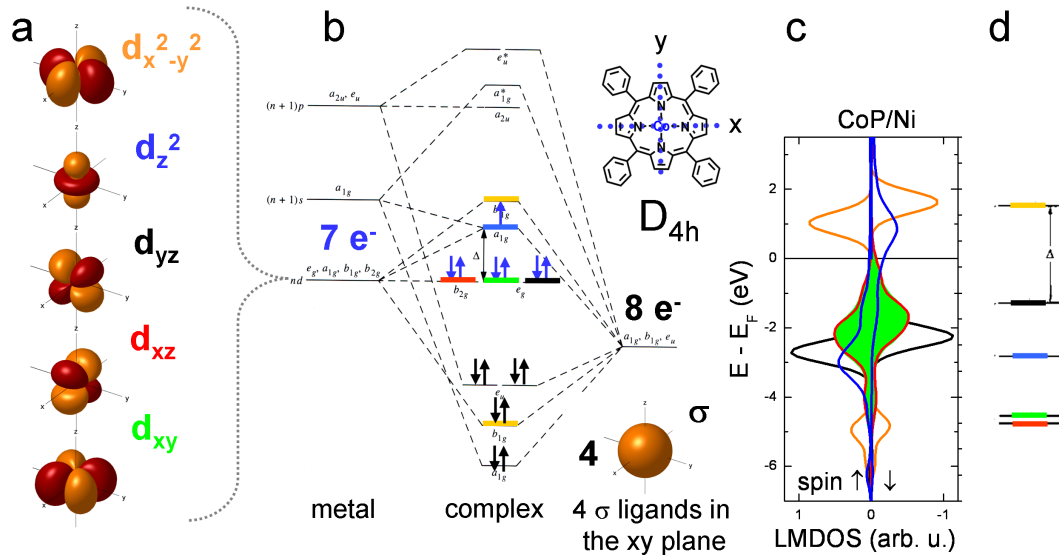
Figure 1.2: Ligand field theory applied to Co(II)-porphyrin. The 3d atomic orbitals (a), a molecular orbital (MO) diagram for a square-planar complex (D_{4h} symmetry) adapted from [15] (b), DFT+U calculation for on-surface Co(II)-porphine (cf. 2.2) (c) and crystal field (CF) diagram (adapted from [15]) for of a square-planar complex (d). In the MO model the porphyrin-ligand is approximated by 4 σ-type (spherical) orbitals (which can be seen as 4 nitrogens with lone-pairs). This simplification is not exactly accurate but it gives already a surprisingly good agreement with the DFT+U calculations. More advanced MO models also exist.[46] In the MO model different states appear, however we are here only interested in those with 3d-character (marked with the respective colors according to the 3d states in (a)). In total, 15 electrons (7 for $3d^7$ of Co(II) and 8 for the 4 N: ligands) have to be filled in. Since the symmetry of $d_{x^2-y^2}$ matches with the symmetry of the ligands, it is split into anti-bonding and bonding states. This hybridization is clearly seen in the DFT+U calculations but not in the CF model. In the MO model, d_{xz}, d_{yz} and d_{xy} are non-bonding (no overlap with σ-ligands). This in good agreement with the DFT+U calculations, although it the porphyrin ligand has some π-character, splitting up d_{xz} and d_{yz} slightly. The MO model and DFT+U calculations correctly [47] place the unpaired electron into the d_{z^2} orbital, while the CF model shows a wrong order of d_{z^2} and d_{xy}. In all 3 models (MO, DFT+U and CF), the d_{xz} and d_{yz} orbitals are degenerate - this is a consequence of the square-planar ligand / crystal field.

1.4 Outline

This thesis is based on five publications concerned with on-surface coordination chemistry.[[1–5]] Four of them report on the on-surface magnetochemistry [[1–4]] of square-planar complexes adsorbed on ferromagnetic substrates and the fifth one [[5]] reports on the on-surface charge-transfer between a strong electron acceptor and an alkali-halide.

In section 2.1, I introduce the magnetochemical approach to control the induced magnetic moment in Co(II)-porphyrin on a Ni thin film, i.e. the spin in the Co(II)-ion is "switched-off" by axial-ligation with nitric oxide.[[1]] This demonstration is based on a combination of two fundamental pieces of work: i) one describing the induced magnetic moment in Mn-porphyrin [14] and ii) the other illustrating the on-surface coordination chemistry of Co-porphyrin.[30]

On the basis of our first communication,[[1]] we have systematically studied the on-surface magnetochemistry of d^7 Co(II), d^6 Fe(II) and d^5 Mn(II)-porphyrin with nitric oxide ligands.[[2]] (section 2.2) In the meantime, Miguel et al. proposed the chemical control over the exchange-interaction strength.[54] This control was proposed on the basis of the surface trans effect [30, 31, 55, 56] which is a simple extension of the well known *trans effect*[4] to surface-chemistry. The trans effect is a competitive chemical interaction between two ligands binding at opposite sides (at *trans* positions) of a metal atom / ion, i.e. binding of one ligand weakens the bond with the other ligand.

Our collaboration with Kartick Tarafder and Peter Oppeneer (Uppsala, Sweden), who provided the DFT+U calculations, resulted in theoretical description of the magnetochemical system Mn-phthalocyanine/Co + NH_3 where the molecule-substrate exchange-interaction strength was significantly reduced upon NH_3-ligation. This effect occurred indeed in our system, which we have shown experimentally.[[2]] Furthermore, from the solution-chemistry knowledge, it should be expected that nitric oxide quenches the spin in Mn(II)-porphyrin.[57] However in our data, we find that after the *on-surface* NO exposure a magnetic moment of ca. 1/2 μ_B remains and it is coupled antiferromagnetically [[2]] to the substrate. This deviation from the solution-chemistry is a consequence of the chemical interaction with the surface. We have proposed the term *spin trans effect* to refer to the influence of the axial ligand, not only on the spin, but also on the *sign and strength of the exchange interaction* with the ferromagnetic substrate.[[2]]

In the course of our studies we wanted to demonstrate that our approach is also suitable to control molecular magnetic moments in a more complex setup. Our goal was to fabricate a supramolecular array where the arrangement of the magnetic centers is defined with atomic precision (section 2.3).[[3]] In order to fabricate this *spin-array*, we have used chemically directed molecular self-assembly. In this strategy, the molecular building-blocks are chemically functionalized such that they self-assemble in the desired way[5].[58] We have chosen to follow the approach by Hipps et al. based on C–F$\cdots$H–C hydrogen-bonds.[59, 60] On this basis we expected that the co-evaporation of a perfluoro-phthalocyanine together with an unsubstituted phthalocyanine will result in a chessboard-like structure of alternating perfluoro-phthalocyanine and phthalocyanine in two dimensions[6]. We knew from our previous studies that self-assembly on ferromagnetic substrates was only possible on oxygen-reconstructed and not on native (clean) Co or Ni.[21] The chessboard structure was self-assembled on an oxygen-reconstructed substrate almost at the first trial, however it took us time to choose the right central metal ions to obtain a spin-array with two different metal centers which both carry a magnetic moment.[7] Ultimately, we

---

[4]*Trans effect* [15] is a broad term referring to thermodynamic and kinetic effects. We are referring here to the *structural trans effect* which can be quantified by changes in bond-lengths.[23]

[5]Like in biological systems.

[6]The chessboard maximizes the number of C–F$\cdots$H–C hydrogen-bonds and is expected to be the thermodynamically most stable arrangement.

[7]Some paramagnetic molecules loose their magnetic dipole moment by the interaction with surfaces, c.f. [61, 62] and [[2]].

used Fe(II)-perfluoro-phthalocyanine[8] co-evaporated together with Mn(II)-phthalocyanine onto oxygen-reconstructed Co substrate. In this array of alternating Mn and Fe magnetic moments we could selectively *switch-off* the Fe's magnetic moments by NH_3-ligation,[56] i.e. we were able to switch the spin-array from its *spin on/on* to its *spin off/on'* state.

Up to this moment only *spin on* $\rightarrow$ *spin off* switches and *spin tuning* have been established, but a *spin on switch* was missing. This magnetochemical operation is introduced in section 2.4.[[4]] For this purpose we have used low-spin d^8 Ni(II) on a Co substrate and converted the Ni-complex to its high-spin (S = 1) state by ligation with NH_3. The ferromagnetic Co substrate induces a magnetic moment in the Ni-porphyrin. Thus, this system presents a first spin-on switch and completes the magnetochemical "tool-kit".

In section 2.5 the on-surface charge-transfer between the strong electron acceptor 7,7,8,8-tetracyano-p-quinodimethane (TCNQ) and alkali-*halides* is investigated.[[5]] The case provides a good argument for what we call spectro-microscopy correlation, i.e. the combination of spectroscopy and microscopy to understand a given system.

- From the scanning tunneling microscopy data we could conclude that the addition of NaCl onto a monolayer of TCNQ on Au(111) leads to a complete reorganization of the self-assembled layer from a brick-wall-like [63] to a windmill-like structure, similarly as in case of sublimation of Mn / Ni / Cs onto a TCNQ-layer.[64–67]

- In the N1s and C1s X-ray photoelectron spectra we could observe that TCNQ adsorbed on Au(111) has no charge and that it only gets negatively charged upon addition of NaCl.[68, 69]

- In the UV photoelectron spectra we could directly spot a new electronic state which corresponded to $TCNQ^-$ [70] and we were able to conclude that the charge-transfer occurs mainly to NaCl and not to the Au substrate. We also found that TCNQ undergoes charge-transfer with Ag(111).[[5]]

- From the Cl2p X-ray photoelectron spectra we could conclude that the amount of chlorine on the sample is decreased, i.e. that 2 Cl^- are oxidized to Cl_2-gas which is evacuated.

This project is related with our ongoing interest the chemistry of TCNQ, i.e. the on-surface [2+2] cycloaddition between TCNQ and acetylene-appended porphyrin [71] and the surface-doping of the organic semiconductor pentacene with fluorine-substituted F_4TCNQ.[72] While we did not study the magnetic-properties of the TCNQ-based layers, the magnetism in such metal-organic layers is certainly a very interesting and promising field.[73–75]

---

[8]Synthesized in the group of Silvio Decurtins.

Results

2.1 Controlling Spins in Adsorbed Molecules by a Chemical Switch

Summary: Here we demonstrate that the induced magnetic moment in the square-planar, low-spin Co(II)-porphyrin adsorbed on a ferromagnetic Ni thin film can be switched from S = 1/2 to S = 0 by axial ligation with a chemical stimulus - nitric oxide (NO). The mechanism of this spin off-switch is based on the hybridization of the singly occupied d_{z^2} orbital with the singly occupied π^* orbital of NO. The experiment is inspired by the seminal work of Flechtner et al. [30] where on-surface coordination-chemistry and the trans effect on surface was explored.

Paper [[1]] is published in Nature Communications
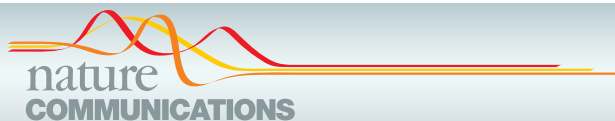
ARTICLE

Controlling spins in adsorbed molecules by a chemical switch

Christian Wäckerlin[1,*], Dorota Chylarecka[1,*], Armin Kleibert[2], Kathrin Müller[1,†], Cristian Iacovita[3], Frithjof Nolting[2], Thomas A. Jung[1] & Nirmalya Ballav[1]

The development of chemical systems with switchable molecular spins could lead to the architecture of materials with controllable magnetic or spintronic properties. Here, we present conclusive evidence that the spin of an organometallic molecule coupled to a ferromagnetic substrate can be switched between magnetic *off* and *on* states by a chemical stimulus. This is achieved by nitric oxide (NO) functioning as an axial ligand of cobalt(II)tetraphenylporphyrin (CoTPP) ferromagnetically coupled to nickel thin-film (Ni(001)). On NO addition, the coordination sphere of Co^{2+} is modified and a NO–CoTPP nitrosyl complex is formed, which corresponds to an *off* state of the Co spin. Thermal dissociation of NO from the nitrosyl complex restores the *on* state of the Co spin. The NO-induced reversible *off–on* switching of surface-adsorbed molecular spins observed here is attributed to a *spin trans* effect.

ARTICLE

Planar organometallic complexes with extended π-conjugation, for example, metalloporphyrins and metallophthalocyanines, have an indispensable role in controlling a wide range of functionalities: chemical reactivity (in biochemistry), optical absorbance (in dyes), optoelectronic conductance (in light harvesting chromophores), as well as the ability to function as electron donors or acceptors (in gas sensors and organic semiconductor devices)[1]. This degree of control is achieved by modifying the coordination of the central metal ion through interaction with its environment, for example, by an external chemical stimulus, as exemplified in nature by the regulation of Fe-porphyrin-to-oxygen affinity within the haemoglobin tetramer[2,3]. Recently, a similar effect has been implemented at surfaces in which the electronic surface–molecular interaction has been controlled by chemical stimuli[4–6]. Furthermore, metalloporphyrins containing unpaired spins have been shown to exhibit exchange coupling to magnetic substrates[7–12]. In view of spintronics[13,14], which has been predominantly emerging for thin-film devices such as spin valves and transistors, it comprises a challenge to control single molecular spins within their specific environment at the spintronic interface. Notably, the molecular spin state for inorganic complexes/polymers in bulk can be controlled by external factors such as temperature, pressure and photon-induced excitation[15–18].

Molecules containing unpaired spins and molecular magnets bearing several coupled magnetic atoms[19] have recently received increasing attention. Unpaired electron spins in a molecule offer a wide range of options towards the tuning of their coupling with the environment. The structure and properties of such molecules can be initially architectured through synthesis and can be further modified by chemical reactions. X-ray magnetic circular dichroism (XMCD) spectroscopy[20,21] allows for the highly sensitive determination of the magnetization of spin systems assembled at surfaces with elemental and chemical specificity. The XMCD technique has also been used to assess the magnetization of adsorbed metalloporphyrin spin systems with respect to ferromagnetic substrates[7–11].

In this article, we demonstrate that the spin of a metalloporphyrin molecule, namely cobalt(II)tetraphenylporphyrin (CoTPP), is magnetically coupled to a ferromagnetic substrate (here nickel (Ni(001))) and can be controlled by nitric oxide (NO) functioning as a chemical stimulus. A reversible *off–on* switching process of the molecular spin, induced by NO, in the presence of the remanent magnetization of the Ni substrate is shown. Addition of NO supersedes the Co–Ni magnetoelectronic interaction by the formation of a NO–CoTPP nitrosyl complex[22,23], which corresponds to the *off state* of the Co spin in CoTPP. Thermal dissociation of NO from the nitrosyl complex restores the initial Co–Ni magnetoelectronic interaction and leads to the *on* state of the Co spin in CoTPP. Thereby, this work provides an example of a *chemical switch* affecting the spin in surface-adsorbed molecules and presents a case for the *spin trans* effect in analogy to the well-established *trans* effect[22–24]. Using stimuli to control single atomic[25] and molecular spins at interfaces and determining their coupling with the environment is of eminent interest in the field of quantum information[26].

Results

Design of the magnetic interface. A cobalt-porphyrin, CoTPP (see Fig. 1a; top panel), has been chosen as a magnetic molecule characterized by one unpaired electron ($S = ½$; magnetic moment M (static) $= 1.73\,\mu_B$, M (effective) $= 1.92\,\mu_B$)[27]. On the basis of its architecture and properties, this molecule is expected to be affected by the up or down magnetization of the ferromagnetic Ni substrate[8]. Atomically clean Ni substrates were prepared by deposition of thin films (~20 monolayers (MLs)) onto clean Cu(001) single crystals in ultrahigh vacuum. About 1 ML of CoTPP molecules was then evaporated onto the freshly prepared non-magnetized Ni(001) substrates kept at room temperature. On such prepared samples the magnetization of the different elemental species, that is, Co and Ni, has been determined by the element-specific XMCD technique[20] (see Fig. 1a; bottom panel).

XMCD spectroscopy. X-ray absorption spectra of circularly polarized synchrotron light with opposite helicities (μ^+ and μ^-) are presented in Figure 1b. They clearly show a difference in absorption, that is, magnetic circular dichroism, at L_2 and L_3 absorption edges
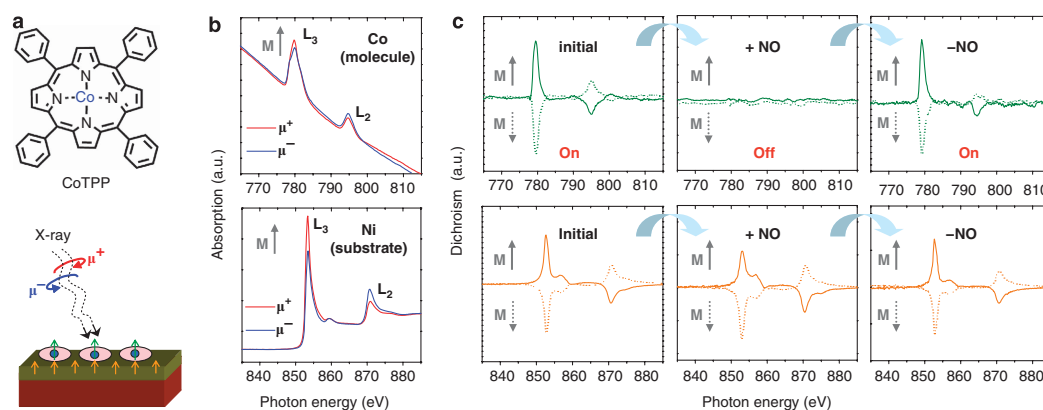

Figure 1 | Magnetic ordering of substrate (Ni) and organic adsorbate (CoTPP) with respect to the NO-induced switching. In all spectra, 'a.u.' represents arbitrary units. (**a**) Chemical structure of the CoTPP molecule (top) and schematic view of the XMCD experiment (bottom). (**b**) Chemical identification of Co and Ni: L-edges X-ray absorption spectra of Co (CoTPP, photon energy range: 765–815 eV) and Ni (substrate, photon energy range: 835–885 eV) acquired with circularly polarized X-ray light from a synchrotron source with opposite helicities (μ^+ and μ^-). The difference in X-ray absorption for the opposite helicities (dichroism) reveals the magnetization of the observed chemical species. (**c**) Spin-switching sequence from left to right as indicated by arrows: L-edges XMCD spectra of Co (top panels) and Ni (bottom panels) recorded on the CoTPP/Ni(001) system after the initial preparation of molecular adlayers (left), after NO addition (centre) and on temperature-induced NO desorption (right). The directions of the remanent substrate magnetization M are indicated by grey arrows to the left of each spectrum. Ferromagnetic ordering of molecular spins with respect to the substrate is observed initially. Reversible 'off–on' switching of Co magnetization is observed with progressing NO addition and temperature-induced NO desorption.

ARTICLE

of both Co (top) and Ni (bottom). In the dichroic spectra, both the magnetic molecule (Co; Fig. 1c; top left panel initial) and the substrate (Ni; Fig. 1c; bottom left panel initial) show a magnetization, as characterized by the two peaks at photon energies corresponding to the L_2 and L_3 edges. A ferromagnetic coupling between CoTPP molecules and the Ni substrate is clearly identified by the same sign of the L_2 and L_3 dichroic signals in the respective spectra. Such ferromagnetic coupling has also been observed for similar molecules with different central metal atoms on various substrates[7–9]. Following numerical calculations based on density functional theory, this coupling occurs by superexchange through nitrogen atoms of the porphyrin ring for these observations[8,28,29].

To investigate the effect of a reaction with a chemical stimulus on the magnetization of CoTPP adsorbed on the Ni substrate, the CoTPP/Ni system was exposed to NO gas at room temperature. After the NO exposure, the initially well-detectable Co magnetization (Fig. 1c; initial) cannot be detected by XMCD anymore (Fig. 1c; +NO). This behaviour is observed irrespective of the substrate magnetization and provides clear evidence that the magnetization of Co in CoTPP is switched *off*—an effect that goes far beyond earlier observations[7,8,21] and allows for the switching of individual molecular spins. As expected for a thin film, the Ni substrate magnetization was only marginally affected by the NO adsorption. We assign the *off* state of the molecular spin to the pairing of the initially unpaired Co spin, with the unpaired spin supplied by NO in the formation of a NO–CoTPP complex[22,23,30] as discussed further below.

To probe the reversibility of the process the sample temperature was temporarily increased to ~615 K, leading to the removal of NO from the NO–CoTPP complex. This implies the reactivation of the Co spin ($S = 1/2$) and the regeneration of the ferromagnetic coupling between CoTPP and Ni as clearly reflected in the XMCD spectra (Fig. 1c; −NO), that is, the Co spin system was switched *on* again. Consequently, the ferromagnetic coupling of Co magnetic moment to the Ni substrate magnetization is reestablished, as confirmed by the respective dichroic signals (Fig. 1c; −NO).

X-ray photoelectron spectroscopy. To assess the influence of NO ligation on the chemical species involved and on the electronic interaction between CoTPP and Ni, we have employed X-ray photoelectron spectroscopy (XPS) and measured Co2p XP spectra at various stages of the experiment (Fig. 2a). For a monolayer of CoTPP on Ni, the $Co2p_{3/2}$ XPS signal exhibits a multiplet spectral feature, on which the main peak was observed at ~778.2 eV resembling an outermost $(d_{z^2})^1$-open-shell structure (compare CoTPP/Ag(111) system in Flechtner *et al.*[6]). Reaction with NO causes two major changes in the $Co2p_{3/2}$ XPS signal. First, the multiplet spectral feature is replaced by a single peak, which is the expected behaviour for Co, assuming an outermost $(d_{z^2})^2$-closed-shell electronic structure. Second, the main peak position shifts from ~778.2 to ~780.2 eV—the latter value also being observed for the main $Co2p_{3/2}$ peak of CoTPP in multilayers (see Flechtner *et al.*[6]). This behaviour suggests the suppression of the Co–Ni interaction by the stronger NO–Co interaction and correlates the observed chemical shift in XPS to a downshift of the unoccupied d_{z^2} spin level after bonding with NO. On thermal treatment of the NO–CoTPP–Ni system the multiplet feature of the $Co2p_{3/2}$ XPS signal, characterized by the main peak at ~778.2 eV, is observed again, which proves the NO dissociation from the nitrosyl complex—consistent with an earlier report on the *electronic* coupling of the NO–CoTPP–Ag system[6]. Notably, in our system, both the electronic coupling and the ad-molecular magnetization respond simultaneously to NO addition and removal.

Scanning tunnelling microscopy. To further elucidate the nature of the chemical switching effect, it is necessary to study the adsorption geometry of the CoTPP molecules on Ni(001). Our scanning tunnelling microscopy (STM) data (Fig. 2b–d) show that the Ni(001) surface exhibits extended terraces that are virtually free of point defects and that CoTPP molecules adsorb spatially in a random distribution on the surface. This is due to a considerable surface-molecular interaction limiting the diffusion length during the deposition process, which then hinders the *frequently* observed self-assembly on metallic substrates[31,32]. This observation is in line with a recent report on the Mn-porphyrin/Co(001) system showing limited or no self-assembly[11]. High-resolution STM images of the CoTPP molecules on Ni(001) (Fig. 2d) reveal a planar orientation on the surface. A quasi-planar orientation has also been found by means of near-edge X-ray absorption fine structure spectroscopy for similar magnetic molecule–substrate interfaces, for example, Mn-porphyrin/Co(001), Fe-porphyrin/Co(001) and Fe-porphyrin/Ni(001)[7,8]. Density functional theory calculations have shown that magnetic exchange coupling requires the metalloporphyrin molecule: (i) in a planar orientation with the metal ion–4N moiety (see 'Co–4N' in Fig. 3a) on the surface and (ii) in a certain distance from the magnetic substrate[8,28,29].

In our STM data, we observe some bright spots (Fig. 2c) that correspond to CoTPP molecules adsorbed on top of the first (incomplete) molecular layer. Molecules in the second layer do not have contact with the Ni substrate and reside comparably far above the surface. Thus, not every CoTPP molecule on our samples undergoes ferromagnetic exchange coupling with the Ni(001) substrate. However, XPS data (Fig. 2a) support that the *vast majority* of CoTPP molecules electronically interact with the Ni(001) substrate. Furthermore, in the STM overview of clean Ni(001) (cf. Fig. 2b), the small black square drawn within the dotted circle represents the corresponding size of one CoTPP molecule. From the molecular dimensions and the step density observed in the STM data, we estimate an upper limit of ~5 to 10% of the molecules (at a coverage of ~1 ML CoTPP), which can reside at low-symmetry sites, for example, step edges. As a result, most of the CoTPP molecules are adsorbed at high-symmetry sites and in planar orientation (Fig. 2c and 2d) and are thereby expected to contribute to the magnetic interaction and to respond well to the spin switching events by NO adsorption/desorption, as observed in the XMCD data (see Fig. 1c).

Discussion

On the basis of the XPS identification of the Co species and the STM observation of a predominantly planar orientation of the molecules, the NO-induced reversible switching between CoTPP and Ni can be attributed to the *trans* effect[6,22–24]. In analogy to the elegant postulate reported in Flechtner *et al.*[6] describing the role of the *trans* effect in interfacial coordination chemistry, the NO ligand coordinating in *trans* position controls the coupling to a second ligand (Ni substrate) acting on the same metalloporphyrin (CoTPP). Bonding of NO with the Co ion presumably changes the 'Co–4N' planar geometry (see Fig. 3a) such that the Co ion is pulled out of the plane towards the NO, whereby the overlap with Ni orbitals is reduced—which assists the switching event. The *trans* effect is frequently used to control chemical reactivity or electron affinity through ligands[22–24] and, as demonstrated here, simultaneously controls the chemical/electronic coupling and the spin state.

The magnetic properties, namely the Co magnetization during the switching process that depends on the Ni substrate magnetization direction, can be uniquely probed for this system by the element-specific XMCD technique. The quenching of the Co XMCD signal observed in our experiments is identified as a consequence of the pairing of the originally unpaired spin in the d_{z^2} orbital on formation of the NO–CoTPP complex. This chemically stimulated process directly affects the Co spin system and the coupling to the substrate, as can be seen from the discussion of the molecular levels (Fig. 3b) involved: the highest occupied molecular orbital
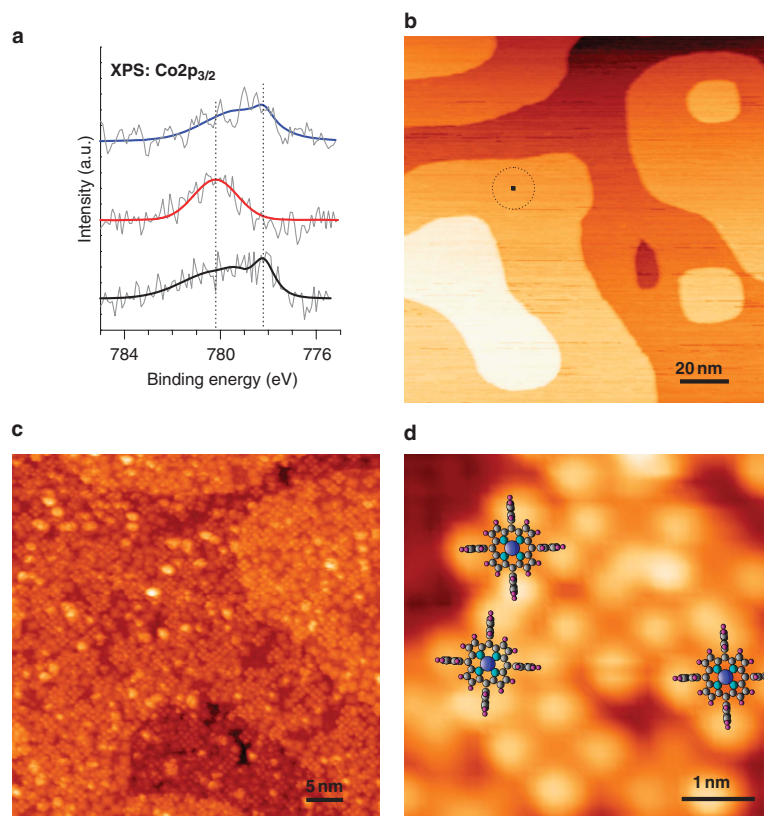
Figure 2 | Probing electronic interaction and visualizing molecules on the surface. (**a**) Co2p$_{3/2}$ XP spectra (raw data and fitted curves) of CoTPP molecules (~1 ML) on Ni(001) before NO exposure (black line), after NO exposure (red line) and on desorption of NO (blue line). The spectral evolution reflects the NO-induced reversible switching of the Co oxidation state and the modified electronic interaction between CoTPP molecules and the Ni surface. Different binding energy positions of the Co2p$_{3/2}$ XPS signal have been marked by dotted lines; 'a.u.' refers to arbitrary units. (**b**) Molecular adsorption on a reactive magnetic substrate: room temperature STM image showing the surface morphology of Ni(001) (150 nm × 150 nm; the size corresponding to one CoTPP molecule is depicted by the black square within the dotted circle). (**c**) Adsorption of CoTPP molecules on the Ni(001) surface (50 nm × 50 nm), where CoTPP is recognized by a four-leaf clover shape in symmetric and planar adsorption geometry while asymmetric conformations can also be detected[38]. (**d**) High-resolution STM: As a guide to the eye, molecular cartoons of CoTPP have been inserted (5 nm × 5 nm). Tunnelling parameters: I = 0.07 nA, U = 0.68 V (**b**) and I = 0.05 nA, U = 1.05 V (**c**, **d**).

of the NO–CoTPP complex[33–35] originates from the interaction of singly occupied molecular orbitals of CoTPP (d_{z^2})[34,35] and NO (π^*)[23], as schematically shown in Figure 3a,b.

On heating the sample, NO dissociates from the NO–CoTPP complex, leaving the CoTPP molecule with an unpaired spin and reestablishing the magnetoelectronic association with the Ni substrate. The dichroic signal at ~778.5 eV (Fig. 1c; top right panel) and the Co XPS data (Fig. 2a; blue line) clearly indicate that the CoTPP molecules remain intact after the temperature-induced dissociation of NO. A scheme for the NO-induced reversible switching of the magnetic response of CoTPP coupled to a ferromagnetic Ni substrate is presented in Figure 3c. Two different mechanisms can be considered: (i) NO reacts with CoTPP from the top and forms the NO–CoTPP complex or (ii) the Ni substrate reacts with NO and consequently affects the CoTPP–Ni interaction. To provide decisive evidence towards mechanism (i) or (ii), we have performed two additional experiments. First, a bare Ni(001) surface was exposed to ~6,000 L (Langmuir) of NO and was subsequently annealed at

~615 K. The O1s (a) and N1s (b) XPS signals (see Fig. 4) remain essentially unchanged on annealing. The shoulder observed at higher binding energies before annealing is assigned to physisorbed species desorbing from the surface on annealing. On the basis of the earlier reported observation of NO dissociation on Ni(001), even at room temperature[36], the two peaks are attributed to Ni–N and Ni–O species, which remain chemisorbed at the annealing temperatures used in our experiment.

In the second experiment, CoTPP (~1 ML) was deposited onto a Ni(001) surface preexposed to NO (~6,000 L). Subsequently, this system was annealed at ~615 K. Interestingly, the Co2p XPS data exhibited almost identical peak positions (Co2p$_{3/2}$ ~780.2 eV) before and after this annealing procedure (see Fig. 5), which indicates that CoTPP remains electronically decoupled from the Ni substrate, that is, the preexposure of NO modifies the Ni(001) substrate such that no NO-induced reversibility can be observed in this temperature window. These results confirm that our experiments on the NO-induced switching are not significantly determined/affected by
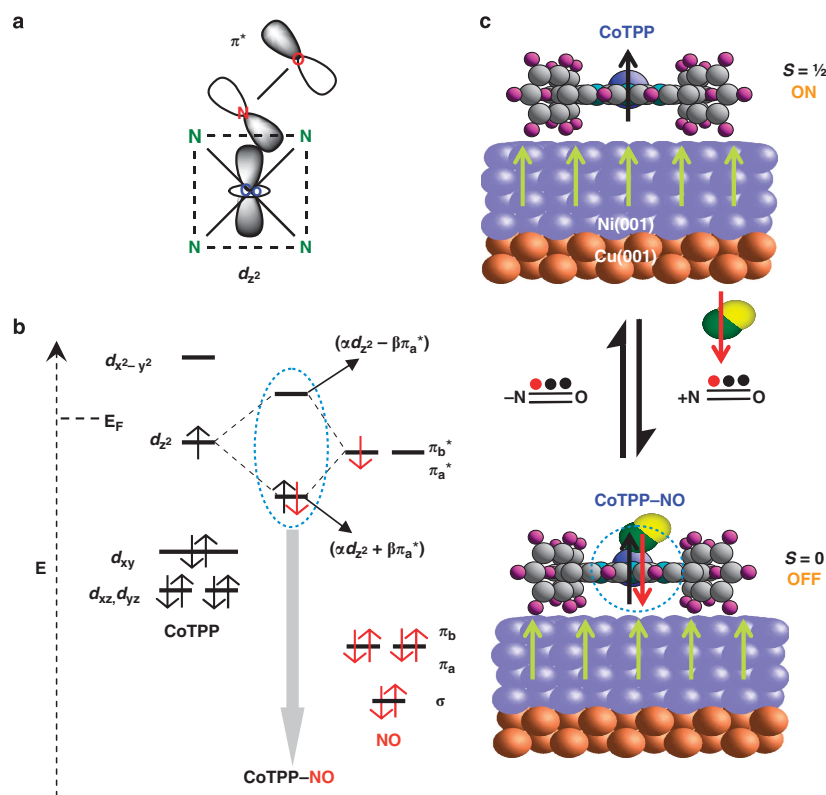
                                                                                        ARTICLE

Figure 3 | Reversible *off-on* switching of a molecular spin. (**a**) A scheme of the NO–CoTPP complex depicting the involvement of the relevant orbitals. The four green N atoms from the pyrrole moieties of the porphyrin represent the coordination with the Co ion and the dashed lines indicate the Co–4N plane that gets a pyramidal distortion on nitrosyl complex formation. (**b**) The electronic levels involved in the chemical reaction between NO acting as a π-ligand and CoTPP. Molecular orbital diagrams (the dashed vertical arrow indicates the energy axis, E) of CoTPP (d^7 configuration: $(d_{xz})^2(d_{yz})^2(d_{xy})^2$ $(d_{z^2})^1(d_{x^2-y^2})^0$ adapted from Wayland *et al.*[34] and Kozuka and Nakamoto[35]) and NO (configuration: $(\sigma)^2(\pi_a)^2(\pi_b)^2(\pi_a{}^*)^1(\pi_b{}^*)^0$ adapted from Huheey *et al.*[23]) showing the presence of unpaired electrons in both CoTPP (d_{z^2}) and NO ($\pi_a{}^*$). On formation of the NO–CoTPP complex (grey arrow), the unpaired spin of CoTPP, which is responsible for the molecular magnetism, is paired up with the unpaired spin supplied by NO in the mixed bonding orbital (highest occupied molecular orbital, HOMO). Consequently, the mixed antibonding orbital (lowest unoccupied molecular orbital, LUMO) is lifted above the Fermi level (E_F) of the Ni substrate. Note that the energy levels of the orbitals within the blue dotted circle have been adapted from the literature: Wayland *et al.*[34] and Kozuka and Nakamoto[35] for the HOMO/LUMO of the NO–CoTPP complex and Flechtner *et al.*[6] for E_F. α and β represent orbital mixing coefficients of d_{z^2} and $\pi_a{}^*$, respectively. (**c**) Schematic representation of the switching process: switching on (top)—the CoTPP molecule is ferromagnetically coupled to the Ni substrate and the Co magnetic moment follows the substrate (Ni) magnetization; switching off (bottom)—on addition of NO, CoTPP ($S = \frac{1}{2}$) forms the NO–CoTPP complex ($S = 0$) and the spin state of NO–CoTPP remains the same, irrespective of the Ni magnetization. Reversibility is shown by the reaction arrows indicating the chemical reaction with NO and the dissociation of NO.

side reactions of NO on the bare fraction of the Ni substrate (< 20%; see Fig. 2b), as the electronic and ferromagnetic exchange coupling between CoTPP and Ni is *restored* after annealing at ~615 K (see Figs 1c and 2a). Thus, the reported experiments are all in agreement with mechanism (i) and are consistent with the involvement of the *trans* effect. Note that the observation of ligand-induced spin switching of porphyrins is not restricted to ferromagnetic substrates, and we expect that this work can be extended to antiferromagnetic or diamagnetic (for example, Cu(100)) substrates as well, using sufficiently high external magnetic fields at low temperature, for example, 6 T and 8 K[21]. The *trans* effect, as used to control the site-specific affinity of porphyrins or phthalocyanines to chemical reactants, is used in this study to control the spin localized at a central metal ion, and thereby provides the case for a *spin trans* effect.

Because of the large body of knowledge about porphyrins and phthalocyanines[1], and their variability established in coordination chemistry, the *spin trans* effect is expected to proceed beyond the case presented here. Spin switching systems on the basis of the presented architecture are expected to be demonstrated using other chemical stimuli (for example, CO), using modified molecular spin systems (for example, metallophthalocyanines), and also for the case of antiferromagnetic exchange coupling[10,11]. Considering the involvement of the chromophoric group in these molecules, the use of other stimuli such as light is foreseeable. By exploiting a *pump-and-probe* approach it might become possible to study *spin dynamics* in surface-supported chemical reactions using the XMCD technique[20].

The reversible *off–on* switching of the electron spin in a surface-supported paramagnetic molecule presented here suggests further
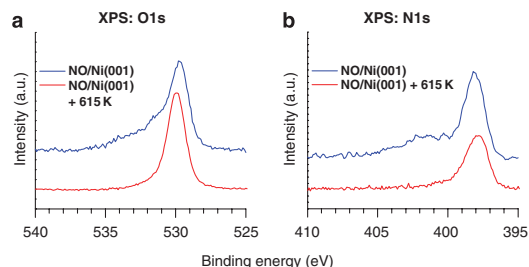
Figure 4 | Effect of NO coadsorption on Ni(001). XPS data recorded on a Ni(001) surface after exposure of ~6,000 L NO. The measurements were taken before (blue) and after (red) annealing at ~615 K. The O1s (**a**) and N1s (**b**) XP spectra clearly show that only the physisorbed NO is removed after annealing. The N/O intensity ratio is reduced after heating by a negligible extent, which suggests that the Ni(001) surface remained covered with nitrogen- and oxygen containing species even after annealing. We tentatively assign these species to chemisorbed Ni–oxygen/Ni–nitrogen and (NO)x. 'a.u.' represents arbitrary units.
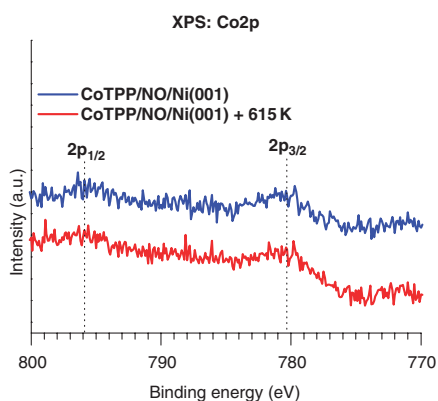

Figure 5 | Role of the *trans* effect in the observed reversibility. About 1 ML of CoTPP was evaporated onto a Ni(001) surface that was previously exposed to ~6,000 L of NO to prepare a CoTPP/NO/Ni(001) system. The system was subsequently annealed at ~615 K, and Co2p XP spectra were recorded before and after annealing. Before annealing, the Co2p$_{3/2}$ peak at ~780.2 eV indicates that there is no electronic interaction between CoTPP and Ni. Interestingly, even after annealing, the CoTPP remained electronically decoupled from the Ni. This control experiment shows that CoTPP on preexposed NO/Ni(001) cannot exhibit reversibility of the magnetoelectronic interaction between CoTPP and Ni (see Figs 1c and 2a). Thereby, the reversibility observed in our main experiment is attributed to gaseous NO species coordinating to the CoTPP adlayer through the *trans* effect[6]. 'a.u.' represents arbitrary units.

studies on organic spintronic interfaces in conjunction with transport measurements. In view of the rapidly advancing capabilities to induce events on the level of single atoms and molecules by scanning probe microscopy, it is anticipated that surface-supported magnetic molecules can be individually switched. The behaviour of such model systems, not only as isolated spin systems and in dependence of their coupling to the substrate/environment but also as elements of quantum-coupled systems, may provide a new

basis for experimental insight into quantum behaviour at further increased complexity.

Methods
Sample preparation and characterization. All experiments were performed in ultrahigh vacuum. Cu(001) single crystals (MaTecK GmbH) were cleaned by repeated Ar$^+$ sputtering/annealing cycles and the impurity level was monitored by recording C1s, O1s, N1s and Ni2p XPS signals. Ni (MaTecK GmbH) thin films (~20 MLs, ~3.5 nm) were deposited by means of electron-beam evaporation in a two-step procedure onto clean Cu(001) single crystals[11]. In the first step, ~10 MLs of Ni were evaporated on Cu(001) kept at room temperature, which provided a sufficient barrier to prevent the Cu atoms from diffusion across the Ni layers. After ~30 min of annealing at ~530 K, another ~10 MLs of Ni were deposited while keeping the sample at ~460 K to obtain atomically flat terraces. During these evaporation steps, the deposition rate was monitored by a quartz crystal microbalance. After deposition of ~20 MLs of Ni on Cu(001), the thin-film substrate was investigated by XPS and low-energy electron diffraction studies to assure that no contamination of the film occurred and that the growing film shows the fcc(001) structure[11]. CoTPP (Sigma-Aldrich) molecules were evaporated (~1 ML) onto a freshly prepared non-magnetized Ni(001) substrate kept at room temperature. The deposition rate was monitored by a quartz crystal microbalance and the molecular coverage on the surface was calibrated by combined XPS and STM measurements. STM images were taken in constant-current mode at room temperature with a Pt/Ir tip and the bias voltages were referred to the grounded sample. The prepared samples were transported to the surfaces/interfaces microscopy (SIM) beamline of the Swiss Light Source (SLS) using a vacuum suitcase (base pressure in the order of ~7.5×10^{-11} Torr), that is, without breaking the vacuum.

XMCD measurements. An external magnetic field of ~125 mT was applied perpendicular to the surface plane of the CoTPP/Ni(001) sample before the XMCD measurements to assure single-domain magnetization of the Ni film along the easy axis (out-of-plane)[8]. The L-edges absorption spectra for both Co and Ni were recorded at normal incidence in total electron yield mode without externally applied magnetic field, that is, in the remanent magnetization of the Ni substrate. The SLS-SIM beamline provides high brilliance X-ray light in the energy range of 130–2,000 eV from two elliptical twin undulators, which permit switching of the photon helicity optically within a few seconds[37]. All spectra were recorded at room temperature and normalized to the incident photon flux. The Ni magnetization was reproducibly reversed by inverting the externally applied magnetic field. XMCD data taken at the SLS-SIM beamline were complemented by XPS/STM measurements using the same sample preparation conditions.

NO dosing and heating. The CoTPP/Ni(001) system was exposed to ~6,000 L of NO (exposure time ~17 min) in the XMCD chamber at room temperature. The sample was subsequently heated to ~615 K to remove NO from the NO–CoTPP complex. Notably, our experiments suggest that cooling the sample to ~100 K reduces the required NO exposure to a considerable extent, whereas the *off–on* electronic switching events can still be consistently observed by the XPS measurements.

References
1. Khadis, K. M., Smith, K. M. & Guilard, R. (eds) in *The Porphyrin Handbook* (Academic Press, Vol. 1–10 (1999) and Vol. 11–20 (2003)).
2. Perutz, M. F. Stereochemistry of cooperative effects of haemoglobin: haem-haem interaction and the problem of allostery. *Nature* **228,** 726–734 (1970).
3. Berg, J. M., Tymoczko, J. L. & Stryer, L. *Biochemistry,* 5th edn (W. H. Freeman and Company, 2002).
4. Williams, F. J. , Vaughan, O. P. H., Knox, K. J., Bampos, N. & Lambert, R. M. First observation of capping/uncapping by a ligand of a Zn porphyrin adsorbed on Ag(100). *Chem. Commun.* 1688–1689 (2004).
5. Vaughan, O. P. H., Williams, F. J., Bampos, N. & Lambert, R. M. A chemically switchable molecular pinwheel. *Angew. Chem. Int. Ed.* **45,** 3779–3781 (2006).
6. Flechtner, K., Kretschmann, A., Steinrück, H.-P. & Gottfried, J. M. NO-induced reversible switching of the electronic interaction between a porphyrin-coordinated cobalt ion and a silver surface. *J. Am. Chem. Soc.* **129,** 12110–12111 (2007).
7. Scheybal, A., Ramsvik, T., Bertschinger, R., Putero, M., Nolting, F. & Jung, T. A. Induced magnetic ordering in a molecular monolayer. *Chem. Phys. Lett.* **411,** 214–220 (2005).
8. Wende, H. *et al.* Substrate-induced magnetic ordering and switching of iron porphyrin molecules. *Nat. Mater.* **6,** 516–520 (2007) [Gatteschi, D. News and Views; Molecular magnets: a coupling powered by nature. *Nat. Mater.* **6,** 471–72 (2007)].
9. Bernien, M. *et al.* Fe-porphyrin monolayers on ferromagnetic substrates: electronic structure and magnetic coupling strength. *Phys. Rev. B.* **76,** 214406 (2007).
10. Bernien, M. *et al.* Tailoring the nature of magnetic coupling of Fe-porphyrin molecules to ferromagnetic substrates. *Phys. Rev. Lett.* **102,** 047202 (2009).

ARTICLE

11. Chylarecka, D. *et al.* Self-assembly and superexchange coupling of magnetic molecules on oxygen-reconstructed ferromagnetic thin film. *J. Phys. Chem. Lett.* **1,** 1408–1413 (2010).

12. Iacovita, C. *et al.* Visualizing the spin of individual cobalt-phthalocyanine molecules. *Phys. Rev. Lett.* **101,** 116602 (2008).

13. Rocha, A. R., Garcia-Suarez, V. M., Bailey, S. W., Lambert, C. J., Ferrer, J. & Sanvito, S. Towards molecular spintronics. *Nat. Mater.* **4,** 335–339 (2005).

14. Dediu, V. A., Hueso, L. E., Bergenti, I. & Taliani, C. Spin routes in organic semiconductors. *Nat. Mater.* **8,** 707–716 (2009).

15. Gütlich, P. & Goodwin, H. A. (eds) *Topics in Current Chemistry Series: Spin Crossover in Transition Metal Compounds*, Vol. 233–235 (Springer, 2004).

16. Kahn, O. & Martinez, C. J. Spin-transition polymers: from molecular materials toward memory devices. *Science* **279,** 44–48 (1998).

17. Gütlich, P., Hauser, A. & Spiering, H. Thermal and optical switching of spin states in iron(II) complexes. *Angew. Chem. Int. Ed.* **33,** 2024–2054 (1994).

18. Bousseksou, A., Molnár, G. & Matouzenko, G. Switching of molecular spin states in inorganic complexes by temperature, pressure, magnetic field and light: towards molecular devices. *Eur. J. Inorg. Chem.* **2004,** 4353–4369 (2004).

19. Mannini, M. *et al.* Magnetic memory of a single-molecule quantum magnet wired to a gold surface. *Nat. Mater.* **8,** 194–197 (2009).

20. Stöhr, J. & Siegmann, H. C. in *Springer Series in Solid-State Sciences, Magnetism: from Fundamentals to Nanoscale Dynamics*, Vol. 152 (Springer, 2006).

21. Gambardella, P. *et al.* Supramolecular control of the magnetic anisotropy in two-dimensional high-spin Fe arrays at a metal surface. *Nat. Mater.* **8,** 189–193 (2009).

22. Cotton, F. A., Wilkinson, G. , Murillo, C. A. & Bochmann, M. *Advanced Inorganic Chemistry*, 6th edn (Wiley-Interscience, 1999).

23. Huheey, J. E., Keiter, E. A. & Keiter, R. L. *Inorganic Chemistry: Principles of Structure and Reactivity* 4th edn (Prentice Hall, 1997).

24. Hartley, F. R. The *cis*- and *trans*-effects of ligands. *Chem. Soc. Rev.* **2,** 163–179 (1973).

25. Hirjibehedin, C. F., Lutz, C. P. & Heinrich, A. J. Spin coupling in engineered atomic structures. *Science* **312,** 1021–1024 (2006).

26. Leuenberger, M. N. & Loss, D. Quantum computing in molecular magnets. *Nature* **410,** 789–793 (2001).

27. Eaton, S. S. & Eaton, G. R. Magnetic susceptibility of porphyrins. *Inorg. Chem.* **19,** 1095–1096 (1980).

28. Ali, Md.E., Sanyal, B. & Oppeneer, P. M. Tuning the magnetic interaction between manganese porphyrins and ferromagnetic Co substrate through dedicated control of the adsorption. *J. Phys. Chem. C* **113,** 14381–14383 (2009).

29. Oppeneer, P. M., Panchmatia, P. M., Sanyal, B., Eriksson, O. & Ali, Md.E. Nature of the magnetic interaction between Fe-porphyrin molecules and ferromagnetic surfaces. *Prog. Surf. Sci.* **84,** 18–29 (2009).

30. Richter-Addo, G. B., Legzdins, P. & Burstyn, J. Introduction: nitric oxide chemistry. *Chem. Rev.* **102,** 857–860 (2002).

31. Barlow, D. E., Scudiero, L. & Hipps, K. W. Scanning tunnelling microscopy study of the structure and orbital-mediated tunneling spectra of cobalt(II) phthalocyanine and cobalt(II) tetraphenylporphyrin on Au(111): mixed composition films. *Langmuir* **20,** 4413–4421 (2004).

32. Buchner, F. *et al.* Chemical fingerprints of large organic molecules in scanning tunneling microscopy: imaging adsorbate-substrate coupling of metalloporphyrins. *J. Phys. Chem. C.* **113,** 16450–16457 (2009).

33. Ghosh, A. Metalloporphyrin-NO bonding: building bridges with organometallic chemistry. *Acc. Chem. Res.* **38,** 943–954 (2005).

34. Wayland, B. B., Minkiewicz, J. V. & Abd-Elmageed, M. E. Spectroscopic studies for tetraphenylporphyrincobalt(II) complexes of CO, NO, O_2, RNC, and (RO_3P), and a bonding model for complexes of CO, NO, and O_2 with cobalt(II) and iron(II) porphyrins. *J. Am. Chem. Soc.* **96,** 2795–2801 (1974).

35. Kozuka, M. & Nakamoto, K. Vibrational studies of (tetraphenylporphyrinato) cobalt(II) and its adduct with CO, NO, and O_2 in gas matrices. *J. Am. Chem. Soc.* **103,** 2162–2168 (1981).

36. Sandell, A., Nilsson, A. & Mårtensson, N. Adsorption of NO on Ni(100). *Surf. Sci.* **251–252,** 971–978 (1991).

37. Flechsig, U. *et al.* Performance measurements at SLS SIM beamline. *AIP Conf. Proc.* **1234,** 319–322 (2010).

38. Jung, T. A., Schlittler, R. R. & Gimzewski, J. K. Conformational identification of individual adsorbed molecules with the STM. *Nature* **386,** 696–698 (1997).

Author contributions

N.B. planned the study and the experimental sessions. C.W., D.C. and N.B. conducted most of the experiments, analysed the data and prepared the figures for the paper. A.K., K.M., C.I. and F.N. provided essential assistance during the beamtime experiments. A.K. and F.N. supervised and checked the XMCD experiments and the analysis. N.B. and T.A.J. supervised and checked the XPS, STM and XAS experiments; and they also assembled the paper and references with inputs from the coauthors.

Additional information

How to cite this article: Wäckerlin, C. *et al.* Controlling spins in adsorbed molecules by a chemical switch. *Nat. Commun.* 1:61 doi: 10.1038/ncomms1057 (2010).

2.2 On-surface Coordination Chemistry of Planar Molecular Spin Systems: Novel Magnetochemical Effects Induced by Axial Ligands

Summary: On the basis of our previous letter based on d^7 low-spin S = 1/2 Co(II)-porphyrin and spin-bearing NO, we explore the on-surface magnetochemistry of d^6 intermediate-spin Fe(II) porphyrin and d^5 high-spin Mn(II)-porphyrin on ferromagnetic substrates. We show that the magnetic moment can be tuned (Fe-porphyrin + NO) and that, in some systems, the outcome of the on-surface-coordination is clearly distinct from the case observed in solution. Specifically, the NO-Mn-porphyrin complex is expected to exhibit an S = 0 spin state; on the surface we find that a non-zero spin-state remains and it is antiferromagnetically coupled to the ferromagnetic substrate. Thus, we show that the axial ligation can invert the sign of the exchange-coupling from ferromagnetic to antiferromagnetic. The experimental data is complemented by DFT+U calculations performed by Peter Oppeneer and Kartick Tarafder. The calculations show increased distance between the metal-ion in the porphyrin and the surface after NO-ligation. This is a clear sign for the presence of a trans effect on surface [29–31] here affecting also the spin-state (e.g. in Mn-porphyrin). This surface trans effect has been shown the reduce the *chemical* interaction with the substrate.[30, 31] We show in a joint theoretical and experimental study that this reduced chemical interaction due to axial ligation can result in a *decreased exchange interaction strength* in MnPc/Co + NH_3.
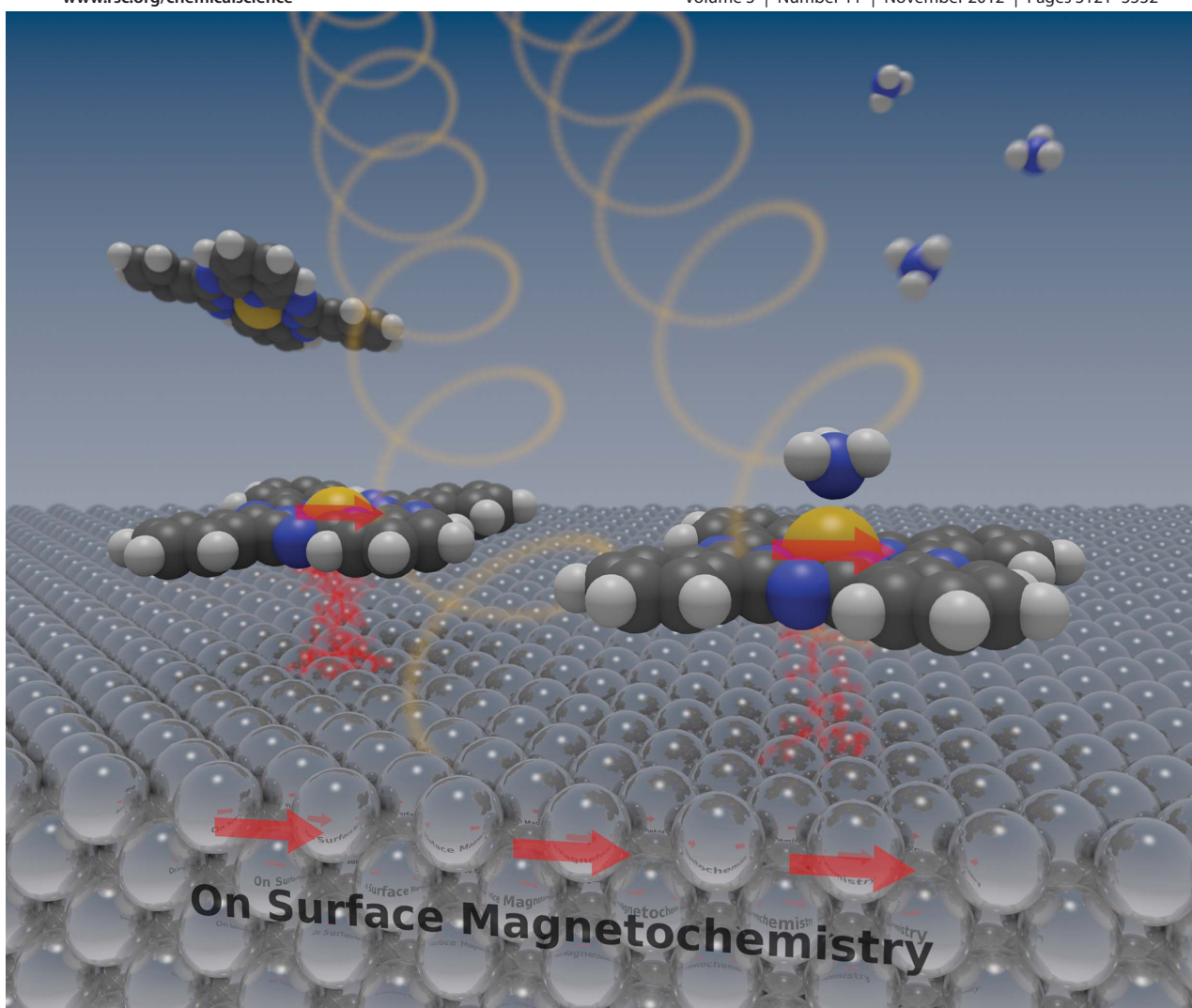
Paper [[2]] is published in Chemical Science.

Chemical Science

On Surface Magnetochemistry

RSC Publishing

Chemical Science

EDGE ARTICLE

On-surface coordination chemistry of planar molecular spin systems: novel magnetochemical effects induced by axial ligands†

Christian Wäckerlin,‡[a] Kartick Tarafder,‡[b] Dorota Siewert,[a] Jan Girovsky,[a] Tatjana Hählen,[a] Cristian Iacovita,[c] Armin Kleibert,[d] Frithjof Nolting,[d] Thomas A. Jung,*[a] Peter M. Oppeneer*[b] and Nirmalya Ballav*[e]

Paramagnetic transition-metal complexes assembled on surfaces are of great interest for potential applications in organic spintronics. The magnetochemical interactions of the spin of the metal centers with both ferromagnetic surfaces and optional axial ligands are yet to be understood. We use a combination of X-ray magnetic circular dichroism (XMCD) and quantum-chemical simulations based on density functional theory (DFT + U) to investigate these metal–organic interfaces with chemically tunable magnetization. The interplay between an optional axial ligand (NO, spin $S = 1/2$ or NH_3, $S = 0$) and Ni and Co ferromagnetic surfaces affecting the spin of Co(II) tetraphenylporphyrin (d^7, $S = 1/2$), Fe(II) tetraphenylporphyrin (d^6, $S = 1$), Mn(II) tetraphenylporphyrin (d^5, $S = 5/2$) and Mn(II) phthalocyanine (d^5, $S = 3/2$) is studied. We find that the structural *trans* effect on the surface rules the molecular spin state, as well as the sign and strength of the exchange interaction with the substrate. We refer to this observation as the surface spin-*trans* effect.

Introduction

A large portfolio of concepts in coordination chemistry of porphyrin- and phthalocyanine-based metal–organic complexes has been developed to rationalize the broad spectrum of physico-chemical functionalities.[1] Recently, coordination chemistry on the surface is being explored.[2–6] In the specific case of competitive coordination, which is usually referred to as the *trans* effect,[7] the ligand on one side of a metal–organic complex is affecting the ground state energy or the binding/unbinding kinetics with the second ligand on the opposite side. To understand coordination chemistry with the surface acting as a ligand,[8–10] square-planar complexes and their reaction with axial ligands like NO, CO, NH₃ affecting the molecule–substrate bonding have been monitored experimentally.

This has been performed by measurements of the spectral characteristics in X-ray photoelectron spectroscopy (XPS),[9–11] in UV photoelectron spectroscopy (UPS)[9,10] and in scanning tunneling microscopy/spectroscopy (STM/STS).[10,6] The term surface *trans* effect has recently been introduced to describe the observed reduction in bonding with the 'surface-ligand'.[10]

Magnetochemical interactions of spin-bearing, square-planar transition metal complexes, like porphyrins and phthalocyanines, with ferromagnetic surfaces offer a unique platform to fabricate metal–organic interfaces with stable magnetization at room temperature that are of great interest for organic spintronics. The search to gain control over the magnetic properties of these interfaces has revealed a number of important findings: paramagnetic complexes on surfaces may be magnetized by their specific bonding interactions with the ferromagnetic (FM) surface.[12–20] Also, the coordination of surface-ligands to paramagnetic metal-porphyrins and phthalocyanines often results in a significant hybridization and/or charge transfer.[21–26] Furthermore, it has been demonstrated that the spin state in cobalt porphyrin adsorbed on a ferromagnetic Ni substrate can be controlled by axial coordination on the open site, *e.g.* by NO[27]. The present work is aimed at answering the fundamentally important question arising from the above findings: to what extent can classical coordination chemistry concepts, which do not consider the surface specific molecule–substrate interaction, be used to understand the on-surface magnetochemistry of metal–organic complexes?

We show that the effect of axial coordination on the spin of planar coordination complexes like porphyrins and phthalocyanines supported on FM substrates can only be understood by inclusion of the surface-ligand into the considerations. Our studies demonstrate that on-surface axial ligation can lead to (i)

[a]Laboratory for Micro- and Nanotechnology, Paul Scherrer Institut, 5232 Villigen, Switzerland. E-mail: thomas.jung@psi.ch
[b]Department of Physics and Astronomy, Uppsala University, Box 516, S-751 20 Uppsala, Sweden. E-mail: peter.oppeneer@fysik.uu.se
[c]Department of Physics, University of Basel, 4056 Basel, Switzerland
[d]Swiss Light Source, Paul Scherrer Institut, 5232 Villigen, Switzerland
[e]Department of Chemistry, Indian Institute of Science Education and Research (IISER), Pune - 411008, India. E-mail: nballav@iiserpune.ac.in
† Electronic supplementary information (ESI) available: experimental section; additional STM, XAS, XMCD and DFT + *U* data; evaluation of exchange coupling strength. See DOI: 10.1039/c2sc20828h
‡ Contributed equally.

spin states that are decisively changed by the interaction with the substrate, (ii) a change in the spin alignment (sign of the exchange coupling: parallel or anti-parallel) or (iii) a modification of the strength of the exchange coupling. These findings are based on X-ray magnetic circular dichroism (XMCD) spectroscopy and density functional theory calculations with additional Hubbard interactions taken into account (DFT + U). Points (i) and (ii) are revealed in the magnetochemistry of metal-tetraphenylporphyrins (CoTPP, FeTPP and MnTPP) sandwiched between a FM surface (Co or Ni thin films) and the NO ligand. To demonstrate (iii), we investigate the strongly chemisorbed[28] Mn-phthalocyanine/Co (MnPc/Co) system under the influence of the non-spin-bearing NH_3 ligand in comparison to the spin-bearing NO ligand. Therefore, the on-surface coordination of metal–organic molecules is shown to lead to novel magnetochemical effects beyond those of classical coordination chemistry. Hence, our observations classify as evidence for the surface spin-*trans* effect. Moreover, our data provide case studies for engineering magnetic metal–organic interfaces in future spintronic applications.

Results

Research design

The electronic and magnetic properties of both the ad-molecules and the substrates were investigated by X-ray absorption spectroscopy (XAS) and XMCD spectroscopy (Fig. 1a). In the latter technique, circularly polarized X-rays from a synchrotron source with opposite helicities were used to perform the absorption experiments.[29] XMCD, the difference of the XAS for opposite helicities, measured at the $L_{2,3}$-adsorption edges of the 3d
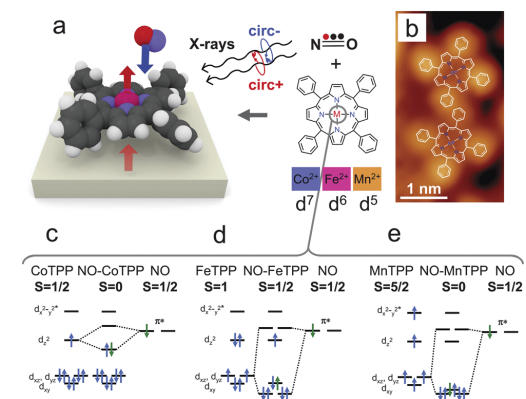

Fig. 1 (a) A schematic representation of the X-ray magnetic circular dichroism (XMCD) experiment on metal-tetraphenylporphyrin (metal-TPP) adsorbed on a ferromagnetic thin film substrate. The magnetic moment of the transition metal centers, which is induced by exchange interaction with the substrate, was studied by XMCD before and after NO coordination. (b) Scanning tunneling microscopy (STM) of CoTPP on Ni showing that the molecules lie flat on the substrate. As a guide to the eye, the chemical schemes have been superimposed on the STM data. (c–e) Molecular orbital (MO) diagrams depicting the reactions of Co, Fe and Mn TPPs with NO in the absence of the surface-ligands.

transition metals provides information on the magnetization of both the substrates and the adsorbed transition-metal complexes, separately, in an element-specific manner. Our experimental observations are complemented by density functional theory (DFT + U) calculations in order to reveal the effects of the axial ligation onto the electronic and spin states. In the DFT + U approach, the strong Coulomb interactions that are present within the open 3d-shell of the central metal ion are captured by the supplemented Hubbard U and exchange constant J. This approach has been shown to provide the correct spin state for free molecules, as well as for substrate-absorbed metal-porphyrins.[15,17,30] To manage computational efforts, we carried out numerical calculations of the on-surface metal-porphyrins (metal-P), *i.e.* without phenyl substitution.[13,16,17,31]

In addition, scanning tunneling microscopy (STM) experiments provide insight into the 2D arrangement of the spin-bearing molecules at a molecular level and into the morphology of the samples in general (Fig. 1b and S1 in the ESI†). X-ray photoelectron spectroscopy (XPS) is primarily used to monitor the surface composition, *i.e.* substrate metal film thickness, molecular coverage and stoichiometry.

We have systematically studied the adsorption of d^7, d^6 and d^5 transition metal-porphyrins (Co(II)TPP, Fe(II)TPP and Mn(II)TPP) respectively onto the FM substrates. The spin of these square-planar complexes has been investigated with respect to the substrate-molecular bonding and the competitive axial ligation with NO. In the free molecules, the low-spin ($S = 1/2$),[9] intermediate-spin ($S = 1$)[32] and high-spin ($S = 5/2$)[33] states of CoTPP, FeTPP and MnTPP, respectively, were reconfigured to low-spin ($S = 0, 1/2, 0$)[9,34–36] upon NO ($S = 1/2$) coordination. As a basis for the discussion of the on-surface coordination in the focus of this paper, molecular orbital (MO) diagrams[37] illustrating the NO binding in the absence of the surface-ligand are provided (Fig. 1c–e).

XMCD experiments performed on the above spin-systems allow us to investigate the complex electronic and spin configurations that arise from the competitive interaction between the surface-ligand and the axial NO ligand. In addition to providing one unpaired electron, NO can undergo a non-innocent electron-transfer reaction.[38] Thus, to assess the influence of the axial coordination onto the strength of the exchange coupling with the surface-ligand, we have chosen to study the strongly chemisorbed MnPc/Co system and its response to innocent[38] and non-spin-bearing NH_3 ($S = 0$).

XAS and XMCD spectroscopy

Fig. 2 compares the Co, Fe and Mn $L_{2,3}$-edges XAS and XMCD spectra recorded on CoTPP/Ni, FeTPP/Ni, MnTPP/Co and MnPc/Co systems. In the native state, *i.e.* before axial ligation, the observed energy positions of the L_3-edge XAS signals appear at ~779.8, ~709.2, ~640.7 and ~640.0 eV, respectively, suggesting considerable electronic interaction of the central metal ion with the axial surface-ligand, since the oxidation states of the respective central metal ions seem to be ≤+2 in comparison to the molecular bulk states.[13,18,27,28,39] The XMCD signals clearly demonstrate that there is a stable magnetic moment of the ad-molecule. This magnetic order in the sub-monolayer regime of paramagnetic molecules on FM substrates originates from the considerable
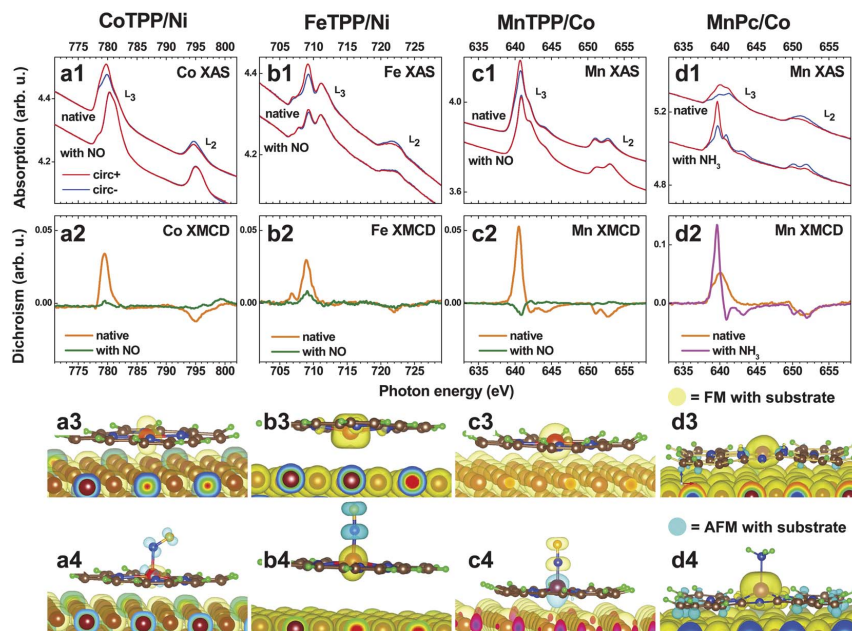
Fig. 2 XAS of CoTPP/Ni (a1), FeTPP/Ni (b1), MnTPP/Co (c1) and MnPc/Co (d1) measured at the respective L-edges, before and after exposure with the gaseous ligand (NO or NH_3). The corresponding XMCD spectra (a2–d2), clearly demonstrate an induced magnetic moment in the molecular spin systems. Positive dichroism at the L_3 edges corresponds to ferromagnetic exchange coupling with the substrate. NO ligation modifies the XAS peak shape. The XMCD spectra show the respective magnetic response of the spin bearing molecules; the magnetic moment in CoTPP/Ni is almost completely quenched, for FeTPP/Ni it is modified and reduced, while for MnTPP/Co it is also reduced, but the sign of the XMCD signal is inverted. This corresponds to an antiferromagnetically coupled magnetic moment. In the case of MnPc/Co (at low temperatures), the increased circular dichroism after NH_3 coordination indicates an increased spin. The magnetization density isosurface plots from the DFT + U calculation of the respective systems before (a3–d3) and after addition of the ligand (a4–d4) illustrate the spin density distribution and the bonding geometry. The light yellow isosurface denotes spin densities parallel to the substrate (ferromagnetic) and the light blue isosurface denotes spin densities antiparallel (antiferromagnetic) to the substrate spin.

exchange interaction between the substrate and the ad-molecule.[7–10,13,16] From the parallel orientations of the $L_{2,3}$-edges XMCD signals of Co, Fe and Mn with respect to those of the substrates (Fig. S2 in the ESI†), a FM coupling is concluded in all native cases. Angular-dependent XMCD measurements reveal a collinear alignment of the molecular spins with the substrate magnetization.[13] Notably, it is not always the case that the paramagnetic molecule retains its spin upon adsorption; as for example, for Co(II) phthalocyanine (CoPc)[21,40–43] on Ni substrate we do not observe an XMCD signal (Fig. S3 in the ESI†).

NO coordination leads to almost complete quenching of the XMCD signal in CoTPP/Ni, while for FeTPP/Ni and for MnTPP/Co the XMCD signal is reduced, but still present (Fig. 2a2–c2). Remarkably, the dichroic signal in NO-exposed MnTPP/Co is oriented antiparallel with respect to the substrate. Thus, the NO–CoTPP ($S = 0$) and NO–FeTPP ($S = 1/2$) in the on-surface configuration behave in first approximation as anticipated by MO theory (Fig. 1c and d). However, MO theory predicts a spin state ($S = 0$) for NO–MnTPP (Fig. 1e), which is not seen in our experiment. Moreover, the reversed sign of the circular dichroism of NO–MnTPP, indicates an antiferromagnetic (AFM) coupling, which is contrary to the usually observed

FM coupling found in experiments on comparable systems.[12,13,27,28]

The XAS of the transition metal centers are also significantly modified upon NO exposure (Fig. 2a1–c1): this modification can be primarily related to (i) a change in the availability of empty states for the transition of 2p core electrons to the unoccupied 3d levels being excited by the X-ray photons, and/or (ii) the change in the oxidation states of the metal ions after ligation with NO.[9–11] The Co, Fe and Mn L_3-edge XAS signals are observed with their maxima at ∼780.4, ∼709.3 and ∼640.9 eV, respectively, after the NO ligation. The stronger shift of the X-ray absorption peak upon NO coordination for CoTPP (+0.4 eV) compared to NO–FeTPP (+0.1 eV) and NO–MnTPP (+0.2 eV) resembles the versatile coordination chemistry of NO, which is related to the NO–central metal (M) bond angle. The NO–M bond is known to be bent (∼120°) for NO–CoTPP and linear (∼180°) in case of NO–MnTPP; NO–FeTPP is found to have an intermediate bond-angle.[44] In the case of bent M–NO where back-bonding is less important, NO is sometimes described as the anionic π-ligand (NO⁻) with the tendency to withdraw charge from the metal center, whereas with an efficient back-bonding in the case of the linear (∼180°) bond the increase of the metal

oxidation state is smaller. The DFT + U calculations of the on-surface complexes reproduce these bond angles (Fig. 2a4–d4).

A surprisingly different system is given by MnPc/Co (intermediate spin state of $S = 3/2$ in the absence of the substrate[45]), which strongly chemisorbs to the Co substrate.[28] We have studied the strength of the magnetic coupling to the surface before and after NH_3 coordination by measuring the dependence of the XMCD/XAS ratio as a function of the temperature. NH_3 ($S = 0$) was chosen, since NO coordination with the d^5 ion in NO–MnTPP/Co (Fig. 2c) leads to a low spin state, *i.e.* a smaller XMCD. For MnPc/Co (Fig. 2d1 and d2) we find that the Mn XMCD/XAS ratio (Fig. S4 in the ESI†), *i.e.* the magnetization, exhibits almost no temperature dependence in the range of 45–373 K, thus providing evidence for a strong molecule–substrate magnetic coupling. After coordination with NH_3, the XMCD/XAS ratio shows a strong decrease when approaching room temperature (Fig. S4 in the ESI†), thus indicating a significantly weaker exchange coupling. However, while the exchange interaction is reduced, the data recorded at ∼80 K indicate a sizeable increase of the spin after NH_3 coordination (Fig. 2d1 and d2).

In the following diccusion, the experimental results of all four spin-systems are interpreted at a microscopic level by means of DFT + U calculations, as illustrated in the magnetization density plots (Fig. 2a3–d3 and a4–d4). The DFT + U calculations predict magnetization changes that are completely consistent with the XMCD measurements. This is further discussed in the next sections, evidencing towards the surface spin-*trans* effect.

Discussion

On-surface magnetochemistry in low-spin and high-spin metal-porphyrins: NO coordination to CoP/Ni and MnP/Co

The mechanism of NO binding with low-spin d^7 Co(II) and high-spin d^5 Mn(II) porphyrin in the free molecule and the formation of low-spin ($S = 0$) nitrosyl complexes[9,36] can be rationalized by the MO diagrams shown earlier (Fig. 1c and e). In the low-spin Co(II) porphyrin, only the singly occupied d_{z^2} is available for bonding, thus the NO binding results in a σ-bond with the singly occupied π* orbital of NO, whereas in the high-spin Mn(II) porphyrin the availability of singly occupied d_π orbitals (*i.e.* d_{xz} and d_{yz}) results in π-bonding with NO – schematically shown in the insets in Fig. 3. Our experimental and theoretical results on these two systems confirm that on the surface, NO binding proceeds in the same fashion. This is reflected in (i) the higher electron affinity of σ-binding NO, as confirmed in the observed stronger shift upon reaction with NO in Co XAS with respect to Mn XAS, (ii) the calculated M–NO bond angles (Fig. 2a4 and c4) and (iii) the hybridization of the d states with NO (Fig. 3b and d).

Recent DFT + U calculations showed that metal-porphyrins can chemisorb or physisorb on metallic substrates.[31] In the case of chemisorbed metal–organic molecules, van der Waals interaction corrections can be neglected. In our DFT + U calculations for chemisorbed CoP/Ni (Fig. 3a), the hybridization of the singly occupied d_{z^2} orbital with the substrate yields a reduced spin state of ∼0.71 μ_B on Co. For the on-surface NO-complex (Fig. 3b), we find a magnetic moment of ∼0.04 μ_B on Co, *i.e.* the spin is almost completely quenched and the local magnetic density of states (LMDOS) is now equally distributed over the two spin-channels
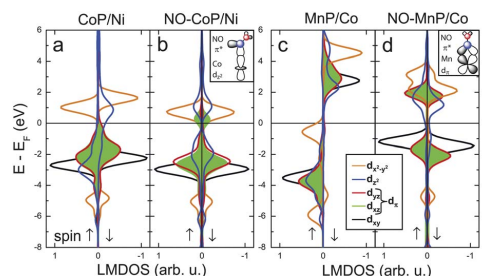

Fig. 3 The 3d orbital local magnetic density of states (LMDOS) is shown for CoP/Ni (a), NO–CoP/Ni (b), MnP/Co (c) and NO–MnP/Co (d) in the chemisorbed case. Without NO, both CoP and MnP are found to be ferromagnetically (FM) coupled with the respective substrates. The out of plane d_{z^2} and d_π orbitals of CoP and MnP are hybridized with the substrate, as reflected in the broadening of the respective states. In the case of CoP/Ni, the hybridization of d_{z^2} leads to a reduction of the spin below the initial value of $S = 1/2$. The binding of NO onto the surface-supported CoP can be rationalized in the formation of a σ-bond with d_{z^2} of Co (depicted in the inset), as seen in the separation of the state. In the case of MnP, a π-bond between d_π of Mn and π* of NO is formed, as depicted in the inset. The NO binding is found to weaken the hybridization of the d states with the substrate. The spin state of the on-surface NO–CoP is approximately zero ($S \approx 0$) in good agreement with considerations neglecting the substrate ($S = 0$). In contrast, the spin state of the on-surface NO–MnP complex cannot be rationalized in neglect of the surface where a spin state of $S = 0$ is expected. Consistent with the experiments, a spin state between $S = 1/2$ and $S = 0$ is found to be antiferromagnetically coupled to the substrate.

(spin ↑ and spin ↓). The quenching of the spin is in accordance to our experimental results (Fig. 2a1 and a2) and similar to the outcome for the free molecule (Fig. 1c). The hybridization of the d_{z^2} with the substrate is reduced in favor of hybridization with NO and separation into bonding and antibonding states. Notably, the distance between the Co-ion and the substrate is increased only slightly (by 0.06 Å from initial 2.34 Å), thus reflecting that NO exerts here only a small structural *trans* effect.[7,44] Notably, the observed reduction of the magnetic moment due to hybridization with the substrate is consistent with our XMCD data of Co-octaethylporphyrin/Ni (CoOEP/Ni) and CoPc/Ni systems, where we find that the magnetic moment is more strongly reduced in CoOEP/Ni, which has less bulky substituents than CoTPP and is even quenched in the case of CoPc/Ni (Fig. S2 in the ESI†). In contrast to CoP/Ni, the influence of the surface-ligand on the spin is clearly visible in MnP/Co (Fig. 3c and d); without NO, the spin state is slightly reduced to ∼4.35 μ_B on Mn (between $S = 2$ and 5/2, *cf.* ref. 31). NO binding affects all d-states and yields a significant structural *trans* effect, as reflected in the increased distance (by 0.3 Å from initial from 2.11 Å) between the Mn-ion and the surface. This leads to a decreased hybridization between the substrate and d_π (now hybridized with NO and separated into bonding and antibonding states) and of d_{z^2} (now mostly unoccupied orbitals of Mn). Importantly, while reducing the spin significantly towards a low-spin state ($S = 0$), a magnetic moment of −0.49 μ_B remains AFM-coupled with the substrate. In Mn-XMCD (Fig. 2c2), this is expressed by the inverted sign of the circular dichroism.

X-ray diffraction (XRD) data of NO–CoTPP in bulk shows a displacement of the Co ion from the center of 0.09 Å, a value which is slightly larger than our calculated Co lift-up on the surface. The Co–N(NO) bond length (1.83 Å) and angle ($\leq 128.5°$) correspond very well with the calculated on-surface bond length (1.82 Å) and angle (~ 123.6 °). In the case of NO–MnTPP in bulk,[46] XRD data shows a Mn–N(NO) bond length of 1.64 Å and a linear (177.8°) Mn–N–O bond.[47] This corresponds very well with the calculated on-surface Mn–N(NO) bond length (1.63 Å) and angle (177.0°). The displacement of the Mn ion from the center (0.34 Å) is comparable to the calculated value for the on-surface configuration. Overall, the structural characteristics of the calculated on-surface Co, Fe and Mn porphyrins correspond very closely with the XRD data of the bulk species. However, this is not the case for the spin states, the most remarkable feature being provided by the AFM coupled spin in the on-surface NO–MnTPP complex.

On-surface magnetochemistry (FeP/Ni + NO): tuning of the molecular spin

In contrast to d^7 Co and d^5 Mn porphyrins where a quenching of the magnetic moment is anticipated, the case of NO coordination with d^6 Fe porphyrin is expected to yield the low-spin $S = 1/2$ complex[35] (Fig. 1d). The mechanism of NO binding to Fe porphyrin can be seen as an intermediate between the two previously discussed d^7 and d^5 complexes and is primarily reflected in a Fe–NO angle of $\sim 170°$ for FeP – in between 120° (d^7) and 180° (d^5). Furthermore, the intermediate spin state ($S = 1$) of Fe(II) porphyrin may change its spin state easily, *e.g.* the histidine-bound natural Fe-porphyrin is high-spin ($S = 2$).[48]

It is worth mentioning that from all three on-surface metal-porphyrins reacting with the NO-ligand, it is the Fe-porphyrin that shows the best reversibility upon heating. NO is completely desorbed from the FeTPP on-surface complex at ~ 260 °C (Fig. S5 in the ESI†), thus at lower temperature than CoTPP (~ 340 °C) and in contrast to MnTPP, which is found to be irreversibly bound within the experimental range up to 400 °C. This reflects the distinctive bonding fashion and strength between NO and Co, Fe and Mn ions.

Our DFT + U calculations (Fig. S7 in the ESI†) for FeP on the Ni surface have been performed for the molecule, being in both the physisorbed and chemisorbed conformation. The calculations yield spin states between $S = 3/2$ and $S = 2$ in the case of physisorption ($\sim 3.73 \, \mu_B$) and chemisorption ($\sim 3.57 \, \mu_B$). For the physisorbed and chemisorbed NO–FeP complex we find spin states of $\sim 1.93 \, \mu_B$ and $\sim 3.49 \, \mu_B$, respectively. On the basis of the observed reduction of the Fe-XMCD signal (Fig. 2a and b) and the calculations suggesting that the exchange coupling strength is not reduced significantly (Fig. S6 in the ESI†), we favor the physisorbed FeP configuration which shows a significant reduction of the spin state.

On-surface magnetochemistry (MnPc/Co + NH₃): tuning the exchange coupling

We now discuss the on-surface magnetochemistry of the MnPc/Co system ($S = 3/2$) and the subsequent effect induced by σ-donating axial NH₃ ligand. Without an axial NH₃ ligand, our

calculations for chemisorbed MnPc on Co (Fig. 4) find a magnetic moment of $\sim 3.25 \, \mu_B$ (spin state in between $S = 3/2$ and $S = 2$) and a strong hybridization between the surface and the out-of plane d-orbitals (d_{z^2} and d_π). Note that in spite of their out-of-plane orientations these d-orbitals carry an in-plane magnetic moment induced by the substrate. The calculations also yield a high coupling energy of ~ 189 meV. Experimentally, this is reflected in the nearly constant XMCD/XAS ratio as a function of temperature (Fig. S4 in the ESI†), which yields a lower limit for the exchange energy in the order of ~ 103 meV, as discussed further in the ESI.†

In the calculations for MnPc/Co with axial NH₃, the ligand pulls the Mn-ion out of the phthalocyanine plane by ~ 0.42 Å from initially 2.30 Å and leads to an increased spin of $\sim 4.45 \, \mu_B$ (between $S = 2$ and $S = 5/2$). In the corresponding experimental data, the higher spin state is expressed by a higher XMCD/XAS ratio observed at lower temperatures (Fig. 2d1 and d2). Remarkably, in our calculations the exchange coupling energy was found to be reduced to only ~ 4 meV. In the temperature-dependent XAS/XMCD data, the reduction of the exchange energy is reflected in a significant decrease of the relative XMCD signal with increasing temperature (Fig. S4 in the ESI†). The data yield an accordingly reduced exchange energy of ~ 31 meV. Notably, a manipulation of the exchange energy has been
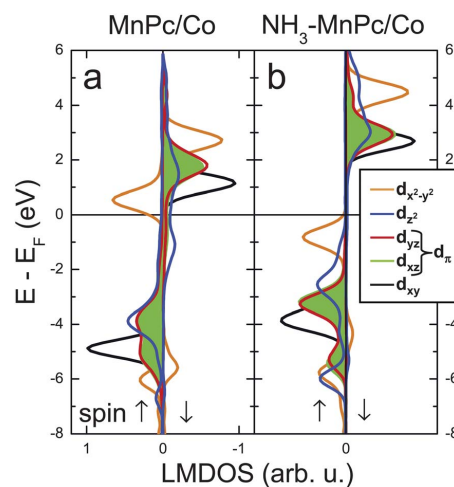

Fig. 4 The 3d LMDOS for MnPc/Co (a) and NH₃–MnPc/Co (b), in the chemisorbed case. Without NH₃, the out of plane d_{z^2} and d_π orbitals are significantly hybridized with the substrate, as recognized by their broadening. In the NH₃-coordinated complex, the hybridization with the substrate is weakened providing narrower d-states. In the calculated on-surface structure, the Mn-ion is pulled out of the plane towards the NH₃ (Fig. 2d4). The spin state of Mn is increased from approximately intermediate spin to approximately high-spin. This is experimentally observed in the increased XMCD/XAS ratio at low temperatures (Fig. S4 in the ESI†). The weaker hybridization with the substrate is reflected in a strong reduction of the calculated magnetic coupling strength. This is confirmed by a stronger decrease of the XMCD/XAS ratio of the NH₃-complex in our experiments performed with increasingly higher temperature. A ferromagnetic coupling is found before and after NH₃ coordination.

claimed for Fe porphyrin, on the basis of the observed reduction of the circular dichroism after NO exposure,[49] but the system has not been measured at different temperatures. We also note that the calculations and experiments for FeTPP/Ni and NO–FeTPP/Ni do not show significant differences in the exchange energy (Fig. S6 in the ESI†). The here presented MnPc/Co + NH_3 case unambiguously demonstrates the relation between axial coordination and exchange energy, i.e. surface spin-trans effect.

Conclusions

The presented data provide an insight into the on-surface magnetochemistry of spin-bearing square-planar complexes. The spins of the complexes (CoTPP, FeTPP, MnTPP and MnPc) are, before coordination with the optional axial ligand, found to be ferromagnetically coupled to the ferromagnetic substrate. The DFT + U calculations reveal a significant hybridization between the d-states in the transition-metal centers and the surface-ligand and show how the hybridization is affecting the spin states in the on-surface complexes. Subsequent axial coordination with the gaseous ligands (NO or NH_3) was found to lead (i) to a rearrangement of the electronic structure in general agreement with coordination chemistry and (ii) to induction of a structural trans effect on the surface with a magnitude depending on the exact chemical species involved. The structural trans effect is concluded from the calculated increase of the distance between the transition-metal center and the substrate, as well as from the decrease of the hybridization with the surface-ligand. In the XMCD data of d^7, d^6, d^5 porphyrins and NO this is reflected respectively by a quenching of the spin in CoTPP/Ni, a modification of the spin in FeTPP/Ni, and most notably a remaining magnetic moment in MnTPP/Co whose alignment with the substrate changed from FM to AFM by axial-ligation. The last system, namely MnPc/Co demonstrates that an axial ligand (here NH_3) may lead to a reduction of the exchange coupling strength. Hence, our data provide compelling evidence that on-surface axial-ligation leads to a trans effect, which influences the molecular spin state, as well as the sign and strength of the exchange interaction. We therefore propose the term surface spin-trans effect for the consequences of the structural trans effect on the spin and the exchange coupling's sign and strength.

The surface spin-trans effect is anticipated to serve as a powerful concept in the design of tailor-made spin-tunable metal–organic interfaces, which may find applications in magnetochemical sensors, in components for future spintronic devices or quantum computing building-blocks. Our study underlines that on-surface magnetochemistry is emerging as a novel arena challenging the notions of classical coordination chemistry.

Acknowledgements

Notes and references

1 K. M. Kadish, K. M. Smith and R. Guilard, The Porphyrin Handbook, Academic Press, 1999.
2 J. V. Barth, Annu. Rev. Phys. Chem., 2007, 58, 375–407.
3 T. Kudernac, S. Lei, J. A. A. W. Elemans and S. De Feyter, Chem. Soc. Rev., 2009, 38, 402.
4 L. Bartels, Nat. Chem., 2010, 2, 87–95.
5 K. Seufert, M.-L. Bocquet, W. Auwärter, A. Weber-Bargioni, J. Reichert, N. Lorente and J. V. Barth, Nat. Chem., 2011, 3, 114–119.
6 K. Seufert, W. Auwärter and J. V. Barth, J. Am. Chem. Soc., 2010, 132, 18141–18146.
7 B. J. Coe and S. J. Glenwright, Coord. Chem. Rev., 2000, 203, 5–80.
8 T. Lukasczyk, K. Flechtner, L. R. Merte, N. Jux, F. Maier, J. M. Gottfried and H.-P. Steinrück, J. Phys. Chem. C, 2007, 111, 3090–3098.
9 K. Flechtner, A. Kretschmann, H.-P. Steinrück and J. M. Gottfried, J. Am. Chem. Soc., 2007, 129, 12110–12111.
10 W. Hieringer, K. Flechtner, A. Kretschmann, K. Seufert, W. Auwärter, J. V. Barth, A. Görling, H.-P. Steinrück and J. M. Gottfried, J. Am. Chem. Soc., 2011, 133, 6206–6222.
11 C. Isvoranu, B. Wang, K. Schulte, E. Ataman, J. Knudsen, J. N. Andersen, M. L. Bocquet and J. Schnadt, J. Phys.: Condens. Matter, 2010, 22, 472002.
12 A. Scheybal, T. Ramsvik, R. Bertschinger, M. Putero, F. Nolting and T. A. Jung, Chem. Phys. Lett., 2005, 411, 214–220.
13 H. Wende, M. Bernien, J. Luo, C. Sorg, N. Ponpandian, J. Kurde, J. Miguel, M. Piantek, X. Xu, P. Eckhold, W. Kuch, K. Baberschke, P. M. Panchmatia, B. Sanyal, P. M. Oppeneer and O. Eriksson, Nat. Mater., 2007, 6, 516–520.
14 M. Bernien, X. Xu, J. Miguel, M. Piantek, P. Eckhold, J. Luo, J. Kurde, W. Kuch, K. Baberschke, H. Wende and P. Srivastava, Phys. Rev. B: Condens. Matter Mater. Phys., 2007, 76, 214406.
15 P. M. Panchmatia, B. Sanyal and P. M. Oppeneer, Chem. Phys., 2008, 343, 47–60.
16 M. Bernien, J. Miguel, C. Weis, M. E. Ali, J. Kurde, B. Krumme, P. M. Panchmatia, B. Sanyal, M. Piantek, P. Srivastava, K. Baberschke, P. M. Oppeneer, O. Eriksson, W. Kuch and H. Wende, Phys. Rev. Lett., 2009, 102, 047202.
17 P. M. Oppeneer, P. M. Panchmatia, B. Sanyal, O. Eriksson and M. E. Ali, Prog. Surf. Sci., 2009, 84, 18–29.
18 D. Chylarecka, C. Wäckerlin, T. K. Kim, K. Müller, F. Nolting, A. Kleibert, N. Ballav and T. A. Jung, J. Phys. Chem. Lett., 2010, 1, 1408–1413.
19 D. Chylarecka, T. K. Kim, K. Tarafder, K. Müller, K. Gödel, I. Czekaj, C. Wäckerlin, M. Cinchetti, M. E. Ali, C. Piamonteze, F. Schmitt, J.-P. Wüstenberg, C. Ziegler, F. Nolting, M. Aeschlimann, P. M. Oppeneer, N. Ballav and T. A. Jung, J. Phys. Chem. C, 2011, 115, 1295–1301.
20 A. Lodi Rizzini, C. Krull, T. Balashov, J. J. Kavich, A. Mugarza, P. S. Miedema, P. K. Thakur, V. Sessi, S. Klyatskaya, M. Ruben, S. Stepanow and P. Gambardella, Phys. Rev. Lett., 2011, 107, 177205.
21 J. Brede, N. Atodiresei, S. Kuck, P. Lazić, V. Caciuc, Y. Morikawa, G. Hoffmann, S. Blügel and R. Wiesendanger, Phys. Rev. Lett., 2010, 105, 047204.
22 S. Stepanow, P. Miedema, A. Mugarza, G. Ceballos, P. Moras, J. Cezar, C. Carbone, F. de Groot and P. Gambardella, Phys. Rev. B: Condens. Matter Mater. Phys., 2011, 83, 220401.
23 N. Tsukahara, K. Noto, M. Ohara, S. Shiraki, N. Takagi, S. Shin and M. Kawai, Phys. Rev. Lett., 2009, 102, 167203.
24 S. Stepanow, A. Mugarza, G. Ceballos, P. Moras, J. C. Cezar, C. Carbone and P. Gambardella, Phys. Rev. B: Condens. Matter Mater. Phys., 2010, 82, 014405.

25 S. Lach, A. Altenhof, K. Tarafder, F. Schmitt, M. E. Ali, M. Vogel, J. Sauther, P. M. Oppeneer and C. Ziegler, *Adv. Funct. Mater.*, 2012, **22**, 989–997.

26 A. Mugarza, C. Krull, R. Robles, S. Stepanow, G. Ceballos and P. Gambardella, *Nat. Commun.*, 2011, **2**, 490.

27 C. Wäckerlin, D. Chylarecka, A. Kleibert, K. Müller, C. Iacovita, F. Nolting, T. A. Jung and N. Ballav, *Nat. Commun.*, 2010, **1**, 61.

28 S. Javaid, M. Bowen, S. Boukari, L. Joly, J.-B. Beaufrand, X. Chen, Y. Dappe, F. Scheurer, J.-P. Kappler, J. Arabski, W. Wulfhekel, M. Alouani and E. Beaurepaire, *Phys. Rev. Lett.*, 2010, **105**, 077201.

29 H. C. Siegmann and J. Stöhr, *Magnetism: From Fundamentals to Nanoscale Dynamics*, Springer, Berlin, 1st edn, 2006.

30 M. E. Ali, B. Sanyal and P. M. Oppeneer, *J. Phys. Chem. B*, 2012, **116**, 5849–5859.

31 M. E. Ali, B. Sanyal and P. M. Oppeneer, *J. Phys. Chem. C*, 2009, **113**, 14381–14383.

32 H. Goff, G. N. La Mar and C. A. Reed, *J. Am. Chem. Soc.*, 1977, **99**, 3641–3646.

33 L. J. Boucher, *J. Am. Chem. Soc.*, 1970, **92**, 2725–2730.

34 B. B. Wayland and J. V. Minkiewicz, *J. Chem. Soc., Chem. Commun.*, 1976, 1015.

35 B. B. Wayland and L. W. Olson, *J. Am. Chem. Soc.*, 1974, **96**, 6037–6041.

36 B. B. Wayland, L. W. Olson and Z. U. Siddiqui, *J. Am. Chem. Soc.*, 1976, **98**, 94–98.

37 J. E. Huheey, *Inorganic Chemistry: Principles of Structure and Reactivity*, HarperCollins College Publishers, New York, 4th edn, 1993.

38 W. Kaim and B. Schwederski, *Coord. Chem. Rev.*, 2010, **254**, 1580–1588.

39 T. Kataoka, Y. Sakamoto, Y. Yamazaki, V. R. Singh, A. Fujimori, Y. Takeda, T. Ohkochi, S.-I. Fujimori, T. Okane, Y. Saitoh, H. Yamagami and A. Tanaka, *Solid State Commun.*, 2012, **152**, 806–809.

40 A. Zhao, Q. Li, L. Chen, H. Xiang, W. Wang, S. Pan, B. Wang, X. Xiao, J. Yang, J. G. Hou and Q. Zhu, *Science*, 2005, **309**, 1542–1544.

41 C. Iacovita, M. Rastei, B. Heinrich, T. Brumme, J. Kortus, L. Limot and J. Bucher, *Phys. Rev. Lett.*, 2008, **101**, 116602.

42 X. Chen, Y.-S. Fu, S.-H. Ji, T. Zhang, P. Cheng, X.-C. Ma, X.-L. Zou, W.-H. Duan, J.-F. Jia and Q.-K. Xue, *Phys. Rev. Lett.*, 2008, **101**, 197208.

43 E. Annese, J. Fujii, I. Vobornik, G. Panaccione and G. Rossi, *Phys. Rev. B: Condens. Matter Mater. Phys.*, 2011, **84**, 174443.

44 G. R. A. Wyllie and W. R. Scheidt, *Chem. Rev.*, 2002, **102**, 1067–1090.

45 C. G. Barraclough, R. L. Martin, S. Mitra and R. C. Sherwood, *J. Chem. Phys.*, 1970, **53**, 1638.

46 W. R. Scheidt and J. L. Hoard, *J. Am. Chem. Soc.*, 1973, **95**, 8281–8288.

47 W. R. Scheidt, K. Hatano, G. A. Rupprecht and P. L. Piciulo, *Inorg. Chem.*, 1979, **18**, 292–299.

48 J. M. Friedman, T. W. Scott, R. A. Stepnoski, M. Ikeda-Saito and T. Yonetani, *J. Biol. Chem.*, 1983, **258**, 10564–10572.

49 J. Miguel, C. F. Hermanns, M. Bernien, A. Krüger and W. Kuch, *J. Phys. Chem. Lett.*, 2011, **2**, 1455–1459.

Electronic Supplementary Information

**On-surface coordination chemistry of planar molecular spin systems:
Novel magnetochemical effects induced by axial ligands**

Christian Wäckerlin[a,‡], Kartick Tarafder[b,‡], Dorota Siewert[a], Jan Girovsky[a], Tatjana Hählen[a], Cristian Iacovita[c], Armin Kleibert[d], Frithjof Nolting[d], Thomas A. Jung[a,*], Peter M. Oppeneer[b,*] & Nirmalya Ballav[e,*]

[a] Laboratory for Micro- and Nanotechnology, Paul Scherrer Institut, 5232 Villigen, Switzerland
[b] Department of Physics and Astronomy, Uppsala University, Box 516, S-751 20 Uppsala, Sweden
[c] Swiss Light Source, Paul Scherrer Institut, 5232 Villigen, Switzerland
[d] Department of Physics, University of Basel , 4056 Basel, Switzerland
[e] Department of Chemistry, Indian Institute of Science Education and Research (IISER), Pune - 411008, India
‡ Contributed equally.

Here, we provide supplementary information complementing the material presented in the article and supporting the therein presented conclusions and the experimental section (in Sec. 1). Specifically, STM data showing the morphology of the samples is presented (in Sec. 2), the XAS and XMCD of the ferromagnetic thin films are discussed (in Sec. 3) and the magnetochemical properties of CoOEP/Ni and CoPc/Ni are presented (in Sec. 4). The reduction/quenching of the XMCD signal in those two systems complements the conclusions discussed in the article. The temperature dependence of the XMCD/XAS ratio of native and NH_3 coordinated MnPc/Co is presented (in Sec. 5). A decrease in the exchange energy for the NH_3-MnPc complex is found in the experiment and in the DFT+U calculations, *i.e.* an influence of axial ligation onto the magnetic coupling. The reversibility of NO coordination with FeTPP/Ni is presented and compared with CoTPP/Ni and MnTPP/Co (in Sec. 6). The impact of the bonding configuration (physisorbed/chemisorbed) onto the spin states of FeP/Ni and NO-FeP/Ni is discussed on the basis of DFT+U calculations (in Sec. 7).

Table of Contents

1 Experimental section

The Ni and Co thin films of 20 monolayer thickness have been grown on Cu(001) single crystals, thereby producing ferromagnetic thin films with well defined magnetic shape-anisotropy in order to re-orient the sample magnetization with a limited external field[1,2]. CoTPP, FeTPPCl, MnTPPCl, MnPc, CoOEP and CoPc were evaporated (~0.7-0.9 ML) onto freshly prepared non-magnetized Ni and Co substrates kept at room temperature. Upon deposition of Fe(III)TPPCl and Mn(III)TPPCl onto Co and Ni substrates, Cl dissociates to form Fe(II)TPP and Mn(II)TPP[3,1].

We have used commercially available transition-metal compounds,. The purity of the 'as deposited' substance is generally higher due to the characteristics of the sublimation process. This is particularly true after thorough degassing at lower than sublimation temperatures. The molecules have been checked occasionally by sublimation with posterior chemical analysis and routinely with XPS [4]. The suppliers and purities (if available) are listed as follows:

- CoTPP, Co(II) tetraphenylporphyrin, Porphyrin Systems, Germany, 98 %
- CoPc, Co(II) phthalocyanine, Sigma-Aldrich, Switzerland
- CoOEP, Co(II) octaethylporphyrin, Sigma-Aldrich, Switzerland
- FeTPPCl, Fe(III) tetraphenylporphyrin chloride, Sigma-Aldrich, Switzerland
- MnTPPCl, Mn(III) tetraphenylporphyrin chloride, Porphyrin Systems, Germany, 98 %
- MnPc, Mn(II) phthalocyanine, Sigma-Aldrich, Switzerland

The quality of the substrates and the epitaxy of the monolayer and multilayer films was monitored by a quartz microbalance and verified in the XPS (monochromatic Al Kα excitation). The evaporation of the molecules was performed with home-built evaporators, the molecules were thoroughly degassed before sublimation, and the stochiometry after sublimation was checked by XPS. The evaporation rates were in the order of 0.5 to 0.25 ML/min, and the pressure during the evaporations was resided in the low 10^{-9} mbar regime. We would like to note that the used transition-metal compounds evaporate well and that XPS studies on multilayer films did not show the presence of impurities. The Co and Ni thin films were produced by electron beam evaporation, the Cu(001) single crystals were prepared by repeated cycles and Ar^+ ion sputtering and annealing. The cleanliness and morphology of the samples was checked by XPS and STM, respectively, c.f. refs. 1,2.

STM images were taken in the constant-current mode at room temperature using W tips. The ferromagnetic thin films were magnetized with an external magnetic field of ~150 mT along the respective easy axis of magnetization. The $L_{2,3}$-edges absorption spectra were recorded in total electron yield (TEY) mode in remanent magnetization of the substrate at the Surface/Interface: Microscopy (SIM) beamline of the Swiss Light Source (SLS)[5]. About 30 Langmuir (L) of NH_3 was dosed on the MnPc/Co system kept at ~80 K. Dosing of NO (~6000 L) on both CoTPP/Ni and MnTPP/Co systems was done at room

temperature while for the FeTPP/Ni system the temperature was kept at 100 K. All measurements were performed in UHV and a portable vacuum chamber was used for sample transfer[1,2].

For the DFT+U calculations, we have used the VASP full-potential plane-wave code[6] with a kinetic energy cut-off of 400 eV. The Perdew-Wang parametrization[7] of the DFT-generalized gradient approximation exchange-correlation functional was used. The Hubbard U and exchange constant J were taken to be 4 eV and 1 eV, respectively. We performed full geometric optimizations of the porphyrin molecules, including their distance and position on the surface, together with a full relaxation of the top substrate layers. Three atomic layers modeled the substrate. Reciprocal space sampling was performed using 2x2x2 Monkhorst-Pack k-points.

To manage computational efforts, we have carried out numerical calculations of the on-surface metallo-porphins (metal-P), *i.e.* without phenyl substitution[3,8–10]. The replacement of the phenyl end groups by hydrogen atoms might influence the magneto-chemical properties in the following ways. First, the phenyl end groups might induce a somewhat shorter or longer bonding distance of the metal-organic macrocycle to the substrate. This might affect the strength of the magnetic coupling of the central metal ion to the substrate. However, we do not expect that the magnetic coupling is changed thereby, for example, from parallel to anti-parallel coupling. It is also worthwhile to note that the current calculations (without phenyl end groups) reproduce fully the experimentally observed magneto-chemical couplings. Also, aspects of the NO or NH_3 bonding to the central metal ion will most likely not be affected. A second way in which the phenyl end groups might affect the coupling of the metal-organic molecule to the substrate could be through inducing a slight deformation of the macrocycle. Some forms of induced chirality have been observed by STM for metal-organic molecules on surfaces[11]. Such stronger chirality might affect the crystal electrical field at the central ion. An answer to the occurrence and possible importance of such deformations might be obtained from future precise STM measurements.
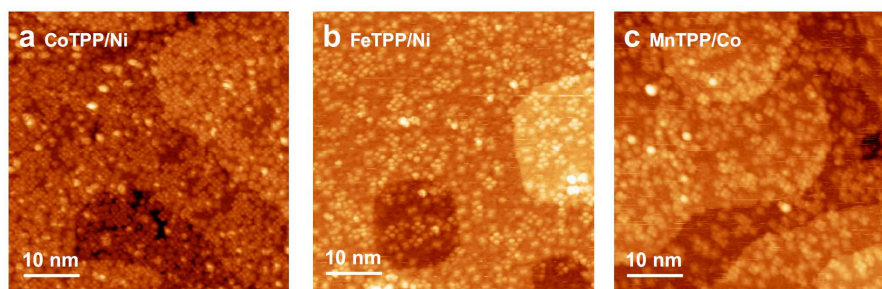
2 STM data

Fig. S1 STM images recorded on sub-monolayer coverages of the metallo-porphyrins on the ferromagnetic thin films: CoTPP/Ni (a), FeTPP/Ni (b) and MnTPP/Co (c).

In STM experiments performed at room-temperature (Fig. S1), we find that the metallo-porphyrins on the here studied ferromagnetic thin films (20 ML of Ni and 20 ML of Co on Cu(001)) do not self-assemble. The molecules are found in different adsorption geometries, *i.e.* conformations and orientations with respect to the substrate. Only a slight ordering between next neighbors is observed, mainly for FeTPP on Ni. The suppression of self-assembly at room temperature indicates a considerable interaction between the molecules and the substrate. This is in contrast to self-assembly as observed on less reactive substrates, *i.e.* oxygen-reconstructed Co/Cu(001)[1]. The STM tunneling parameters used in the shown STM data are: 1.05 V, 50 pA for Figs. 1b and S1a; -1.2 V, -60 pA for Fig. S1b; 1.25 V, 30 pA for Fig. S1c.

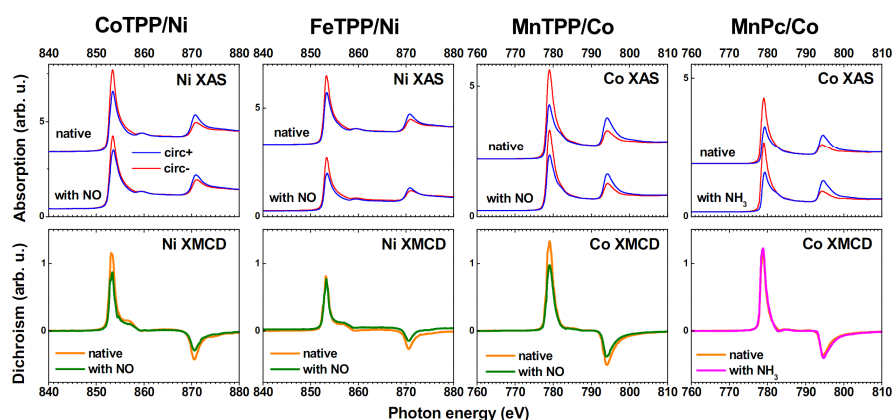## 3 XAS and XMCD of the substrates

Fig. S2 XAS and XMCD of the substrates.

XMCD and XAS data of the substrates of the CoTPP/Ni, FeTPP/Ni, MnTPP/Co and MnPc/Co systems are shown in Fig. S2. Exposure with NO marginally affected the magnetization of the substrate, giving rise to a < 15 % reduction in the XMCD/XAS. When dosing NO/NH$_3$ onto the sample kept at ~100 K, *i.e.* as done for FeTPP/Ni and MnPc/Co no reduction in the XMCD/XAS signals is observed.
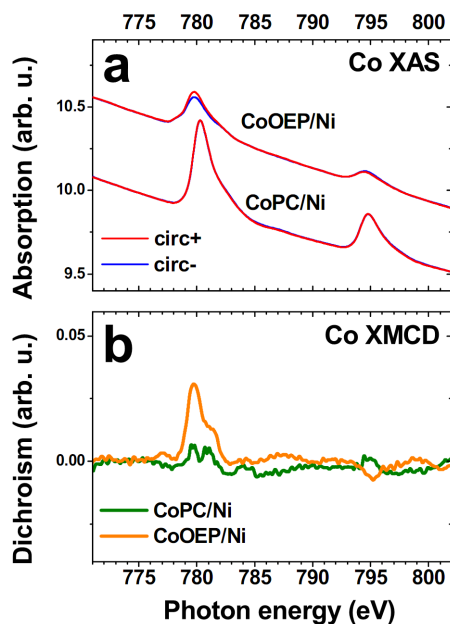
4 XAS and XMCD of CoOEP/Ni and CoPc/Ni

Fig. S3 XAS and XMCD of Co-phthalocyanine (CoPc) and Co-octaethylporphyrin (CoOEP) on Ni, measured at room temperature.

Performing a XAS and XMCD study of CoPc/Ni and CoOEP/Ni (Fig. S3) we find, in comparison to CoTPP/Ni (Figs. 2a1 and 2a2) with an XMCD/XAS ratio at the L_3-edge of ~23%, that the circular dichroism in CoOEP/Ni is reduced to ~15%, while CoPc/Ni shows only small remnant features in the circular dichroism, amounting to ~1.5% at the L_3 edge. Also, CoPc/Ni does not show the circular dichroism signal at the L_2 edge with opposite sign to that at the L_3 edge, as found in the other systems. Thus, the XMCD signal indicates the absence of a dipolar magnetic moment of CoPc on Ni.

In view of the literature[12–15] concerned with CoPc on ferromagnetic substrates and our DFT+U calculations, showing a reduction of the magnetic moment already in CoTPP/Ni (Figs. 3a and 3b), we tentatively explain the observed loss of the magnetic moment in CoPc and the observed reduction in CoOEP/Ni compared to CoTPP/Ni as a result of a strong hybridization of the half-filled d_z^2 orbital with substrate orbitals.

Note that, for CoPc/Au(111) where the absence of a Co XMCD is observed[16], too, this was explained in terms of a coherent superposition a d^7 and d^8 electronic states. This explanation could be considered in the present case as well, however keeping in mind the

decisive differences in the character of the Au and Ni substrates respectively: 6s vs. 3d
bands at the Fermi level and diamagnetism vs. ferromagnetism.

5   Exchange coupling strength in MnPc/Co and NH$_3$-MnPc/Co

The temperature-dependence of the magnetization in MnPc was fitted with the Brillouin
function[17]:

$$B_J(x) = \frac{2J+1}{2J}\coth(\frac{2J+1}{2J}x) - \frac{1}{2J}\coth(\frac{1}{2J}x)$$

In the model, the magnetization in the molecule μ_{mol} depends on the magnetization of the
substrate $\mu_{sub,}$ the absolute temperature T and the exchange energy E_{ex}:

$$\mu_{mol} = \mu_{sub}B_J(\frac{E_{ex}}{k_BT})$$

J is the total angular momentum and k_B the Boltzmann constant. For the fit, J was chosen
in accordance with the DFT+U calculations to be 3/2 for MnPc and 2 for NH$_3$-MnPc. The
exchange energies calculated from the fit vary only slightly with the choice of different
values for J. The approach to extract the exchange energy is discussed in detail in Refs.
[18,9].

The magnetic moment of Co was found to depend only weakly on the temperature
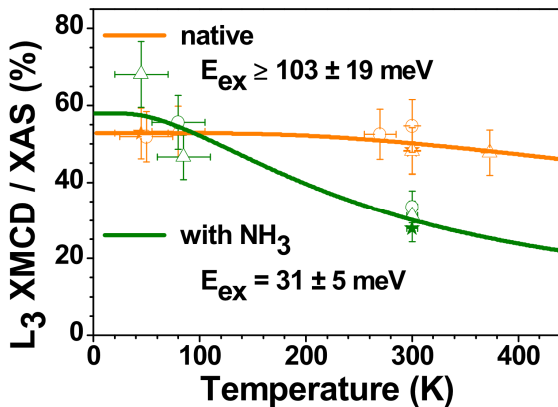$(\sim5\%)$[18], and is therefore assumed to be constant.

Fig. S4 Temperature dependence of the XMCD/XAS ratio of MnPc/Co before and after NH$_3$ exposure. The
symbols (e.g. triangles, etc) mark different experimental runs.

The fit to the temperature dependence (Fig. S4) of MnPc/Co before NH_3 exposure, which yields a value of 103 meV, is to be seen as an estimate of a lower limit since the XMCD/XAS ratio was found to vary only slightly within the measured temperature range. In comparison, for FeOEP/Co, a high exchange energy of 70 meV was found [9].

After exposure to NH_3 with the sample kept at 70 K, and variation of the temperature, a significant temperature dependence of the XMCD/XAS ratio was found. The estimated exchange energy is ~31 meV.

Note, that the herein shown temperature dependence data before and after NH_3 exhibits significant scatter and high error bars mainly due to limitations in the control of the exact temperature, the coverage and the fact that at room temperature NH_3 was found to desorb slowly with a lifetime of a few hours.

The decrease of the exchange energy from $\geq$ 103 meV to 31 meV, is in *qualitative* agreement with the DFT+U calculations which yield values of 189 meV without NH_3 and 4 meV with NH_3.

6 Reversible coordination of NO on FeTPP/Ni and temperature dependence

Our XAS/XMCD experiments on FeTPP/Ni reveal that the coordination of NO onto FeTPP/Ni shows a very good reversibility by annealing to 260°C (Fig. S5).

The spin on Co of CoTPP/Ni is recovered by annealing to 340°C, a significantly higher temperature than for FeTPP/Ni, which opens up the possibility for structural changes on the reactive substrate as indicated by an incomplete (~70%) response to subsequent NO exposure. Notably, we found that NO coordination onto MnTPP/Co was not reversible in the experimental range up to 400°C.

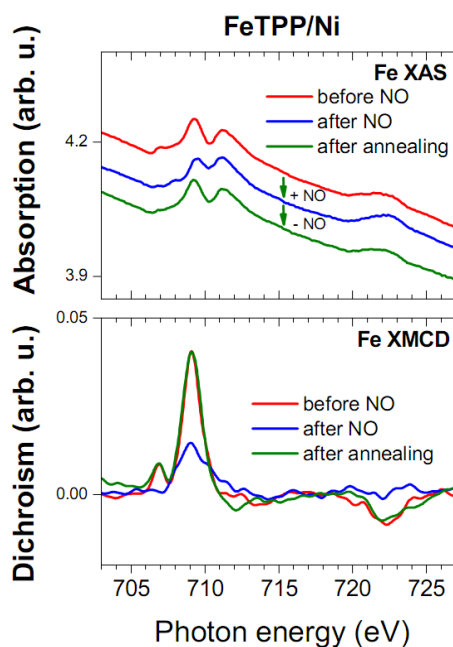**Fig. S5** XAS and XMCD of FeTPP/Ni for the native, NO-dosed and annealed system.
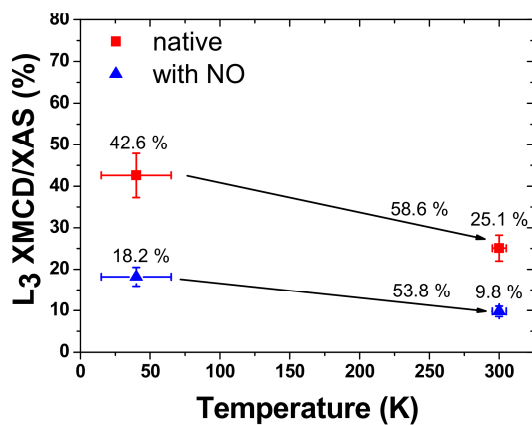

Fig. S6 Temperature dependence of the XMCD/XAS ratio of FeTPP/Ni before and after NO exposure. Compared to ~40K, the XMCD/XAS ratio of the room temperature data is reduced by 58.6 and 53.8 % respectively. This difference is within our error-bars, i.e. we do not observe a significant change of the exchange energy in FeTPP/Ni (+NO).

We have measured the XMCD/XAS ratio (Fig. S6) of FeTPP/Ni and NO-FeTPP/Ni at low temperature and at room temperature. However, the respective data taken at ~40 K and 300 K for FeTPP/Ni (before and after NO coordination) showed only a small difference in the Fe-XAS/XMCD ratio thereby suggesting that the magnetic exchange coupling strength was not significantly affected by the NO coordination. These observations are further confirmed by DFT+U calculations revealing an exchange energy of 114 meV for FeP/Ni and of 110 meV for NO-FeP/Ni.

7   FeP/Ni + NO: physisorption vs. chemisorption

In case of the intermediate-spin system FeTPP (S=1), the axial ligation with NO (S=1/2) is expected to lead to an S=1/2 state of NO-FeTPP if the surface is neglected (Fig. 1d). This is achieved by the unpaired spin of the NO in combination with the high ligand-field strength of NO imposing a low-spin electronic configuration in the nitrosyl complex.
The coordination of NO with FeTPP affecting the spin-state of Fe^{2+} ion is reflected by the Fe-XAS/XMCD spectra presented in Figs. 2c and 2d. Specifically, the vanishing of the Fe-XAS/XMCD shoulder peak at ~707.1 eV and diminishing of the main peak at ~709.2 eV is a signature of NO coordination. Importantly, the coordination of NO to FeTPP was found to be reversible by annealing to 260°C (*c.f.* Fig. S5).

In the DFT+U calculations we have considered both the *physisorbed* and *chemisorbed* FeP/Ni configuration (Fig. S7). In the latter adsorption configuration, the Fe ion distance to the top Ni layer is 2.19 Å and the Fe magnetic moment is 3.57 μ_B, *i.e.* a spin state between S=3/2 and S=2, with tiny magnetic moments existing on the N and C atoms in the molecule. Hence, the molecular spin has increased from S=1 for FeP in the gas phase. Ferromagnetic coupling of the FeP to the Ni is identified.

With NO, the molecule is significantly distorted and the Fe atom is pulled towards the NO leaving a distance of 2.55 Å to the surface. The Fe-NO bond angle is 169.5° and the Fe-NO bond length is 1.76 Å. Surprisingly, the magnetic moment of Fe is reduced only slightly to 3.49 μ_B. This small decrease in the Fe spin found in the DFT+U calculations for *chemisorbed* FeP on Ni is clearly not enough to explain the observed Fe-XMCD data obtained after NO exposure.
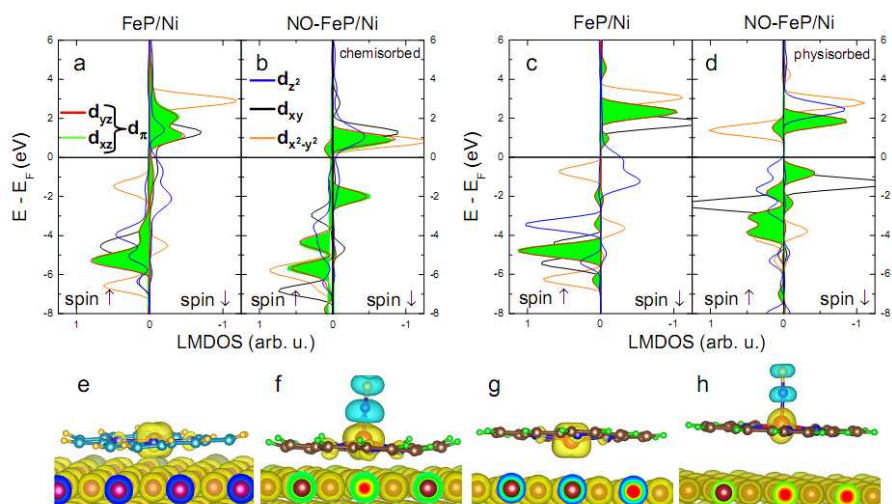
Fig. S7 Results of DFT+U calculations for FeP on Ni before and after NO coordination. Fe 3d orbital LMDOS for FeP/Ni (a) and NO-FeP/Ni (b) chemisorbed, and FeP/Ni (c) and NO-FeP/Ni (d) physisorbed on Co. Spin density isosurfaces for FeP/Ni and NO-FeP/Ni on Co, in chemisorbed (e&f) and physisorbed (g&h) configuration. Light yellow color denotes a spin density parallel to that of the Co substrate, light blue color an antiparallel spin density.

In the case of physisorbed FeP/Ni configuration, where the influence of the surface is weaker, the situation is different: the Fe magnetic moment is strongly reduced from 3.73 μ_B to 1.93 μ_B upon NO coordination (corresponding to a spin state close to S=1/2). Such a change in the molecular spin state is close to the expectations for the gas phase and can be seen as an effect of the strong ligand field of the NO-ligand resulting in an up-shift of the formerly singly occupied $d_{x^2-y^2}$ state which is almost completely unoccupied after NO coordination and a down-shift and occupation of the formerly singly occupied d_{xy} orbital. With NO, the distance from the surface is increased from 3.11 Å to 3.69 Å and Fe-NO bond length is 1.76 Å. Thus on the basis of our presented data, we prefer to assign the FeTPP/Ni system to be in rather physisorbed than chemisorbed configuration since the observed change in the XMCD in combination with the temperature dependence XAS/XMCD intensity ratio is consistent only with physisorption.

The calculated values are in good agreement with X-ray diffraction data on bulk NO-FeTPP, where a Fe-N-O angle of 149° and a Fe-N(NO) bond length of 1.72 Å is reported[19]. In this case, the NO-induced displacement of the Fe ion is 0.21 Å. This is clearly higher then in case of the NO-Co porphyrin bond.

In case of FeTPP/Ni, we find that the interaction with the substrate leads to an increase of the spin. Furthermore, we find that in contrast to CoTPP/Ni, NO exerts a significant

structural trans-effect. Not surprisingly, the coordination of NO (one unpaired electron) with d^6-Fe(II) (even number of electrons) does not result in a loss of the spin as for d^7-Co(II) (odd-number of electrons).

References

1. D. Chylarecka, C. Wäckerlin, T. K. Kim, K. Müller, F. Nolting, A. Kleibert, N. Ballav, and T. A. Jung, *J. Phys. Chem. Lett.*, 2010, **1**, 1408–1413.
2. C. Wäckerlin, D. Chylarecka, A. Kleibert, K. Müller, C. Iacovita, F. Nolting, T. A. Jung, and N. Ballav, *Nat. Commun.*, 2010, **1**, 61.
3. H. Wende, M. Bernien, J. Luo, C. Sorg, N. Ponpandian, J. Kurde, J. Miguel, M. Piantek, X. Xu, P. Eckhold, W. Kuch, K. Baberschke, P. M. Panchmatia, B. Sanyal, P. M. Oppeneer, and O. Eriksson, *Nat. Mater.*, 2007, **6**, 516–520.
4. P. Fesser, C. Iacovita, C. Wäckerlin, S. Vijayaraghavan, N. Ballav, K. Howes, J. Gisselbrecht, M. Crobu, C. Boudon, M. Stöhr, T. A. Jung, and F. Diederich, *Chem. Eur. J.*, 2011, **17**, 5246–5250.
5. U. Flechsig, F. Nolting, A. Fraile Rodríguez, J. Krempaský, C. Quitmann, T. Schmidt, S. Spielmann, D. Zimoch, R. Garrett, I. Gentle, K. Nugent, and S. Wilkins, *AIP Conf. Proc.*, 2010, **1234**, 319–322.
6. G. Kresse and J. Furthmüller, *Phys. Rev. B*, 1996, **54**, 11169–11186.
7. J. P. Perdew and Y. Wang, *Phys. Rev. B*, 1992, **45**, 13244–13249.
8. M. E. Ali, B. Sanyal, and P. M. Oppeneer, *J. Phys. Chem. C*, 2009, **113**, 14381–14383.
9. M. Bernien, J. Miguel, C. Weis, M. E. Ali, J. Kurde, B. Krumme, P. M. Panchmatia, B. Sanyal, M. Piantek, P. Srivastava, K. Baberschke, P. M. Oppeneer, O. Eriksson, W. Kuch, and H. Wende, *Phys. Rev. Lett.*, 2009, **102**, 047202.
10. P. M. Oppeneer, P. M. Panchmatia, B. Sanyal, O. Eriksson, and M. E. Ali, *Prog. Surf. Sci.*, 2009, **84**, 18–29.
11. A. Mugarza, R. Robles, C. Krull, R. Korytár, N. Lorente, and P. Gambardella, *Phys. Rev. B*, 2012, **85**.
12. C. Iacovita, M. Rastei, B. Heinrich, T. Brumme, J. Kortus, L. Limot, and J. Bucher, *Phys. Rev. Lett.*, 2008, **101**, 116602.
13. J. Brede, N. Atodiresei, S. Kuck, P. Lazić, V. Caciuc, Y. Morikawa, G. Hoffmann, S. Blügel, and R. Wiesendanger, *Phys. Rev. Lett.*, 2010, **105**, 047204.
14. E. Annese, J. Fujii, I. Vobornik, G. Panaccione, and G. Rossi, *Phys. Rev. B*, 2011, **84**, 174443.
15. S. Lach, A. Altenhof, K. Tarafder, F. Schmitt, M. E. Ali, M. Vogel, J. Sauther, P. M. Oppeneer, and C. Ziegler, *Adv. Funct. Mater.*, 2012, **22**, 989–997.
16. S. Stepanow, P. Miedema, A. Mugarza, G. Ceballos, P. Moras, J. Cezar, C. Carbone, F. de Groot, and P. Gambardella, *Phys. Rev. B*, 2011, **83**, 220401.
17. C. Kittel, *Introduction to solid state physics*, Wiley, New York, 7th ed., 1996.
18. M. Bernien, PhD Dissertation, Freie Universität Berlin, 2009.
19. W. R. Scheidt and M. E. Frisse, *J. Am. Chem. Soc.*, 1975, **97**, 17–21.

2.3 Two-Dimensional Supramolecular Electron Spin Arrays

Summary: In this study we show the formation of a nanoscale array of Fe and Mn spin-systems arranged in an alternating, chessboard-like fashion. The nanoscale array is produced by mere co-evaporation of the molecular building-blocks. The work is based on a number of important concepts: i) the molecular self-assembly of planar molecules based on C–F$\cdots$H–C hydrogen-bonds [59, 60], ii) the previous observation from our group that porphyrins/phthalocyanines self-assemble only on oxygen-reconstructed Co or Ni and not on native (clean) substrates [21] and iii) the magnetochemical spin-switching effect by axial ligation with a suitable chemical agent. In this work, we use Fe(II)-perfluoro-phthalocyanine (synthesized in the group of S. Decurtins) and Mn(II)-phthalocyanine as molecular building blocks, an oxygen-reconstructed Co thin film as the ferromagnetic substrate and NH_3 as the axial ligand. Remarkably, the mechanism responsible for Fe(II)-perfluoro-phthalocyanine's spin off-switch is analogous to the mechanism in the spin on-switch, i.e. the interaction with the lone-pair of NH_3 increases the energy of the d_{z^2} orbital.[[4]] However, in case of intermediate-spin Fe-perfluoro-phthalocyanine the d_{z^2} orbital is initially singly occupied. Rising the d_{z^2} energy level results in a situation where the low-spin (S = 0) state is preferred. In case of Mn(III)-phthalocyanine (as identified by XAS), NH_3-coordination could not quench the spin-state.

Paper [[3]] is published in Advanced Materials

COMMUNICATION

Two-Dimensional Supramolecular Electron Spin Arrays

Christian Wäckerlin,* Jan Nowakowski, Shi-Xia Liu,* Michael Jaggi, Dorota Siewert, Jan Girovsky, Aneliia Shchyrba, Tatjana Hählen, Armin Kleibert, Peter M. Oppeneer, Frithjof Nolting, Silvio Decurtins, Thomas A. Jung,* and Nirmalya Ballav*

In the pursuit of future spintronic applications, investigations of addressable atomic and molecular arrangements of spin systems on surfaces have received increasing attention in recent years.[1–3] Common to this work is that spin-bearing ad-surface atoms are probed individually by scanning tunneling microscopy/spectroscopy (STM/STS) and that they are arranged by atomic repositioning techniques. This piece by piece assembly technique is very time-consuming and therefore impractical for technological applications. Further, the limited resolution of lithography does not yet allow for the production of spin-systems with atomic precision. In the present work, we demonstrate that spontaneous molecular self-assembly[4,5] is able to provide an interesting alternative. A well-defined supramolecular spin-array on a ferromagnetic substrate is obtained by the self-assembly of appropriately functionalized square-planar molecular building-blocks.[6–16] In these unique bi-molecular arrays the electron spin state can be reversibly controlled by a chemical stimulus[17,18] acting specifically on one of the two metal centers. Our approach involves a combination of supramolecular chemistry for *engineering* the spin arrays and coordination chemistry for *manipulating* them. A selective magnetic control over specific sublattices in large area spin arrays has therefore been achieved.

The on-surface self-assembly of spin-bearing molecules is obtained by decorating the substrate with oxygen atoms[11] and by supramolecular arrangement of the molecular building blocks which is directed by functional groups. The incorporation of fluorine-substituents into the Fe-phthalocyanine enables the formation of intermolecular C–F···H hydrogen-bonds with the Mn-phthalocyanine.[19,20] The such generated bi-molecular chessboard pattern is thermodynamically the most stable arrangement as the number of hydrogen-bond interactions is maximized (**Figure 1**). Specifically, we use a perfluorinated iron(II) phthalocyanine ($FeF_{16}Pc$)[21] and a manganese(II) phthalocyanine (MnPc) as the molecular building blocks. Thereby a 2D *spin array* of alternating Fe–Mn–Fe spins (Fe–Mn pitch: ~1.65 nm) is produced by mere co-evaporation of the molecules. Here, we have assembled the molecules on a c(2×2) oxygen-reconstructed Co(001) surface,[11] but we show that the chessboard-like assembly also takes place on other surfaces, e.g. on Ag(111) (Supporting Information). Note that, in absence of fluorine-functionalization, the molecules occupy random sites in the self-assembled layer (Supporting Information).

The electronic configuration and the corresponding magnetization of the transition metal centers in the $FeF_{16}Pc$ and MnPc molecular building blocks and in the Co substrate are probed by X-ray absorption (XA) spectroscopy (XAS) and X-ray magnetic circular dichroism (XMCD).[22] XMCD, the difference between XA spectra obtained with circular plus and minus (circ+/circ-) polarized X-rays, provides a measure of the magnetization for each element. The dichroism measured at the $L_{3,2}$ absorption edges allows for the element-specific detection of the magnetic moments in the Fe and Mn ions of the supramolecular array and in the Co atoms of the substrate (Figure 1). The presence of a negative XMCD signal (the direction of the substrate XMCD signal is defined as positive) at the L_3 edge denotes an antiferromagnetic (AFM) spin alignment of the Fe and Mn ions in the molecules with respect to the oxygen-reconstructed substrate.[23,11] We call the initial state of the supramolecular spin array, in which both Fe- and Mn-lattices bear an AFM-coupled spin, the spin ON/ON state (**Figure 2**a,e). The oxidation states can be identified from the XA spectra. Specifically, the Mn L_3 XA peak-shape and position (maximum at ~641.7 eV) of MnPc on the oxygen-reconstructed cobalt surface identify it as Mn(III) Pc, in contrast to the molecule in bulk.[24] In the case of $FeF_{16}Pc$, the L_3 XA peak-shape and position (maxima at ~710.0 eV) can be assigned to $Fe(II)F_{16}Pc$.[25]

C. Wäckerlin, J. Nowakowski, Dr. D. Siewert,
J. Girovsky, T. Hählen, Prof. T. A. Jung
Laboratory for Micro and Nanotechnology
Paul Scherrer Institute
5232 Villigen-PSI, Switzerland
E-mail: christian@waeckerlin.com;
thomas.jung@psi.ch
Dr. S.-X. Liu, M. Jaggi, Prof. S. Decurtins
Department of Chemistry and Biochemistry
University of Berne
Freiestrasse 3, 3012 Bern, Switzerland
E-mail: liu@iac.unibe.ch
A. Shchyrba
Department of Physics
University of Basel
4056 Basel, Switzerland
Dr. A. Kleibert, Prof. F. Nolting
Swiss Light Source
Paul Scherrer Institute
5232 Villigen-PSI, Switzerland
Prof. P. M. Oppeneer
Department of Physics and Astronomy
University of Uppsala
Box 516, S-751 20 Uppsala, Sweden
Prof. N. Ballav
Department of Chemistry
Indian Institute of Science Education and Research
Pune 411008, India
E-mail: nballav@iiserpune.ac.in
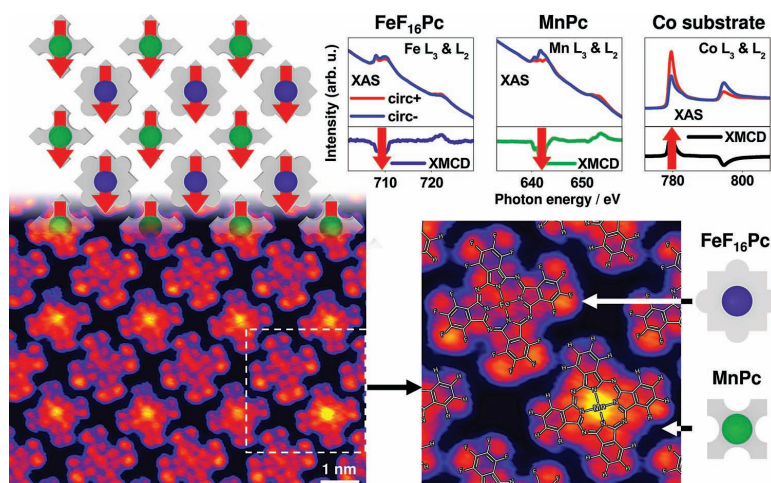
DOI: 10.1002/adma.201204274

COMMUNICATION

Figure 1. Bottom-up assembly of the supramolecular spin array. Chemical structures of FeF$_{16}$Pc and MnPc are superimposed on the scanning tunneling microscopy (STM) image which directly visualizes the supramolecular chessboard-like 2D lattice and the intramolecular electronic structure. Thus, the resulting molecular array consists of two superimposed spin-bearing lattices: Fe (dark-blue spheres in jigsaw pieces) and Mn (green spheres in jigsaw pieces). X-ray absorption spectroscopy (XAS) and X-ray magnetic circular dichroism (XMCD) on the respective L$_{3,2}$ edges indentify the antiparallel orientation of the Fe or Mn magnetic moments in the self-assembled 2D array with respect to the magnetization of the oxygen-covered ferromagnetic Co substrate. This antiparallel alignment stems from the super-exchange interaction via the oxygen-reconstruction. The data shown here are obtained at 70 K, but the spin-alignment as well as the supramolecular arrangement is strong enough to be observed up to room temperature.

We selectively control the electron spin states in the self-assembled array by the metal center's specific response to a chemical stimulus.[17,18] This approach is inspired by the biochemical oxygen transport and storage through O$_2$ coordination to the metal-organic heme group. The coordination and desorption of NH$_3$, the chemical stimulus chosen in this study, switch the spin states of the self-assembled supramolecular array (Figure 2). The axial NH$_3$-ligation is imposed by dosage of 100 Langmuir while the sample has been kept at ~70 K. The electronic structures of *both* the Fe and Mn are consequently modified, as reflected in the characteristically different peak shapes observed in both XA spectra (Figure 2b,f). The coordination with NH$_3$ via its lone-pair results in an increased energy of the $3d_{z^2}$ orbital, consequently yielding a low-spin (S = 0) configuration in NH$_3$-ligated Fe(II)F$_{16}$Pc which corresponds to a vanished Fe-XMCD signal as seen in Figure 2b. Note that NH$_3$-ligation is distinctly different from the axial coordination with nitric oxide (NO, S = 1/2) where the observed annihilation of the spin has been attributed to the unpaired electron in the NO ligand.[26] In the case of NH$_3$-ligated Mn(III)Pc, the coordination *does not* quench the spin (Figure 2f) but merely modifies it, as evidenced by the modified XMCD peak-shape, cf. ref. [16] Since the Fe spin is quenched, whereas the Mn spin remains in a modified spin ON' state, this results in a spin OFF/ON' state of the supramolecular chessboard. The relatively weak binding between NH$_3$ and the ad-complexes allows desorption of the NH$_3$ ligand and restoration of the original spin ON state by annealing to 300 K (Figure 2c,g). Repeated exposure to NH$_3$ leads to the spin OFF/ON' state of the supramolecular

spin array, demonstrating reversibility of the switching process (Figure 2d,h). Importantly, the substrate is not affected by the adsorption/desorption cycles (Figure 2i–l).

Besides the selective spin switching we observe characteristic, site-specific differences in the ammonia bonding by direct STM experiments. The native spin array (**Figure 3**a,b) appears with distinct imaging contrast at a sample bias-voltage of +1.9 V. Under these conditions, the FeF$_{16}$Pc macrocycle appears larger than the MnPc macrocycle and an eight-lobed feature is observed. The feature corresponds well to the macrocycle's lowest unoccupied molecular orbital as also depicted in Figure 1. Upon exposure to NH$_3$ at a sample temperature of 78 K, we observe the ligands on both FeF$_{16}$Pc and MnPc molecules at a bias voltage of +0.4 V (Supporting Information). After increasing the sample temperature to ~130 K, the NH$_3$ ligands are only found on the MnPc molecules, where they are seen as shaky, streak-like features which appear and disappear between individual scan lines (Figure 3c). Note that at both temperatures a low current set-point is important to minimize the interaction with the STM tip and to avoid NH$_3$ desorption. These data directly reveal a higher affinity of NH$_3$ to Mn(III)Pc over Fe(II)F$_{16}$Pc. This selectivity constitutes an additional parameter to control the spin in the self-assembled bi-molecular array. We may note here, that the formation constants of NH$_3$ complexes with metal ions are not yet well known, since aqueous phase coordination chemistry of NH$_3$ is limited as most metal ions do not form stable ammonia complexes, but react with hydroxide. Nevertheless, the estimation of the formation constants of NH$_3$ complexes for a large selection of metal ions also demonstrates
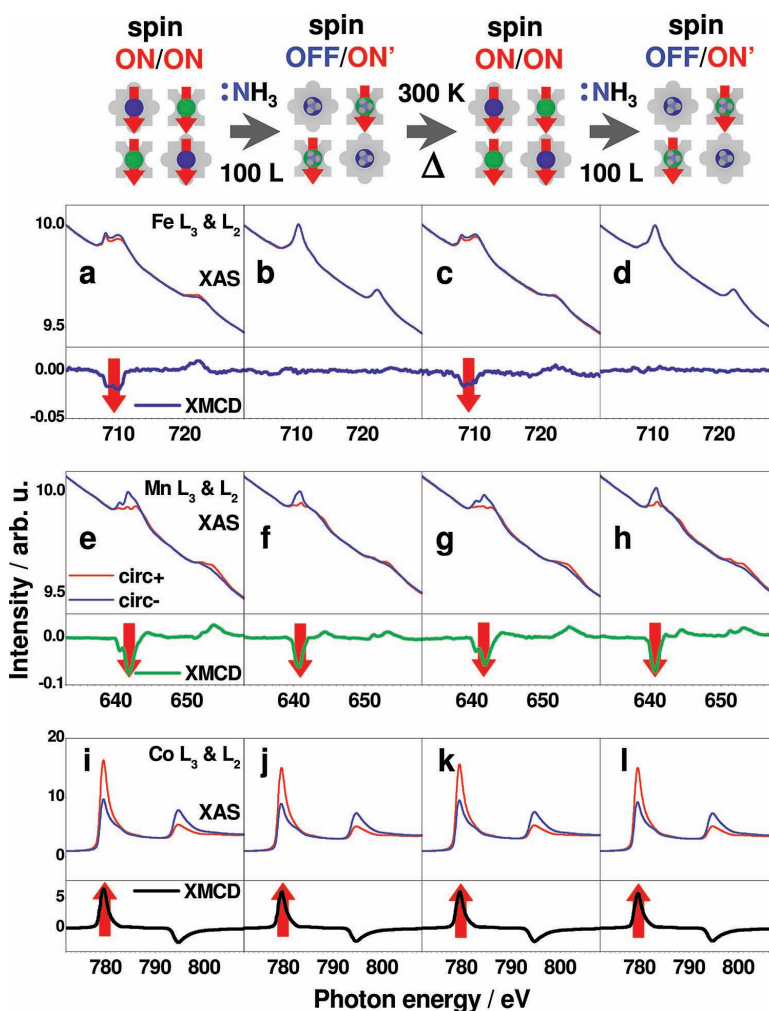
COMMUNICATION

Figure 2. Reversible and selective manipulation of the electron spin states in the Fe and Mn lattices on the oxygen covered Co substrates. X-ray absorption spectroscopy (XAS) and X-ray magnetic circular dichroism (XMCD) of the Fe (a-d), Mn (e-h) and Co (i-l) $L_{3,2}$ edges of the respective Fe(II)F_{16}Pc (with dark-blue centers) and Mn(III)Pc (with green centers) molecules and the oxygen-reconstructed Co substrate. The complex electronic structure of the transition metal ions is reflected in the XAS (red and blue for circ+ and circ- X-rays respectively). XMCD is a measure for the magnetic moment induced by the ferromagnetic substrate. The spins in the bi-molecular array (a,e) are controlled by consecutive ammonia (NH$_3$)-ligation to both complexes (b,f), thermal NH$_3$ desorption (c,g) and subsequent NH$_3$-ligation (d,h). As a result, the spin of FeF$_{16}$Pc is selectively switched between the spin ON and OFF states (a-d), while the electronic structure of MnPc is modified but the molecules remain spin ON respective spin ON' (a slightly modified state with close to identical magnetization after forming the NH$_3$-complex) during the whole process (e-h). The magnetic moment in the substrate remains unchanged during the cycles (i-l).

a considerably higher affinity for Mn(III) over Fe(II) ions.[27,28] In vacuum, the coordination of NH$_3$ with FePc[29] is consistent with our observations.

The interaction with the oxygen-reconstructed substrate results in the formation of two mirror-domains of the self-assembled 2D lattices.[11] These mirror domains of self-assembled

molecules differ not only in their orientation with respect to the substrate but also in the relative orientation of the molecular building blocks. The FeF$_{16}$Pc and MnPc molecules are found to be rotated by +/− 14° with respect to the <110> directions of the substrate, leading to organizational chirality.[30] (Figure 3 and Supporting Information). Thereby a 2D magnetic lattice
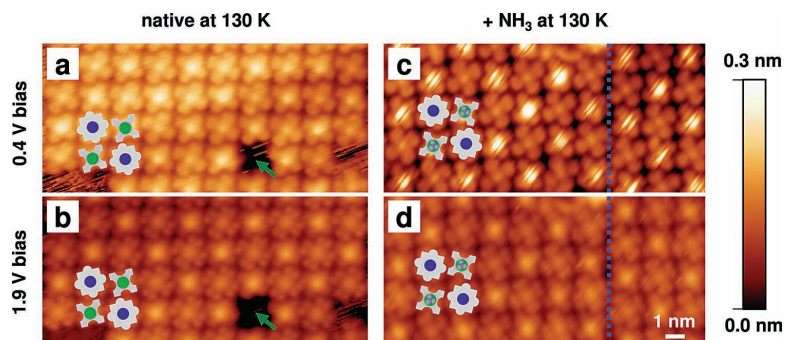
Figure 3. Direct observation of the coordinated NH₃ ligands by STM. The bi-molecular lattice is imaged at different bias voltages before (native, a,b) and after NH₃ exposure (c,d). The FeF₁₆Pc and MnPc molecules are represented by jigsaw pieces with dark-blue and green centers, respectively. The coordinating NH₃ can be observed at ∼0.4 V bias voltage as elevated streaks (c). At ∼130 K, NH₃ is only observed on the MnPc molecules. The green arrows and the blue dotted lines denote a vacancy defect where one molecule is missing (a,b) and a phase-shift domain boundary in the supramolecular lattice (c,d), respectively.

without an inversion symmetry is obtained, as currently discussed in the context of magneto-chiral effects.[31]

The combination of on-surface *supramolecular chemistry* with *coordination chemistry* provides a facile and unique approach to manufacture extended supramolecular arrays with switchable spin states. This methodology works irrespective of the lateral extent of the 2D spin array. The observation of Mn(III)Pc as the on-surface species, also demonstrates that it is important to further explore the influence of the surface *trans* effect on the electronic[32] as well as on the spin states[16,17] of coordination complexes. Together with the ability to chemically turn OFF the spin states of one species in the supramolecular array leading to spin ON/ON and OFF/ON' states, the present approach opens the possibility to gain selective magnetic control over large area spin arrays.

The spin array can be fabricated on other, non-magnetic, superconducting[33] or antiferromagnetic[34] substrates since self-assembly is governed by intermolecular interactions between the molecular building-blocks.[19,20] Particularly interesting for future spintronic applications might be antiferromagnetic substrates since they promise to obtain exchange-coupled spin arrays at room temperature, which can be manipulated with external fields independent of the substrate.[35]

Experimental Section

Sample preparation and STM experiments: Cu(001) single crystals were cleaned by cycles of sputtering with Ar⁺ ions and annealing. The preparation of the oxygen-reconstructed Co thin films has been described previously.[11] MnPc (Sigma-Aldrich, Switzerland) and FeF₁₆Pc (synthesized according to ref. [21]) were co-evaporated on the substrate at room temperature. To obtain a ∼50:50 molar ratio of two building blocks, the deposition rates were controlled independently for both molecules. The cleanliness, the Co film thickness, the oxygen induced surface reconstruction, the molecular coverage and the stoichiometry of the surface layers were checked by XPS and STM. The STM experiments were performed using electrochemically etched W tips and cut Pt-Ir tips which were treated in situ by sputtering. Positive bias voltages result in tunneling from the tip into unoccupied states of the samples. The

tunneling parameters used in the STM experiments are summarized in the Supporting Information.

XAS/XMCD measurements and NH₃ dosage: XAS/XMCD measurements were carried out at the Surfaces/Interfaces Microscopy (SIM) beamline of the Swiss Light Source, Paul Scherrer Institute, Switzerland.[36] A portable vacuum chamber with a base pressure in the order of ∼10⁻¹⁰ mbar, as established in previous experiments by our group,[11,13,16,17] has been used for sample transfer without breaking the vacuum. NH₃ (99.98%, water-free, Air Liquide, Germany) was introduced with the sample kept at ∼70 K for XMCD (100 Langmuir) and at 130 K (100 Langmuir) or 78 K (20 Langmuir) for STM. NH₃ was desorbed by annealing to 300 K. The gas-line was cleaned by repeated filling/pumping cycles. The gas-line was pumped by an oil-free pump, the obtained base-pressure of the line was <10⁻¹ mbar, i.e., less than 10⁻⁴ of the NH₃ pressure in the line (∼1 bar).

Supporting Information

Supporting Information is available from the Wiley Online Library or from the author.

COMMUNICATION

[1] A. Yazdani, B. A. Jones, C. P. Lutz, M. F. Crommie, D. M. Eigler, *Science* **1997**, *275*, 1767.

[2] S. Loth, M. Etzkorn, C. P. Lutz, D. M. Eigler, A. J. Heinrich, *Science* **2010**, *329*, 1628.

[3] A. A. Khajetoorians, J. Wiebe, B. Chilian, R. Wiesendanger, *Science* **2011**, *332*, 1062.

[4] G. Whitesides, J. Mathias, C. Seto, *Science* **1991**, *254*, 1312.

[5] S. De Feyter, F. C. De Schryver, *Chem. Soc. Rev.* **2003**, *32*, 139.

[6] A. Scheybal, T. Ramsvik, R. Bertschinger, M. Putero, F. Nolting, T. A. Jung, *Chem. Phys. Lett.* **2005**, *411*, 214.

[7] H. Wende, M. Bernien, J. Luo, C. Sorg, N. Ponpandian, J. Kurde, J. Miguel, M. Piantek, X. Xu, P. Eckhold, W. Kuch, K. Baberschke, P. M. Panchmatia, B. Sanyal, P. M. Oppeneer, O. Eriksson, *Nat. Mater.* **2007**, *6*, 516.

[8] M. Bernien, J. Miguel, C. Weis, M. E. Ali, J. Kurde, B. Krumme, P. M. Panchmatia, B. Sanyal, M. Piantek, P. Srivastava, K. Baberschke, P. M. Oppeneer, O. Eriksson, W. Kuch, H. Wende, *Phys. Rev. Lett.* **2009**, *102*, 047202.

[9] C. Iacovita, M. Rastei, B. Heinrich, T. Brumme, J. Kortus, L. Limot, J. Bucher, *Phys. Rev. Lett.* **2008**, *101*, 116602.

[10] J. Brede, N. Atodiresei, S. Kuck, P. Lazi , V. Caciuc, Y. Morikawa, G. Hoffmann, S. Blügel, R. Wiesendanger, *Phys. Rev. Lett.* **2010**, *105*, 047204.

[11] D. Chylarecka, C. Wäckerlin, T. K. Kim, K. Müller, F. Nolting, A. Kleibert, N. Ballav, T. A. Jung, *J. Phys. Chem. Lett.* **2010**, *1*, 1408.

[12] S. Javaid, M. Bowen, S. Boukari, L. Joly, J.-B. Beaufrand, X. Chen, Y. Dappe, F. Scheurer, J.-P. Kappler, J. Arabski, W. Wulfhekel, M. Alouani, E. Beaurepaire, *Phys. Rev. Lett.* **2010**, *105*, 077201.

[13] D. Chylarecka, T. K. Kim, K. Tarafder, K. Müller, K. Gödel, I. Czekaj, C. Wäckerlin, M. Cinchetti, M. E. Ali, C. Piamonteze, F. Schmitt, J.-P. Wüstenberg, C. Ziegler, F. Nolting, M. Aeschlimann, P. M. Oppeneer, N. Ballav, T. A. Jung, *J. Phys. Chem. C* **2011**, *115*, 1295.

[14] E. Annese, J. Fujii, I. Vobornik, G. Panaccione, G. Rossi, *Phys. Rev. B* **2011**, *84*, 174443.

[15] S. Lach, A. Altenhof, K. Tarafder, F. Schmitt, M. E. Ali, M. Vogel, J. Sauther, P. M. Oppeneer, C. Ziegler, *Adv. Funct. Mater.* **2012**, *22*, 989.

[16] C. Wäckerlin, K. Tarafder, D. Siewert, J. Girovsky, T. Hählen, C. Iacovita, A. Kleibert, F. Nolting, T. A. Jung, P. M. Oppeneer, N. Ballav, *Chem. Sci.* **2012**, *3*, 3154.

[17] C. Wäckerlin, D. Chylarecka, A. Kleibert, K. Müller, C. Iacovita, F. Nolting, T. A. Jung, N. Ballav, *Nat. Commun.* **2010**, *1*, 61.

[18] J. Miguel, C. F. Hermanns, M. Bernien, A. Krüger, W. Kuch, *J. Phys. Chem. Lett.* **2011**, *2*, 1455.

[19] K. W. Hipps, L. Scudiero, D. E. Barlow, M. P. Cooke, *J. Am. Chem. Soc.* **2002**, *124*, 2126.

[20] L. Scudiero, K. W. Hipps, D. E. Barlow, *J. Phys. Chem. B* **2003**, *107*, 2903–2909.

[21] J. G. Jones, M. V. Twigg, *Inorg. Chem.* **1969**, *8*, 2018.

[22] J. Stöhr, H. C. Siegmann, *Magnetism: From Fundamentals to Nanoscale Dynamics*, Springer Berlin, **2006**.

[23] M. Bernien, X. Xu, J. Miguel, M. Piantek, P. Eckhold, J. Luo, J. Kurde, W. Kuch, K. Baberschke, H. Wende, P. Srivastava, *Phys. Rev. B* **2007**, *76*, 214406.

[24] T. Kataoka, Y. Sakamoto, Y. Yamazaki, V. R. Singh, A. Fujimori, Y. Takeda, T. Ohkochi, S.-I. Fujimori, T. Okane, Y. Saitoh, H. Yamagami, A. Tanaka, *Solid State Commun.* **2012**, *152*, 806.

[25] S. Stepanow, P. Miedema, A. Mugarza, G. Ceballos, P. Moras, J. Cezar, C. Carbone, F. de Groot, P. Gambardella, *Phys. Rev. B* **2011**, *83*, 220401.

[26] J. H. Enemark, R. D. Feltham, *Coord. Chem. Rev.* **1974**, *13*, 339.

[27] F. Mulla, F. Marsicano, B. S. Nakani, R. D. Hancock, *Inorg. Chem.* **1985**, *24*, 3076.

[28] A. E. Martell, R. M. Smith, *Critical stability constants*, Plenum Press, New York, **1974**.

[29] C. Isvoranu, B. Wang, K. Schulte, E. Ataman, J. Knudsen, J. N. Andersen, M. L. Bocquet, J. Schnadt, *J. Phys.: Condens. Matter* **2010**, *22*, 472002.

[30] C. Bombis, S. Weigelt, M. M. Knudsen, M. Nørgaard, C. Busse, E. Lægsgaard, F. Besenbacher, K. V. Gothelf, T. R. Linderoth, *ACS Nano* **2010**, *4*, 297.

[31] C. Train, R. Gheorghe, V. Krstic, L.-M. Chamoreau, N. S. Ovanesyan, G. L. J. A. Rikken, M. Gruselle, M. Verdaguer, *Nat. Mater.* **2008**, *7*, 729.

[32] W. Hieringer, K. Flechtner, A. Kretschmann, K. Seufert, W. Auwärter, J. V. Barth, A. Görling, H.-P. Steinrück, J. M. Gottfried, *J. Am. Chem. Soc.* **2011**, *133*, 6206.

[33] K. J. Franke, G. Schulze, J. I. Pascual, *Science* **2011**, *332*, 940.

[34] F. Nolting, A. Scholl, J. Stöhr, J. W. Seo, J. Fompeyrine, H. Siegwart, J.-P. Locquet, S. Anders, J. Lüning, E. E. Fullerton, M. F. Toney, M. R. Scheinfein, H. A. Padmore, *Nature* **2000**, *405*, 767.

[35] A. Lodi Rizzini, C. Krull, T. Balashov, A. Mugarza, C. Nistor, F. Yakhou, V. Sessi, S. Klyatskaya, M. Ruben, S. Stepanow, P. Gambardella, *Nano Lett.* **2012**, *12*, 5703.

[36] U. Flechsig, F. Nolting, A. Fraile Rodríguez, J. Krempaský, C. Quitmann, T. Schmidt, S. Spielmann, D. Zimoch, R. Garrett, I. Gentle, K. Nugent, S. Wilkins, *AIP Conf. Proc.* **2010**, *1234*, 319.

Submitted to **ADVANCED MATERIALS**

Supporting Information

Two-dimensional supramolecular electron spin arrays

By Christian Wäckerlin,[1*] Jan Nowakowski,[1] Shi-Xia Liu,[2*] Michael Jaggi,[2] Dorota Siewert,[1] Jan Girovsky,[1] Aneliia Shchyrba,[3] Tatjana Hählen,[1] Armin Kleibert,[4] Peter M. Oppeneer,[5] Frithjof Nolting,[4] Silvio Decurtins,[2] Thomas A. Jung,[1*] and Nirmalya Ballav[6*]

[1]Laboratory for Micro and Nanotechnology, Paul Scherrer Institute, 5232 Villigen-PSI (Switzerland)
[2]Department of Chemistry and Biochemistry, University of Berne, Freiestrasse 3, 3012 Bern (Switzerland)
[3]Department of Physics, University of Basel, 4056 Basel (Switzerland)
[4]Swiss Light Source, Paul Scherrer Institute, 5232 Villigen-PSI (Switzerland)
[5]Department of Physics and Astronomy, University of Uppsala, Box 516, S-751 20 Uppsala (Sweden)
[6]Department of Chemistry, Indian Institute of Science Education and Research, Pune 411008 (India)

[*]**To whom correspondence should be addressed:**
E-mail: christian@waeckerlin.com
E-mail: thomas.jung@psi.ch
E-mail: liu@iac.unibe.ch
E-mail: nballav@iiserpune.ac.in

Figure S1: Formation of the bimolecular array on Ag(111)

The sublimation of the molecular $FeF_{16}Pc$ and MnPc building-blocks onto a structurally different substrate (noble metal, no oxygen-reconstruction, hexagonal symmetry) demonstrates that the formation of the bimolecular Fe—Mn—Fe spin array is dominated more by the intermolecular interactions than by interactions with the substrate (Figure S1). Obviously, interactions with the substrate have to be weak enough to allow for self-assembly. A Moiré-pattern in the bimolecular layer is observed on the Ag(111) substrate.[1]
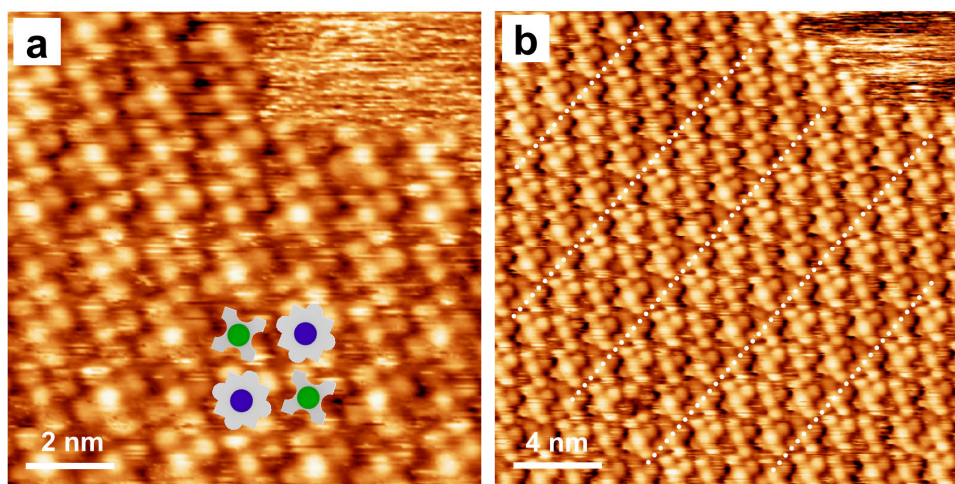

Figure S1. STM of a self-assembled bimolecular layer obtained by co-evaporation of $FeF_{16}Pc$ and MnPc on Ag(111). The slightly smaller MnPc and the slightly bigger $FeF_{16}Pc$ building-blocks are clearly visible in the zoom-in (a). In the larger-scale image (b) the apparent height of the building-blocks is observed to vary slightly (signified by dotted lines). This indicates the presence of a Moiré-pattern, i.e. a superstructure based on the mismatch of the respective lattices of the Ag(111) substrate and the bimolecular lattice.

Figure S2: STM data of non-functionalized building blocks

As a reference, we have co-evaporated FePc (without fluorine-functionalization) with MnPc onto oxygen-reconstructed Co. The STM image (Figure 2) shows the occurrence of self-assembled layers as observed for similar complexes.[2] However, the molecular Fe and Mn building-blocks occupy random places within the 2D lattice, i.e. they form a 2D solid solution. The molecular building blocks are not readily distinguishable as in the case of $FeF_{16}Pc$ and MnPc, but they differ slightly in their apparent brightness.
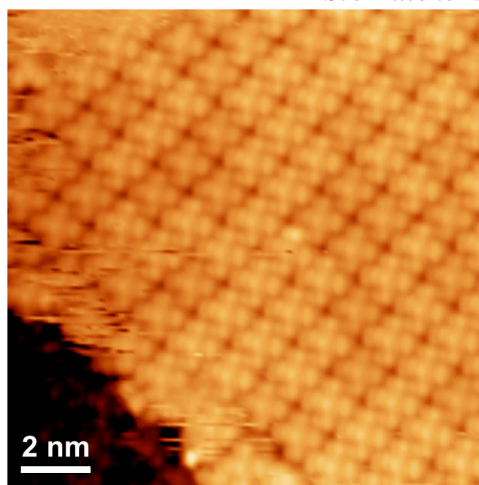
Figure S2. STM of a self-assembled layer obtained by co-evaporation of FePc with MnPc onto oxygen-reconstructed Co, i.e. when using the non-functionalized Fe building-block. Both the FePc and MnPc appear in STM very similar and do not allow for straightforward identification of the Fe and Mn centers, but they have a slight difference in the image-contrast. A self-assembled 2D layer is observed, however the position of the Fe and Mn ions within the layer is random, i.e. the system represents a 2D solid-solution.

Figure S3: Bias-dependent STM data

We have studied the imaging contrast obtained on the bimolecular layer as a function of the bias voltage (Figure S3). At high positive bias voltages (+1.3 to +1.9 V) the $F_{16}Pc$ and Pc macrocycles are well resolved with intramolecular contrast. This contrast can be associated with tunneling into the respective (partially) unoccupied states.[3] A distinctively different contrast is observed at +0.4 V. In case of tunneling into the singly/fully occupied states at negative bias voltages, no pronounced intramolecular contrast is observed; however, a large difference in the apparent height on the metal-centers is found.[4,5]

The oxygen-reconstruction on the Co thin film is expected to result in a significant electronic decoupling of the electronic states in the molecular adsorbate from the substrate's electronic states, thus allows a good intramolecular contrast, cf. the case of Pentacene/NaCl/Cu(111).[6]
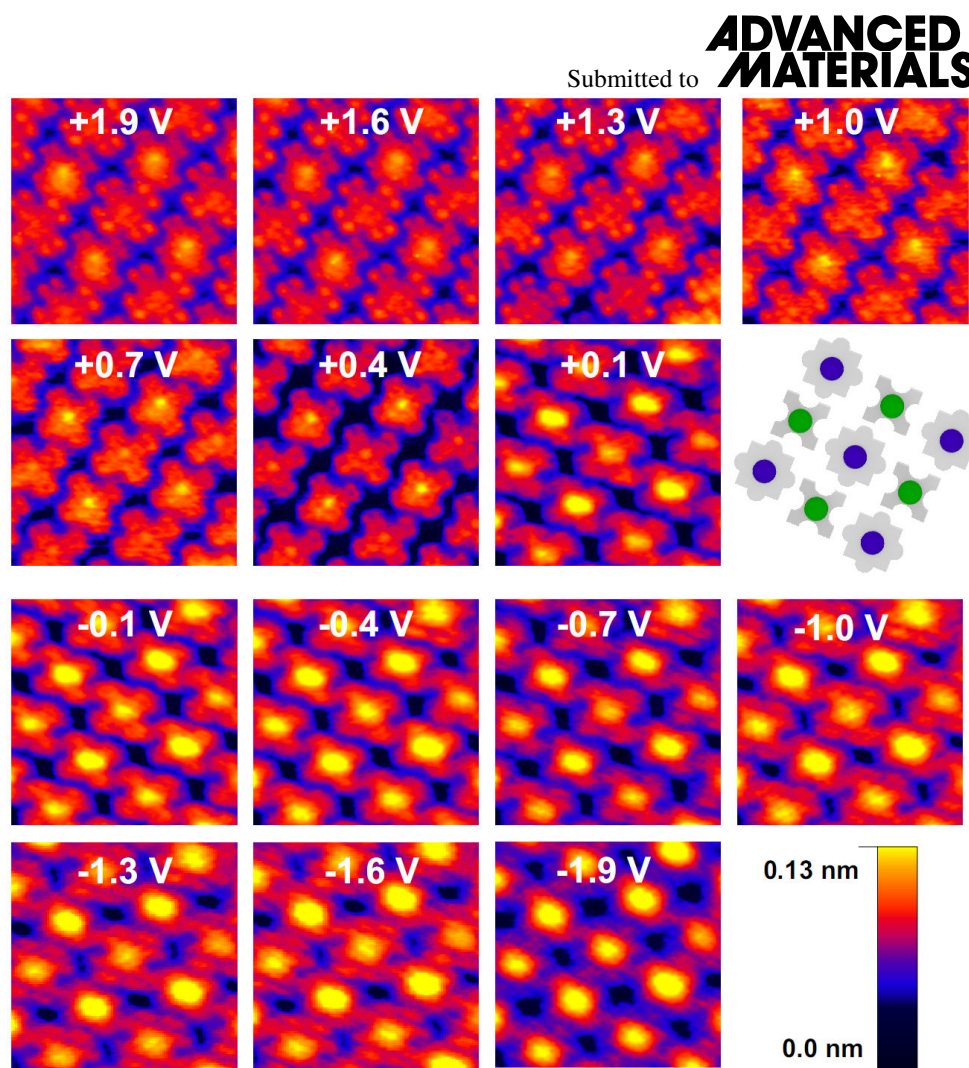
Figure S3. STM data of the same area on bimolecular $FeF_{16}Pc$ + MnPc lattice on oxygen-reconstructed Co. The central molecule is $FeF_{16}Pc$, the arrangement is illustrated by the jigsaw puzzle pieces (dark-blue: Fe, green: Mn). Positive bias voltage values correspond to the tunneling into unoccupied states of the sample, negative voltage values correspond to tunneling from occupied states of the sample. The size of the images is 5 nm x 5 nm.

Figure S4: Direct observation of the NH_3 ligand on both building-blocks at 78K

Figure S4 shows STM data obtained on the bimolecular layer on oxygen-reconstructed Co kept at 78 K, after exposure to NH_3. In this case, if scanning is performed at a low current set point, the NH_3 ligand is observed on both the $FeF_{16}Pc$ and MnPc molecules.
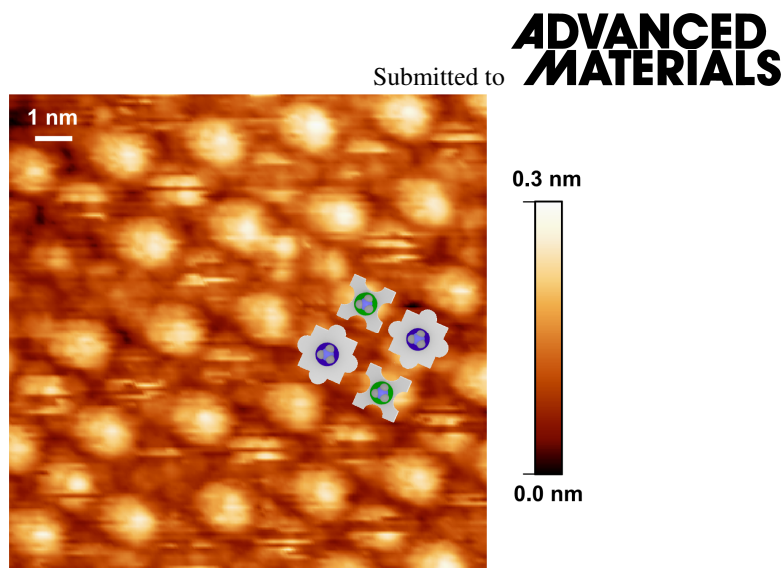
Figure S4. STM data of the bimolecular $FeF_{16}Pc$+MnPc lattice on oxygen-reconstructed Co after exposure to NH_3 (20 Langmuir), imaged at 78 K with a bias voltage of +0.4 V. In this scanning regime (temperature, low current set-point), the NH_3 ligand on MnPc is imaged as a solid bright protrusion. On the $FeF_{16}Pc$ building-block, the NH_3 ligand is imaged as streaks, very similar to the appearance of the NH_3 ligand on MnPc at 130 K (Figure 3c). A minority of the $FeF_{16}Pc$ molecules appear without streaks.

For NH_3 adsorbed on Cu(111)[7], the NH_3 molecule is imaged as a bright protrusion. The transfer of an NH_3 molecule to the tip is reported to cause an apparent elongation of the tip by 0.2 nm. This value corresponds to the observed apparent height of the protrusions on $FeF_{16}Pc$ and MnPc displayed in Figure 3c and Figure S4. Note that these values are considerably larger than the apparent heights observed on unligated $FeF_{16}Pc$ and MnPc. Interestingly, ref. [7] reports the current-induced desorption of NH_3 from the Cu(111) surface. This observation correlates with the requirement for low current set point to observe the NH_3 ligand, and the streak-like appearance of the ligand.

Figure S5: Large scale STM data

The treatment of the Co thin film with O_2 during epitaxy (cf. Methods section and ref. [2]) results in the formation of a c(2x2) reconstruction[2,8]. The oxygen-reconstruction passivates the initially very reactive ferromagnetic thin film and allows the diffusion of the ad-molecules, which is a requirement for self-assembly to occur.[2] The STM micrograph of an oxygen-reconstructed Co thin film is shown in Figure S5a. The oxygen-reconstruction results in rectangular step edges along the <100> crystallographic directions. Fine lines are observed on the oxygen-reconstruction; we tentatively explain those as grain boundaries in the c(2x2) reconstruction, which are related to the oxygen-surfactant mediated growth.

The bimolecular arrays are oriented +/- 14° with respect to the <110> directions (Figure S5b). This is a consequence of the square molecular lattice, characterized by four-fold rotational symmetry, and its placement on a substrate with four-fold rotational symmetry, thus resulting in two energetically equivalent orientations. Thus, the interaction with the substrate breaks the initial inversion symmetry of the ideal chessboard lattice and results in organizational chirality of the 2D spin arrays.

The supramolecular unit cells of the two mirror domains are marked by blue and green squares. Both mirror domains also differ in the rotation of the molecular building blocks within the unit cell as designated by the crosses within the squares. This internal structure is also seen in Figure 3.

In between of the self-assembled molecular arrays, the STM data has a streak-like appearance. We ascribe this to the co-existence of a molecular 2D gas with the self-assembled arrays. At room temperature (Figure S5b), single molecular building blocks at the edges of the self-assembled array are adsorbed/desorbed from the molecular 2D gas. They are imaged only partly (white circles) since they adsorb/desorb during the scanning process, i.e. within seconds.
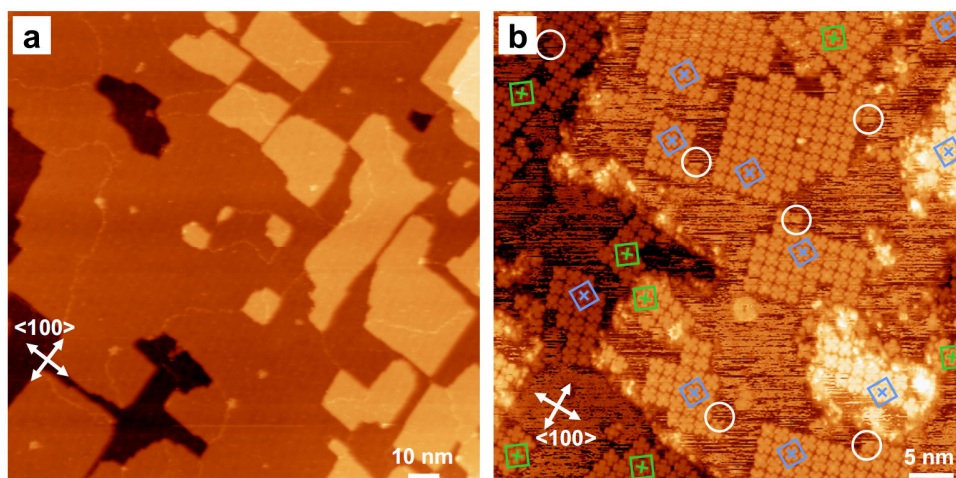

Figure S5. Large scale STM data of the oxygen-reconstructed Co thin film (a) and of the bimolecular co-assembled FeF$_{16}$Pc+MnPc layer on this substrate (b). The exposure of Co to oxygen results in a reconstruction of the Co(001) thin film and leads to the formation of step edges which prefer to follow <100> directions of the substrate. In case of the bimolecular chessboard-lattice two mirror domains of the supramolecular lattice, rotated by +/-14° with respect to the <110> directions of the substrate, are observed.

Table S1: STM imaging parameters

Table S1 summarizes the bias voltage, current set point and sample temperature of the presented STM data. All data were obtained in the constant-current mode. A positive bias voltage corresponds to the tunneling from tip into the sample, i.e. into unoccupied states. The STM data at 78 K were obtained using a sputtered Pt-Ir tip, all other data was obtained using a sputtered W tip. The images were processed with the WSxM software.[9]

Table S1. Imaging parameters of the presented STM data.

Figure	Bias voltage / V	Current set point / pA	Sample temperature / K
1	1.9	20	78
3a	0.4	10	130
3b	1.9	10	130
3c	0.4	10	130
3d	1.9	10	130

S1a	0.3	10	300
S1b	0.35	10	300
S2	0.8	50	300
S3	+1.9 to -1.9	10 to 20	78
S4	0.4	4	78
S5a	1.25	10	300
S5b	1.8	40	300

References

[1] K. J. Franke, G. Schulze, J. I. Pascual, *Science* **2011**, *332*, 940.

[2] D. Chylarecka, C. Wäckerlin, T. K. Kim, K. Müller, F. Nolting, A. Kleibert, N. Ballav, T. A. Jung, *J. Phys. Chem. Lett.* **2010**, *1*, 1408.

[3] J. Ren, S. Meng, Y.-L. Wang, X.-C. Ma, Q.-K. Xue, E. Kaxiras, *J. Chem. Phys.* **2011**, *134*, 194706.

[4] F. Buchner, K.-G. Warnick, T. Wölfle, A. Görling, H.-P. Steinrück, W. Hieringer, H. Marbach, *J. Phys. Chem. C* **2009**, *113*, 16450.

[5] K. W. Hipps, X. Lu, X. D. Wang, U. Mazur, *J. Phys. Chem.* **1996**, *100*, 11207.

[6] J. Repp, G. Meyer, S. Stojković, A. Gourdon, C. Joachim, *Phys. Rev. Lett.* **2005**, *94*, 026803.

[7] L. Bartels, M. Wolf, T. Klamroth, P. Saalfrank, A. Kühnle, G. Meyer, K.-H. Rieder, *Chem. Phys. Lett.* **1999**, *313*, 544.

[8] C. Sorg, N. Ponpandian, M. Bernien, K. Baberschke, H. Wende, R. Wu, *Phys. Rev. B* **2006**, *73*, 064409.

[9] I. Horcas, R. Fernández, J. M. Gómez-Rodríguez, J. Colchero, J. Gómez-Herrero, A. M. Baro, *Rev. Sci. Instrum.* **2007**, *78*, 013705.

2.4 Ammonia Coordination Introducing a Magnetic Moment in On-Surface Low-Spin Porphyrin

Summary: In the previous works we have shown that axial coordination can result either in quenching or in tuning of the magnetic moment of a complex. However, no on-surface magnetochemical reaction has been shown until now to *induce* a magnetic moment, i.e. act as a chemical spin on-switch. In this work, we study the d^8 low-spin (S = 0) Ni(II)-porphyrin on a ferromagnetic substrate. The experimental data as well as theoretical calculations show that the axial coordination of NH_3 induces a magnetic moment. The mechanism of this effect is a conversion from low-spin to high-spin caused by NH_3 coordination on surface.

Paper [[4]] is published in Angewandte Chemie International Edition

Angewandte
Communications

Magnetochemistry

Ammonia Coordination Introducing a Magnetic Moment in an On-Surface Low-Spin Porphyrin**

Christian Wäckerlin, Kartick Tarafder, Jan Girovsky, Jan Nowakowski, Tatjana Hählen, Aneliia Shchyrba, Dorota Siewert, Armin Kleibert, Frithjof Nolting, Peter M. Oppeneer, Thomas A. Jung,* and Nirmalya Ballav*

The controlled manipulation of spin states in atoms/molecules is of profound interest towards the design of future spin-based devices.[1,2] A prominent example of how spin states are modified ($S = 2 \leftrightarrow S = 0$) can be found in nature's Fe^{II} porphyrin moiety within hemoglobin and its coordination with the O_2 ligand.[3] Recently, we have implemented this concept in a synthetic on-surface arrangement using metallo-porphyrins adsorbed on ferromagnetic surfaces. By axial coordination with an external NO ligand the induced magnetic moment in the ($S = 1/2$) Co^{II} porphyrin has been switched-off.[4] These experiments depend on a characteristic property of paramagnetic metallo-porphyrins as well as phthalocyanines: their interfacial chemical interaction with the ferromagnetic surface ligand induces a magnetic moment stable up to room temperature.[4,5] Axial coordination can also be used to control the magnetic anisotropy[6] as well as the strength and sign of the exchange interaction.[4b]

Controlling on-surface/interface spin systems[4,5j,k,6,7] is a prerequisite for applications in organic spintronics[1] which makes this research field increasingly popular. Recently, we combined chemically directed self-assembly and coordination chemistry to obtain selectively switchable, highly ordered supramolecular 2D spin arrays.[5j] Concerning chemical control of the magnetic moment, only off-switching[4,5j] and spin-tuning,[4b,5k] that is, switching spin-on→spin-off and spin-on→spin-on' (a modified spin state) have been established. So far this set of on-surface chemical spin operations was incomplete since the spin-off→spin-on case was missing. Generally,

switching the spin in organometallic complexes by external ligands to the on-state is more difficult to achieve than switching to the off-state, since chemical bonding has to overcome the spin-pairing energy. An additional complication arises from the possibility that the surface can modify the spin states before as well as after the axial ligation.[4b] This can also lead to spin-quenching on the surface.[4b,8] Here we report on the first demonstration of an on-surface chemical spin on-switch, for Ni^{II} porphyrins ($S = 0$) adsorbed on a ferromagnetic (FM) Co substrate, by the diamagnetic ($S = 0$) external NH_3 ligand. A schematic representation of this spin on-switch ($S = 0 \leftrightarrow S = 1$) is shown in Figure 1 a.

To study this effect, Ni^{II} tetraphenylporphyrin (NiTPP; see Figure 1 a) molecules were thermally sublimed in ultra-high vacuum onto clean Co thin films on Cu(001) single crystals.[4,5e,f,j] For a description of the methods see the Supporting Information.

In scanning tunneling microscopy (STM) experiments (Figure 1 b), we consistently find the molecules adsorbed in a random fashion on Co and Ni substrates,[4,5f] in contrast to self-assembly of NiTPP on Au and Ag substrates.[9a] Most of the NiTPP molecules on the Co surface can be recognized as rectangular shapes—the so-called saddle-shape conformation[9b] (Figure 1 c), whereas a minority of the molecules is observed as four-leaf clovers,[5f] that is, in the flat, square-planar conformation of the free molecule. The adsorption-induced saddle-shape conformation is characterized by a tetrahedrally distorted macrocycle[9b,c] and its coexistence with

[*] C. Wäckerlin, J. Girovsky, J. Nowakowski, T. Hählen, Dr. D. Siewert, Prof. T. A. Jung
Laboratory for Micro and Nanotechnology
Paul Scherrer Institute, 5232 Villigen-PSI (Switzerland)
E-mail: thomas.jung@psi.ch

Prof. N. Ballav
Department of Chemistry
Indian Institute of Science Education and Research
Pune 411008 (India)
E-mail: nballav@iiserpune.ac.in

Dr. K. Tarafder,[+] Prof. P. M. Oppeneer
Department of Physics and Astronomy, University of Uppsala
Box 516, 75120 Uppsala (Sweden)

A. Shchyrba
Department of Physics, University of Basel
4056 Basel (Switzerland)

Dr. A. Kleibert, Prof. F. Nolting
Swiss Light Source, Paul Scherrer Institute
5232 Villigen-PSI (Switzerland)

[†] Current address:
Materials Science Division, Lawrence
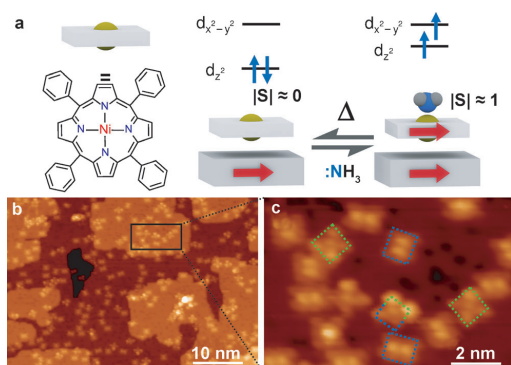Berkeley National Laboratory, Berkeley, CA 94720 (USA)

Figure 1. a) NiTPP and the reversible spin on-switch ($S=0\leftrightarrow S=1$). The molecular orbital diagram shows that the NH_3 ligand increases the energy of the $3d_{z^2}$ orbital and thus allows a $S=1$ high-spin state. b) Constant current STM image of NiTPP on Co(001) without NH_3 (tunneling parameters: 20 pA, 650 mV, W-tip). The considerable molecule–surface interaction leads to irregular arrangement of the ad-molecules. c) The zoom-in STM image shows that the NiTPP molecules are found in either one of two conformations: saddle-shape (blue rectangles) and flat (green squares).

the flat conformation has been observed in our previous studies.[4] Note, that an intermediate conformation (half flat, half saddle-shape) is also observed (Figure 1c, marked half

green, half blue). STM data obtained after exposure to NH_3 at 78 K depict bright blurry protrusions which partly have a streak-like appearance[5j, 10] (see the Supporting Information). This suggests considerable degrees of freedom of the NH_3 ligand or partial removal of NH_3 during the scanning process.[5j, 10]

The electronic and magnetic properties of both ad-molecules (NiTPP) and substrate (Co(001) thin films), as well as the magnetochemical effect induced by the NH_3 ligand were investigated by element-specific X-ray absorption spectroscopy (XAS) and X-ray magnetic circular dichroism (XMCD)[11a] measurements (Figure 2) at the Surface/Interface: Microscopy (SIM) beamline of the Swiss Light Source (SLS).[11b] For 3d transition metals, the absorption cross-section at the $L_{3;2}$ edges ($2p\rightarrow3d$ electronic transitions) provides element-specific information on the magnetization of the surface adsorbed transition-metal complexes (here NiTPP) and the substrate (here Co) separately.

Figure 2 shows the Ni and Co $L_{2;3}$ edge XAS/XMCD signals sequentially obtained at about 70 K with the substrate kept in its remanent magnetization on the native NiTPP/Co system (a), after exposure to NH_3 gas (b), after thermal desorption of NH_3 (c) and, finally, after re-exposure to NH_3 gas (d). Note that the Ni $L_{3;2}$ edge XAS is affected by far-edge oscillations, originating from the Co thin-film substrate, giving rise to a slowly varying background in XAS/XMCD signals. In the main panels we show the spectra upon subtraction of the background measured on a reference substrate.
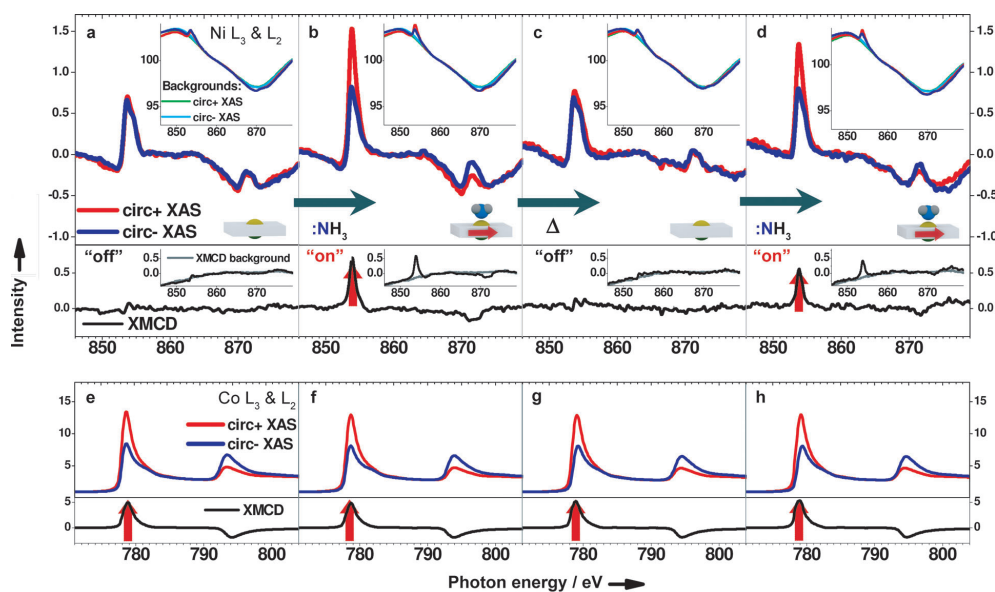
Figure 2. XAS/XMCD of Ni in the molecule and the Co substrate of the native NiTPP/Co (a,e), after exposure to NH_3 gas (b,f), after thermal desorption (Δ) of NH_3 (c,g) and after re-exposure to NH_3 gas (d,h). The spectra were recorded at about 70 K. At the Ni $L_{3;2}$ edge XAS/XMCD data, the respective backgrounds as shown in the insets (green/cyan for circ+/circ- XAS and gray for XMCD), have been subtracted. The original spectra (red/blue for circ+/circ- XAS and black for XMCD) are also shown in the insets. In absence of NH_3 (a,c), no XMCD signal is observed in Ni (spin-off state). The red arrows indicate the presence of magnetic dipole moments.

Angewandte
Communications

For native NiTPP/Co, the absence of an XMCD signal demonstrates that the adsorption of the molecules on the Co substrate alone does not induce a magnetic dipole moment in the Ni^{2+} central ion (Figure 2 a). The exposure with NH_3, however, results in a clear XMCD signal evidencing the presence of a magnetic moment on the Ni^{2+} center (Figure 2 b). Annealing to 300 K restores the initial spin-off state and subsequent NH_3 exposure leads to the recovery of the spin-on state (Figure 2 c and d). The spin-on state is characterized by a FM coupling to the substrate as indicated by the parallel red arrows in Figure 2. Such coupling for paramagnetic porphyrins and phthalocyanines in contact with ferromagnetic substrates has been observed earlier[5a] and studied in detail.[4,5] However, in the case presented here the FM coupled spin, confirmed by the observed change in the sign of the Co and Ni XMCD signals after remagnetizing the substrate in the opposite direction, is observed only in presence of the axial NH_3 ligand. The magnetic signature of the substrate remains unaffected (see Co-XMCD signals in Figure 2 e–h) in the sequential processes of NH_3 coordination/decoordination, that is, the switching between the molecular spin-off and spin-on states occurs in the presence of the substrate magnetization and its exchange interaction with the central metal ion of the molecule.

The origin of the induced magnetic moment is related to the increase of the coordination number of the Ni ion upon exposure to NH_3. Four-coordinated Ni^{2+} complexes are usually in the low-spin (S = 0) state.[12] Ni^{2+} ions with a coordination number of five (square pyramidal) or six (octahedral) are usually paramagnetic high-spin (S = 1) species.[13] However, the nature of the ligand, that is, whether it acts as a σ donor or as a π acceptor, plays a crucial role for the thermodynamic stability of the coordination bond.[13c] Notably, we can observe this low-spin to high-spin transition also by X-ray photoelectron spectroscopy (XPS) as an increase in the full-width-at-half-maximum of the $Ni2p_{3/2}$ spectral feature (see the Supporting Information).

To explain our experimental observations and to provide detailed insight into the on-surface molecular spin-switching, numerical simulations based on density functional theory were performed taking additional Hubbard interactions (DFT + U) into account (Figure 3). The calculations were performed on Ni–porphine, that is, without phenyl substitution, to manage the computational efforts.[4b,5b–e,14] Note that in view of the coexistence of different conformations, local experiments, for example, spin-polarized STM, would be desirable to correlate conformation and magnetochemistry. For Ni–porphine on Co (NiP/Co), we find that the 3d orbital local magnetic density of states (LMDOS) of Ni is equally distributed over the two spin-channels, that is, spin ↑ and spin ↓; hence the magnetic dipole moment of NiP on Co is not present (S = 0). The calculated electronic configuration, approximately $(d_{xy})^2 (d_{yz},d_{xz})^4 (d_{z^2})^2 (d_{x^2-y^2})^0$, corresponds well to the free Ni^{II} porphyrin.

Through NH_3 coordination, the 3d LMDOS of Ni^{2+} changes into $(d_{xy})^2 (d_{yz},d_{xz})^4 (d_{z^2})^1 (d_{x^2-y^2})^1$, revealing singly occupied and FM coupled d_{z^2} and $d_{x^2-y^2}$ orbitals. The magnetic moment is about 1.61 μ_B on the Ni ion and 0.06 μ_B on each of the nitrogen atoms of the porphyrin. Moreover, the Ni ion is
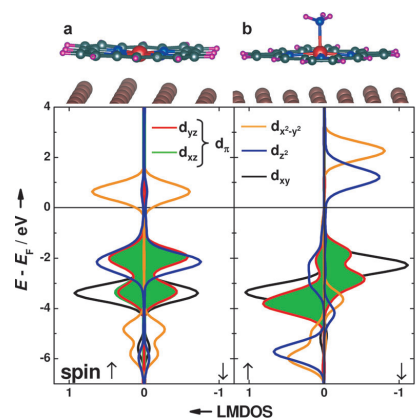

Figure 3. DFT + U calculations presenting the spin-projected 3d orbital local magnetic density of states (LMDOS) for the Ni-porphine/Co system with S = 0 before (a) and with S = 1 after (b) reaction with NH_3. The given energies are with respect to the Fermi-level (E_F). The calculations show that the NH_3 ligation leads to an increased energy of the d_{z^2} orbital (because of interaction with the lone-pair of the NH_3 ligand), shifting it closer in energy to the $d_{x^2-y^2}$ orbital and allowing for a high-spin (S = 1) state being FM coupled to the Co substrate.

pulled-up from the porphyrin plane towards the NH_3 ligand. Note that, depending on the electronic configuration NH_3 can also act as a spin–off switch.[5j,7] The calculated Ni–Co distance for NH_3-NiP/Co (3.59 Å) is significantly longer than the value obtained for the native NiP/Co (3.09 Å) system, consistent with the observation of a surface spin-trans effect.[4] Notably, the coordination of the Co surface ligand[4,15] to the Ni^{2+} ion is identified by a broadening of the calculated $3d_{z^2}$ LMDOS, however, this occurs without modification of the total molecular magnetic moment. Furthermore, the calculations show an increase of the Ni–$N_{porphine}$ distance from 1.98 to 2.05 Å. This increase has been attributed for a similar system to the reduced formal bond order because of the presence of an unpaired electron in the anti-bonding $d_{x^2-y^2}$ orbital of NH_3–NiTPP.[13b] Note, that the NH_3-induced FM coupled spin density is distributed across the nitrogen atoms of the Ni–porphyrin and the NH_3 ligand (0.06 μ_B). The spin density sums up to about 1.92 μ_B, corresponding to a molecular spin state of S = 1, consistent with the two singly occupied levels seen in Figure 3 b.

In conclusion, we have provided evidence for the capability of NH_3 to act as an on-switch for the spin of the NiTPP/Co system and confirmed the surface spin-trans effect.[4] Notably, the observation of a magnetic moment in the molecule only after exposure to NH_3 rules out that the ligand quenches the magnetic moment of the substrate. The presented findings are of fundamental interest and provide a showcase for magnetochemistry in an on-surface setting. The consequence of ligation-induced transitions on spin multiplicity and magnetic moment are uniquely probed by XPS and XMCD, respectively. Moreover, they open-up new possibilities to control magnetic moments down to the single-molecule level by chemical stimuli. Possible applications

Angewandte
Chemie
International Edition

include the use of this system in a magnetochemical sensor and in molecular spintronics.

[1] a) O. Kahn, K. J. Martinez, *Science* **1998**, *279*, 44–48; b) V. A. Dediu, L. E. Hueso, I. Bergenti, C. Taliani, *Nat. Mater.* **2009**, *8*, 707–716.

[2] a) A. A. Khajetoorians, J. Wiebe, B. Chilian, R. Wiesendanger, *Science* **2011**, *332*, 1062–1064; b) S. Sanvito, *Chem. Soc. Rev.* **2011**, *40*, 3336.

[3] J. M. Berg, J. L. Tymoczko, L. Stryer, *Biochemistry*, W. H. Freeman, New York, **2002**.

[4] a) C. Wäckerlin, D. Chylarecka, A. Kleibert, K. Müller, C. Iacovita, F. Nolting, T. A. Jung, N. Ballav, *Nat. Commun.* **2010**, *1*, 61; b) C. Wäckerlin, K. Tarafder, D. Siewert, J. Girovsky, T. Hählen, C. Iacovita, A. Kleibert, F. Nolting, T. A. Jung, P. M. Oppeneer, N. Ballav, *Chem. Sci.* **2012**, *3*, 3154–3160.

[5] a) A. Scheybal, T. Ramsvik, R. Bertschinger, M. Putero, F. Nolting, T. A. Jung, *Chem. Phys. Lett.* **2005**, *411*, 214–220; b) H. Wende, M. Bernien, J. Luo, C. Sorg, N. Ponpandian, J. Kurde, J. Miguel, M. Piantek, X. Xu, P. Eckhold, W. Kuch, K. Baberschke, P. M. Panchmatia, B. Sanyal, P. M. Oppeneer, O. Eriksson, *Nat. Mater.* **2007**, *6*, 516–520; c) M. Bernien, J. Miguel, C. Weis, M. E. Ali, J. Kurde, B. Krumme, P. M. Panchmatia, B. Sanyal, M. Piantek, P. Srivastava, K. Baberschke, P. M. Oppeneer, O. Eriksson, W. Kuch, H. Wende, *Phys. Rev. Lett.* **2009**, *102*, 047202; d) M. E. Ali, B. Sanyal, P. M. Oppeneer, *J. Phys. Chem. C* **2009**, *113*, 14381–14383; e) D. Chylarecka, T. K. Kim, K. Tarafder, K. Müller, K. Gödel, I. Czekaj, C. Wäckerlin, M. Cinchetti, M. E. Ali, C. Piamonteze, F. Schmitt, J.-P. Wüstenberg, C. Ziegler, F. Nolting, M. Aeschlimann, P. M. Oppeneer, N. Ballav, T. A. Jung, *J. Phys. Chem. C* **2011**, *115*, 1295–1301; f) D. Chylarecka, C. Wäckerlin, T. K. Kim, K. Müller, F. Nolting, A. Kleibert, N. Ballav, T. A. Jung, *J. Phys. Chem. Lett.* **2010**, *1*, 1408–1413; g) M. Bernien, X. Xu, J. Miguel, M. Piantek, P. Eckhold, J. Luo, J. Kurde, W. Kuch, K. Baberschke, H. Wende, P. Srivastava, *Phys. Rev. B* **2007**, *76*, 214406; h) S. Javaid, M. Bowen, S. Boukari, L. Joly, J.-B. Beaufrand, X. Chen, Y. Dappe, F. Scheurer, J.-P. Kappler, J. Arabski, W. Wulfhekel, M. Alouani, E. Beaurepaire, *Phys. Rev. Lett.* **2010**, *105*, 077201; i) N. Atodiresei, J. Brede, P. Lazicacute, V. Caciuc, G. Hoffmann, R. Wiesendanger, S. Blügel, *Phys. Rev. Lett.* **2010**, *105*, 066601; j) C. Wäckerlin, J. Nowakowski, S.-X. Liu, M. Jaggi, D. Siewert, J. Girovsky, A. Shchyrba, T. Hählen, A. Kleibert, P. M. Oppeneer, F. Nolting, S. Decurtins, T. A. Jung, N. Ballav, *Adv. Mater.* **2013**, DOI: 10.1002/adma.201204274; k) J. Miguel, C. F. Hermanns, M. Bernien, A. Krüger, W. Kuch, *J. Phys. Chem. Lett.* **2011**, *2*, 1455–1459.

[6] P. Gambardella, S. Stepanow, A. Dmitriev, J. Honolka, F. M. F. de Groot, M. Lingenfelder, S. S. Gupta, D. D. Sarma, P. Bencok, S. Stanescu, S. Clair, S. Pons, N. Lin, A. P. Seitsonen, H. Brune, J. V. Barth, K. Kern, *Nat. Mater.* **2009**, *8*, 189–193.

[7] C. Isvoranu, B. Wang, K. Schulte, E. Ataman, J. Knudsen, J. N. Andersen, M. L. Bocquet, J. Schnadt, *J. Phys. Condens. Matter* **2010**, *22*, 472002.

[8] a) N. Tsukahara, K. Noto, M. Ohara, S. Shiraki, N. Takagi, S. Shin, M. Kawai, *Phys. Rev. Lett.* **2009**, *102*, 167203; b) J. Brede, N. Atodiresei, S. Kuck, P. Lazić, V. Caciuc, Y. Morikawa, G. Hoffmann, S. Blügel, R. Wiesendanger, *Phys. Rev. Lett.* **2010**, *105*, 047204.

[9] a) L. G. Teugels, L. G. Avila-Bront, S. J. Sibener, *J. Phys. Chem. C* **2011**, *115*, 2826–2834; b) W. Auwärter, K. Seufert, F. Klappenberger, J. Reichert, A. Weber-Bargioni, A. Verdini, D. Cvetko, M. Dell'Angela, L. Floreano, A. Cossaro, G. Bavdek, A. Morgante, A. P. Seitsonen, J. V. Barth, *Phys. Rev. B* **2010**, *81*, 245403; c) F. Buchner, I. Kellner, W. Hieringer, A. Görling, H.-P. Steinrück, H. Marbach, *Phys. Chem. Chem. Phys.* **2010**, *12*, 13082.

[10] L. Bartels, M. Wolf, T. Klamroth, P. Saalfrank, A. Kühnle, G. Meyer, K.-H. Rieder, *Chem. Phys. Lett.* **1999**, *313*, 544–552.

[11] a) J. Stöhr, H. C. Siegmann, *Magnetism: From Fundamentals to Nanoscale Dynamics*, Springer, Berlin, **2006**; b) U. Flechsig, F. Nolting, A. Fraile Rodríguez, J. Krempaský, C. Quitmann, T. Schmidt, S. Spielmann, D. Zimoch, R. Garrett, I. Gentle, K. Nugent, S. Wilkins, *AIP Conf. Proc.* **2010**, *1234*, 319–322.

[12] F. A. Cotton, G. Wilkinson, A. C. Murillo, M. Bochmann, *Advanced inorganic chemistry*, Wiley, New York, **1999**.

[13] a) L. X. Chen, W. J. H. Jäger, G. Jennings, D. J. Gosztola, A. Munkholm, J. P. Hessler, *Science* **2001**, *292*, 262–264; b) H. Duval, V. Bulach, J. Fischer, R. Weiss, *Inorg. Chem.* **1999**, *38*, 5495–5501; c) S. Thies, C. Bornholdt, F. Köhler, F. D. Sönnichsen, C. Näther, F. Tuczek, R. Herges, *Chem. Eur. J.* **2010**, *16*, 10074–10083; d) S. Venkataramani, U. Jana, M. Dommaschk, F. D. Sonnichsen, F. Tuczek, R. Herges, *Science* **2011**, *331*, 445–448.

[14] P. M. Oppeneer, P. M. Panchmatia, B. Sanyal, O. Eriksson, M. E. Ali, *Prog. Surf. Sci.* **2009**, *84*, 18–29.

[15] a) K. Flechtner, A. Kretschmann, H.-P. Steinrück, J. M. Gottfried, *J. Am. Chem. Soc.* **2007**, *129*, 12110–12111; b) M. G. Betti, P. Gargiani, R. Frisenda, R. Biagi, A. Cossaro, A. Verdini, L. Floreano, C. Mariani, *J. Phys. Chem. C* **2010**, *114*, 21638–21644; c) W. Hieringer, K. Flechtner, A. Kretschmann, K. Seufert, W. Auwärter, J. V. Barth, A. Görling, H.-P. Steinrück, J. M. Gottfried, *J. Am. Chem. Soc.* **2011**, *133*, 6206–6222.

Supporting Information

Ammonia Coordination Introducing a Magnetic Moment in On-Surface Low-Spin Porphyrin

Christian Wäckerlin, Kartick Tarafder, Jan Girovsky, Jan Nowakowski, Tatjana Hählen, Aneliia Shchyrba, Dorota Siewert, Armin Kleibert, Frithjof Nolting, Peter M. Oppeneer, Thomas A. Jung and Nirmalya Ballav

Table of Contents

Experimental

The Co thin films (20 monolayers) were grown on Cu(001) single crystals[1–3] by electron beam evaporation. NiTPP (Sigma-Aldrich, Switzerland) was evaporated (~0.7 − 0.9 monolayers for the XMCD experiments; lower coverage for the STM experiments) onto the Co thin films kept at room temperature. The quality of the samples (thickness, morphology, stoichiometry, absence of contamination) was checked by XPS (monochromatic Al Kα excitation) and STM.

The XAS/XMCD data were measured at the Surface/Interface: Microscopy (SIM) beamline of the Swiss Light Source (SLS).[4] The Co thin films were magnetized with an external magnetic field of ~150 mT along the easy axis of magnetization (in-plane). The XAS/XMCD data were recorded in total electron yield with the Co substrate kept in its remanent magnetization. All experiments were performed in ultra-high vacuum; a portable vacuum chamber was used for sample transfer to the beamline.[1–3] NH_3 was dosed (20 Langmuir) onto the samples kept at 70 K.

The STM data were recorded in the constant current mode at room temperature using sputtered W and Pt-Ir tips. Positive bias voltage corresponds to tunneling from the tip into unoccupied states of the sample.

The calculations presented here are based on density-functional theory +U, where the strong Coulomb interactions in the open 3d-shell are implemented by the supplementary Hubbard U (4 eV) and exchange constant J (1 eV). We used the VASP full-potential plane wave code,[5] with a kinetic energy cut-off of 400 eV. The used generalized gradient approximation was parameterized according to Perdew-Burke-Ernzerhof.[6] The calculations were performed on Ni-porphine, i.e. without phenyl

1

substitution, to manage the computational efforts.[7–10] We performed full geometric optimization of the porphine molecule and its distance and position on the surface in combination with a full relaxation of the top surface layer (3 layers in total model the surface). Reciprocal space sampling was performed using 2x2x2 Monkhorst-Pack k-points.

XPS data of NiTPP/Co + NH$_3$

Figure S1 displays Ni2p$_{3/2}$ XPS data of NiTPP/Co/Cu(001) before and after exposure to NH$_3$ The data reveal an increased full width at half maximum (FWHM) after NH$_3$ exposure which is consistent with the formation of the high-spin Ni-complex. Note that the reverse effect (the observation of a decreased FWHM) has been observed for the transition "open-shell → closed-shell" in the cases of CoTPP+NO[2,11] and FePc+NH$_3$.[12] The Ni2p$_{3/2}$ peak maximum shifts only very slightly upon NH$_3$ exposure (from 853.1 eV to 853.2 eV). This very small peak shift is consistent with the small peak shifts of +0.2 eV observed for ZnTPP/Ag(111)+NH$_3$[13] and -0.2 eV for FePc/Au(111)+NH$_3$[12] and suggests a predominantly neutral character of the ammonia ligand.
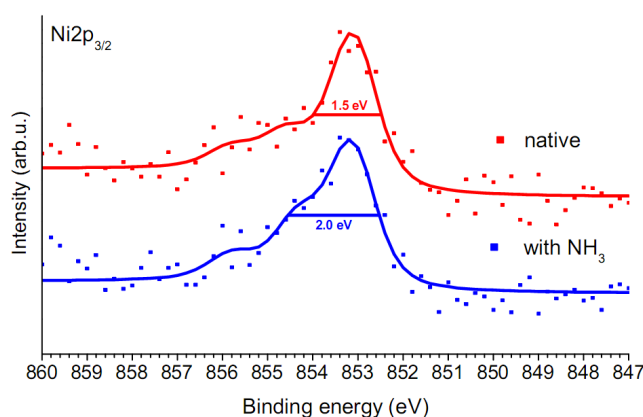

Figure S1 Ni2p$_{3/2}$ XPS data (background subtracted) of NiTPP/Co/Cu(001) before and after exposure to NH$_3$ (100 Langmuir). The sample is kept at 120 K during the experiment. The peak-width of the Ni2p$_{3/2}$ signal is significantly increased by multiplet effects upon exposure to NH$_3$.

2

STM data of NiTPP/Co + NH$_3$

Figure S2 exhibits STM data of a submonolayer of NiTPP/Co/Cu(001) before and after NH$_3$ exposure. The data was obtained at 78 K using a PtIr-tip. Before exposure to NH$_3$ (Fig. S2a), the NiTPP molecules are clearly resolved as square and rectangular shapes for the corresponding flat (minority) and saddle-shape (majority) conformations. After exposure to NH$_3$ (Fig. S2b&c), the free surface is observed to be covered with ammonia. We find that a low-current set-point and bias-voltage is necessary to minimize the interaction with the STM tip and to avoid "picking-up"/desorbing ammonia. These findings are fully consistent with the reported desorption of NH$_3$/Cu(111) by tunneling electrons.[14]. In ref. [14], ammonia is imaged as a relatively big (up to ~1 nm), bright protrusion. Indeed, in our STM experiments we observe the ammonia-ligand as bright protrusions. Some of the bright protrusions have a streak-like appearance, i.e. they appear and disappear between individual scan-lines. We interpret this as the signature of the NH$_3$-ligand having considerable degrees of freedom when coordinated with NiTPP and may be released/excited by the STM experiments even at low bias voltage and tunneling current. Note that intramolecular resolution was not obtained on the NH$_3$-NiTPP/Co samples in extensive measurements, in contrast to NiTPP/Co without NH$_3$, where intramolecular resolution is obtained regularly. We tentatively explain this by the presence of a monolayer of NH$_3$ being attached to the free area on the Co-substrate.
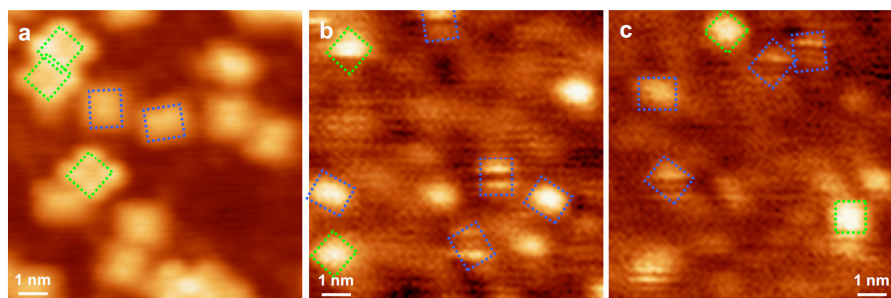
Figure S2 STM data of NiTPP/Co recorded at 78 K. Before NH$_3$ exposure (a), the NiTPP molecules are clearly resolved in the saddle-shape (majority, blue rectangles) and flat (minority, green squares) conformations (25 pA, 400 mV) as discussed in the main-text. After exposure with 50 Langmuir of NH$_3$ (b,c) the ammonia ligands are imaged as bright protrusions which partly have a streak-like appearance (3 pA, 400 mV).

References

[1]   D. Chylarecka, C. Wäckerlin, T. K. Kim, K. Müller, F. Nolting, A. Kleibert, N. Ballav, T. A. Jung, *J. Phys. Chem. Lett.* **2010**, *1*, 1408–1413.

[2]   C. Wäckerlin, D. Chylarecka, A. Kleibert, K. Müller, C. Iacovita, F. Nolting, T. A. Jung, N. Ballav, *Nat. Commun.* **2010**, *1*, 61.

3

[3]   D. Chylarecka, T. K. Kim, K. Tarafder, K. Müller, K. Gödel, I. Czekaj, C. Wäckerlin, M. Cinchetti, M. E. Ali, C. Piamonteze, et al., *J. Phys. Chem. C* **2011**, *115*, 1295–1301.

[4]   U. Flechsig, F. Nolting, A. Fraile Rodríguez, J. Krempaský, C. Quitmann, T. Schmidt, S. Spielmann, D. Zimoch, R. Garrett, I. Gentle, et al., *AIP Conf. Proc.* **2010**, *1234*, 319–322.

[5]   G. Kresse, J. Furthmüller, *Phys. Rev. B* **1996**, *54*, 11169–11186.

[6]   J. P. Perdew, K. Burke, M. Ernzerhof, *Phys. Rev. Lett.* **1996**, *77*, 3865–3868.

[7]   M. E. Ali, B. Sanyal, P. M. Oppeneer, *J. Phys. Chem. C* **2009**, *113*, 14381–14383.

[8]   M. Bernien, J. Miguel, C. Weis, M. E. Ali, J. Kurde, B. Krumme, P. M. Panchmatia, B. Sanyal, M. Piantek, P. Srivastava, et al., *Phys. Rev. Lett.* **2009**, *102*, 047202.

[9]   P. M. Oppeneer, P. M. Panchmatia, B. Sanyal, O. Eriksson, M. E. Ali, *Prog. Surf. Sci.* **2009**, *84*, 18–29.

[10] H. Wende, M. Bernien, J. Luo, C. Sorg, N. Ponpandian, J. Kurde, J. Miguel, M. Piantek, X. Xu, P. Eckhold, et al., *Nat. Mater.* **2007**, *6*, 516–520.

[11] K. Flechtner, A. Kretschmann, H.-P. Steinrück, J. M. Gottfried, *J. Am. Chem. Soc.* **2007**, *129*, 12110–12111.

[12] C. Isvoranu, B. Wang, K. Schulte, E. Ataman, J. Knudsen, J. N. Andersen, M. L. Bocquet, J. Schnadt, *J. Phys.: Condens. Matter* **2010**, *22*, 472002.

[13] K. Flechtner, A. Kretschmann, L. R. Bradshaw, M.-M. Walz, H.-P. Steinruck, J. M. Gottfried, *J. Phys. Chem. C* **2007**, *111*, 5821–5824.

[14] L. Bartels, M. Wolf, T. Klamroth, P. Saalfrank, A. Kühnle, G. Meyer, K.-H. Rieder, *Chem. Phys. Lett.* **1999**, *313*, 544–552.

4

2.5 Assembly of 2D Ionic Layers by Reaction of Alkali Halides with the Organic Electrophile 7,7,8,8-tetracyano-p-quinodimethane (TCNQ)

Summary: The organic compound TCNQ is a strong electron acceptor which is of interest
in the fields of molecular electronics and surface-chemistry.[76, 77] Its high electron-affinity is
due to its electronic structure: like its relative 1,4-Benzoquinone, the bonds in the central carbon
6-ring are *not* delocalized, but the uptake of 1 or 2 electrons allows for partial/full delocalization
which is energetically favored.[78] On surface, the charge-transfer between organic electron-
acceptors and alkali-metals,[79] transition-metals [66] and molecular electron-donors [73] has
been studied. In this context we are interested to find out if *alkali-halides* (e.g. NaCl) instead
of alkali-metals can be used to produce such structures. On the basis of STM, XPS and UPS
we find that TCNQ undergoes charge-transfer with NaCl (or LiCl) to form an ionic layer. This
is possible because TCNQ can oxidize even halides (e.g. $Cl^- + e^- \rightarrow 1/2\, Cl_2$).[76, 77] The
surface-chemistry of small organic molecules and alkali-halides is of renewed interest - cf. the
recent publications from the Tait-group.[80, 81]

Paper [[5]] is published in Chemical Communications.

ChemComm

COMMUNICATION

Assembly of 2D ionic layers by reaction of alkali halides with the organic electrophile 7,7,8,8-tetracyano-*p*-quinodimethane (TCNQ)†‡

Christian Wäckerlin,[a] Cristian Iacovita,[b] Dorota Chylarecka,[a] Petra Fesser,[c] Thomas A. Jung*[a] and Nirmalya Ballav*[d]

Sublimation of alkali halides (NaCl and LiCl) onto a pre-assembled hydrogen-bonded layer of TCNQ on Au(111) resulted in the formation of 2D ionic layers *via* a direct charge-transfer reaction without involvement of the substrate. The presented approach allows for the fabrication of different ionic layers, decoupled from the substrate and offering new, potentially interesting properties.

Recently, the observation of chemical reactions at surfaces by scanning probe microscopes has gained significant attention, both for individual reagents being moved into sufficient proximity, as well as for the observation of an ensemble of molecules confined to surfaces.[1] Among the general case of redox reactions performed in surface confinement[2] we here put the emphasis on those which can be used to influence the self-assembly.

The remarkable electron-affinity of 7,7,8,8-tetracyano-*p*-quinodimethane (TCNQ) permits not only charge-transfer (CT) with metals and organic electron-donors, but also CT by oxidation of halogens, *i.e.* in alkali halides.[3a,b] The products of the reaction show interesting properties, *i.e.* high conductivity or magnetism.[3] In this paper, we study the reaction of NaCl and LiCl with TCNQ on a surface and discuss the CT processes between the adsorbates as well as with the substrate.

We use a CT reaction between sublimed TCNQ and NaCl, both in a submonolayer regime, on Au(111) as a design concept to fabricate two-dimensional (2D) ionic layers.[4] In this 'solvent free' dry ultra-high vacuum environment, we perform spectro-microscopy correlation experiments involving scanning tunneling microscopy (STM) and photoelectron
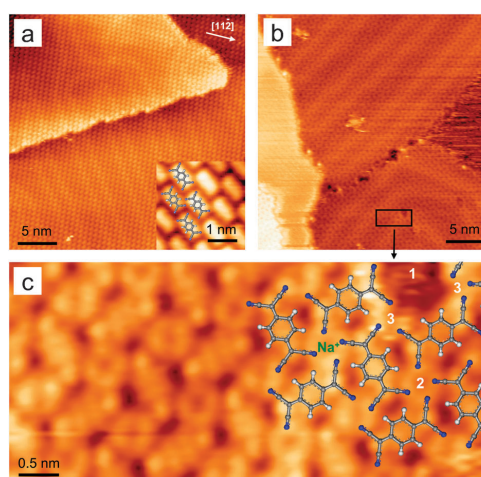
a Laboratory for Micro- and Nanotechnology, Paul Scherrer Institute, 5232 Villigen, Switzerland. E-mail: thomas.jung@psi.ch; Fax: +41-56-310-2646; Tel: +41-56-310-4518
b Department of Physics, University of Basel, 4056 Basel, Switzerland
c Laboratory for Organic Chemistry, Department of Chemistry and Applied Biosciences, ETH Zürich, 8093 Zürich, Switzerland
d Department of Chemistry, Indian Institute of Science Education and Research, Pune 411008, India. E-mail: nballav@iiserpune.ac.in
† This article is a part of a ChemComm web-based themed issue on molecule-based surface chemistry.
‡ Electronic supplementary information (ESI) available: Data on the reaction of TCNQ/Au(111) with LiCl, additional STM data and general experimental conditions including STM tunneling parameters. See DOI: 10.1039/c1cc12519b

Fig. 1 STM image of (a) TCNQ layer on Au(111) and (b,c) TCNQ layer on Au(111) after addition of NaCl.

spectroscopy to demonstrate that CT exclusively occurs between the reactants, and not with the Au(111) substrate.

The self-assembly of TCNQ on Au(111) samples as probed by STM (Fig. 1a) has been predominantly attributed to H-bonding of the cyano groups.[5] Sublimation of NaCl onto TCNQ/Au(111) drastically changes the molecular arrangement as clearly visible in both large scale (Fig. 1b) and high resolution STM images (Fig. 1c). The latter image contains a vacancy defect '**1**' in the 2D molecular layer which allows for the unambiguous identification of the adsorption geometry. The four-round protrusions '**2**' appear due to the arrangement of four-cyanogroups from the adjacent four TCNQ molecules. This assigned structure is supported by the fact that next to the vacancy '**3**' only three protrusions are observed.

In order to explore the mechanism behind the drastic change in the molecular assembly of TCNQ upon addition of NaCl we have employed X-ray photoelectron spectroscopy (XPS) (Fig. 2a). TCNQ in a multilayer exhibits a single N1s core-level signal with a binding energy of $\sim$399.1 eV and a C1s signal composed of two components ($\sim$284.95 eV and $\sim$286.3 eV; ratio $\sim$8:4)
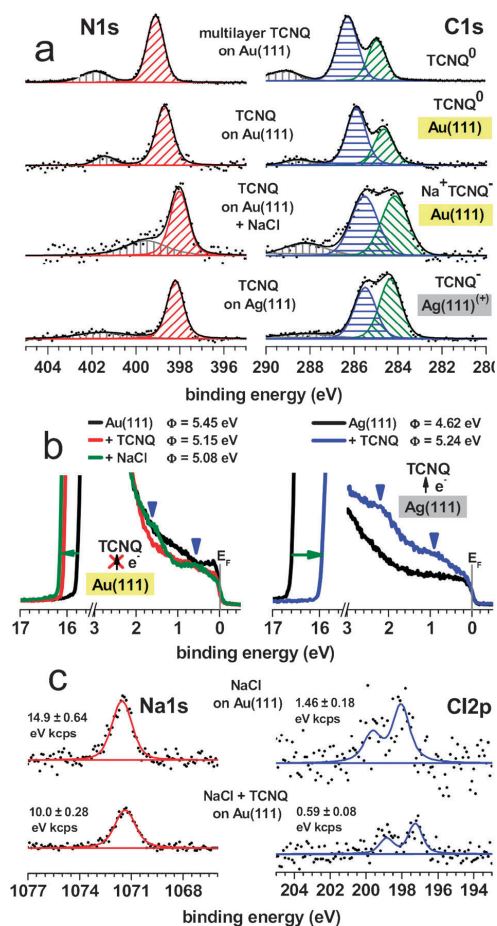
Fig. 2 Photoemission spectroscopy data towards the assignment of the species in the reacted and reorganized surface layer: (a) N1s and C1s XP spectra show evidence for neutral (TCNQ/Au(111)) and negatively charged TCNQ, accompanied by aromatization (TCNQ + NaCl/Au(111) and TCNQ/Ag(111)) derived from the characteristic C1s peak shapes.[6a,b] (b) UP spectra provide evidence for a substrate-to-molecule CT in the case of TCNQ/Ag(111) while no such CT occurs for TCNQ/Au(111) and TCNQ + NaCl/Au(111). The green arrows indicate the shift in the secondary electron cut-off which relates to the sample work function (Φ).[7b] (c) Na1s and Cl2p XP spectra of NaCl/Au(111) before and after addition of TCNQ show a decrease of the Cl/Na ratio, indicating the loss of chlorine. The numbers give the integrated peak intensity of the respective signals.

characteristic for neutral TCNQ as observed in bulk TCNQ. Our results are in good agreement with studies of bulk TCNQ[6a] and in particular also reproduce the shake-up features.[6a,b] For a monolayer of TCNQ on Au(111), both the N1s (∼398.7 eV) and C1s (∼284.65 eV and ∼285.9 eV) binding energies are slightly reduced presumably due to many-body effects.[7a] The C1s peak shape (i.e. the 8 : 4 ratio) clearly reveals that TCNQ remains neutral on Au(111)—a conclusion

also supported by STM and scanning tunneling spectroscopy data: the herringbone reconstruction persists the deposition of a full monolayer of TCNQ and the highest occupied molecular orbital (HOMO) also survives the adsorption process.[5]

The addition of NaCl significantly lowers the N1s (∼397.95 eV) and C1s (∼284.15 eV and ∼285.55 eV) binding energies and considerably changes the C1s peak shape. Now the two C1s peaks are in ∼6 : 6 ratio, which is characteristic for [TCNQ]⁻, as previously observed for bulk Li⁺[TCNQ]⁻.[6b] Interestingly, without the addition of NaCl, very similar N1s (∼398.2 eV) and C1s (∼284.35 eV and ∼285.5 eV) binding energies as well a similar C1s peak shape are observed in our data for TCNQ/Ag(111). This implies the presence of negatively charged TCNQ through substrate-to-molecule CT, as recently observed for TCNQ on Cu(001)[8a] and for Ag nanoparticles.[8b] The addition of LiCl instead of NaCl onto TCNQ/Au(111) leads to very similar changes in self-assembly and XP spectra (Fig. S1 and S2 in ESI‡) and demonstrates that the reaction of TCNQ with salts provides a general toolbox to direct self-assembly in surface supported layers.

The XPS data together with the STM observations clearly demonstrate that upon addition of NaCl a CT reaction on the Au(111) surface occurred which resulted in the conversion of TCNQ to [TCNQ]⁻. As a consequence of the CT reaction, the initial H-bonded self-assembly was modified towards a 2D ionic layer. In order to clearly distinguish the observed CT reaction between TCNQ and NaCl on Au(111) from substrate-to-molecule CT as observed for TCNQ/Ag(111), we have employed ultra-violet photoelectron spectroscopy (UPS) (Fig. 2b). Besides the valence electronic structure, UPS also yields information on substrate-to-molecule CT which is strongly influencing the vacuum level at the surface due to formation of an additional electric dipole thereby changing the measured sample workfunction (Φ).[7b]

In the case of a substrate-to-molecule CT reaction as evidenced by the TCNQ/Ag(111) XPS data, an increase of the sample workfunction is expected[7b] due to the formation of a negatively charged TCNQ layer. Indeed, this increase amounts to a workfunction change of $\Delta \approx 0.62$ eV (Fig. 2b, right). In the contrary case, in the absence of a substrate-to-molecule CT reaction, the work function is expected to decrease slightly.[7b] For both systems, TCNQ/Au(111) and TCNQ + NaCl/Au(111), the workfunction is decreased by ∼0.30 eV and ∼0.37 eV, respectively, in comparison to the clean Au(111) substrate. This clearly excludes the possibility of a substrate-to-molecule CT reaction (Fig. 2b left, green arrow).

Two cases of CT are observed in this study: TCNQ + NaCl/Au(111) exhibiting CT within the ad-layer and TCNQ/ Ag(111) where CT with the substrate occurs. Both cases lead to the formation of negatively charged TCNQ which can be identified by the occurrence of two new features in the valence region (blue triangles). This corresponds to the (partial) occupation of the former lowest unoccupied molecular orbital (LUMO), very similar to the UP spectra measured on bulk K⁺[TCNQ]⁻.[6c] The STM images, recorded at a bias voltage close to this resonance at ∼1.5 eV, yield a high intra-molecular contrast for the TCNQ + NaCl/Au(111) system (Fig. 1c, cf. Fig. S3 in ESI‡ for more STM data). Notably, similar STM images of intra-molecular resolution have been
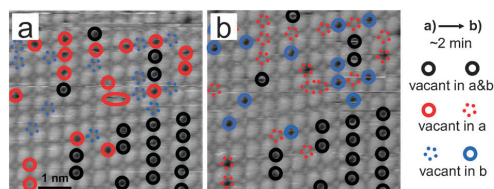
Fig. 3 STM images of TCNQ/Ag(111) in two subsequent scans (a) and (b) with vacancies marked by circles in three colours to visualize their diffusion in the TCNQ host lattice.

obtained by tunneling into presumably the same molecular orbital on the TCNQ/Au(111) system.[5] Note that for TCNQ adsorbed on noble metals (Cu, Ag, Au), charge transfer has been observed in the case of TCNQ/Cu(001)[8a] and TCNQ/Ag(111)[8b] but not for TCNQ/Au(111).

Experimental support for the 'on-surface' redox reaction of TCNQ and NaCl is provided by comparing XPS spectra for NaCl/Au(111) before and after addition of TCNQ. The Na1s and Cl2p XPS signals (Fig. 2c) show a decrease of the Cl/Na ratio by a factor of 1.67 ± 0.11 upon sublimation of TCNQ. This decrease indicates a partial loss of chlorine according to the following reaction: $Cl^- + TCNQ \rightarrow \frac{1}{2}Cl_2 + [TCNQ]^-$.[3a,9] Consequently, the structural rearrangements shown in Fig. 1c can easily be explained on the basis of an ionic assembly of $[TCNQ]^-$ with a Na^+ ion sitting next to four cyano groups '**2**'. The electron charge is fully compensated over the whole layer by the depicted coordination. Notably, adsorbed Cl_2 ($Cl2p_{3/2}$ at ~ 200.2 eV)[10] was not observed, suggesting a rapid sublimation of molecular chlorine into the vacuum.

Fig. 3 represents an STM image of TCNQ on Ag(111). In between the molecules one can identify dots of either dark or bright contrast, which were not observed in the case of TCNQ/Au(111) (Fig. 1a). We tentatively assign these features as Ag vacancies and Ag atoms, respectively. The proposed inclusion of Ag substrate atoms into the layer of TCNQ is qualitatively similar to the rearrangement of substrate atoms observed at the TCNQ/Cu(001)[8a] interface and is induced by CT, in full agreement with our UPS data on TCNQ/Ag(111). Notably, the Ag(111) and the Cu(001) surfaces differ in their symmetry and lattice constants. As a consequence, the epitaxy and interaction of any periodic layer with these substrates are also expected to differ. On Ag(111) the arrangement of the vacancies/depressions is dynamic at room-temperature in the ~ 2 minute interval between the two subsequent STM scans (Fig. 3a and b, for overview STM images see Fig. S4 in ESI‡). Remarkably, the number of vacancies remains practically constant (Table S1 in ESI‡), thereby suggesting that the system is *geometrically frustrated*, *i.e.* the density of the vacancies is governed by geometric constraints in the TCNQ/Ag(111) system.

In summary, we have demonstrated an 'on surface' chemical reaction between TCNQ and NaCl or LiCl on Au(111), which led to the formation of an extended ionic 2D layer. Sublimation of alkali halides is simple and therefore this approach is of a more general use to obtain extended (few hundred nanometer)

2D ionic layers. By choosing various combinations of other salts and electron acceptors similar to TCNQ, ultra-thin ionic layers with tunable electronic and magnetic properties can be prepared without having to rely on *i.e.* alkali metals, where excess atoms can easily undergo CT with the substrate.[11] In particular, the ionic coordination network on the Au(111) surface is found to be decoupled from the substrate.

Notes and references

1 (*a*) A. Gourdon, *Angew. Chem., Int. Ed.*, 2008, **47**, 6950–6953; (*b*) D. F. Perepichka and F. Rosei, *Science*, 2009, **323**, 216–217; (*c*) F. Mohn, J. Repp, L. Gross, G. Meyer, M. S. Dyer and M. Persson, *Phys. Rev. Lett.*, 2010, **105**, 266102; (*d*) P. Fesser, C. Iacovita, C. Wäckerlin, S. Vijayaraghavan, N. Ballav, K. Howes, J. Gisselbrecht, M. Crobu, C. Boudon, M. Stöhr, T. A. Jung and F. Diederich, *Chem.–Eur. J.*, 2011, **17**, 5246–5250.
2 F. Buchner, K. Flechtner, Y. Bai, E. Zillner, I. Kellner, H.-P. Steinrück, H. Marbach and J. M. Gottfried, *J. Phys. Chem. C*, 2008, **112**, 15458–15465.
3 (*a*) L. R. Melby, R. J. Harder, W. R. Hertler, W. Mahler, R. E. Benson and W. E. Mochel, *J. Am. Chem. Soc.*, 1962, **84**, 3374–3387; (*b*) J. Ferraris, D. O. Cowan, V. Walatka and J. H. Perlstein, *J. Am. Chem. Soc.*, 1973, **95**, 948–949; (*c*) R. Jain, K. Kabir, J. B. Gilroy, K. A. R. Mitchell, K.-C. Wong and R. G. Hicks, *Nature*, 2007, **445**, 291–294.
4 (*a*) S. L. Tait, Y. Wang, G. Costantini, N. Lin, A. Baraldi, F. Esch, L. Petaccia, S. Lizzit and K. Kern, *J. Am. Chem. Soc.*, 2008, **130**, 2108–2113; (*b*) T.-C. Tseng, C. Lin, X. Shi, S. L. Tait, X. Liu, U. Starke, N. Lin, R. Zhang, C. Minot, M. A. Van Hove, J. I. Cerdá and K. Kern, *Phys. Rev. B*, 2009, **80**, 155458; (*c*) S. Stepanow, R. Ohmann, F. Leroy, N. Lin, T. Strunskus, C. Wöll and K. Kern, *ACS Nano*, 2010, **4**, 1813–1820; (*d*) X. Q. Shi, C. Lin, C. Minot, T.-C. Tseng, S. L. Tait, N. Lin, R. Q. Zhang, K. Kern, J. I. Cerdá and M. A. Van Hove, *J. Phys. Chem. C*, 2010, **114**, 17197–17204.
5 I. Torrente, K. Franke and J. Pascual, *Int. J. Mass Spectrom.*, 2008, **277**, 269–273.
6 (*a*) J. M. Lindquist and J. C. Hemminger, *J. Phys. Chem.*, 1988, **92**, 1394–1396; (*b*) J. M. Lindquist and J. C. Hemminger, *Chem. Mater.*, 1989, **1**, 72–78; (*c*) W. D. Grobman, R. A. Pollak, D. E. Eastman, E. T. Maas and B. A. Scott, *Phys. Rev. Lett.*, 1974, **32**, 534.
7 (*a*) S. Hüfner, *Photoelectron spectroscopy: principles and applications*, Springer, Berlin, 3rd edn, 2003; (*b*) H. Ishii, K. Sugiyama, E. Ito and K. Seki, *Adv. Mater.*, 1999, **11**, 605–625.
8 (*a*) T.-C. Tseng, C. Urban, Y. Wang, R. Otero, S. L. Tait, M. Alcamí, D. Écija, M. Trelka, J. M. Gallego, N. Lin, M. Konuma, U. Starke, A. Nefedov, A. Langner, C. Wöll, M. Á. Herranz, F. Martín, N. Martín, K. Kern and R. Miranda, *Nat. Chem.*, 2010, **2**, 374–379; (*b*) I. S. Chae, S. W. Kang, J. Y. Park, Y.-G. Lee, J. H. Lee, J. Won and Y. S. Kang, *Angew. Chem., Int. Ed.*, 2011, **50**, 2982–2985.
9 (*a*) J. Farges, A. Brau and P. Dupuis, *Solid State Commun.*, 1985, **54**, 531–535; (*b*) X.-L. Mo, G.-R. Chen, Q.-J. Cai, Z.-Y. Fan, H.-H. Xu, Y. Yao, J. Yang, H.-H. Gu and Z.-Y. Hua, *Thin Solid Films*, 2003, **436**, 259–263; (*c*) E. T. Maas Jr., *Mater. Res. Bull.*, 1974, **9**, 815–826.
10 H. Piao, K. Adib and M. A. Barteau, *Surf. Sci.*, 2004, **557**, 13–20.
11 J. L. LaRue, J. D. White, N. H. Nahler, Z. Liu, Y. Sun, P. A. Pianetta, D. J. Auerbach and A. M. Wodtke, *J. Chem. Phys.*, 2008, **129**, 024709.

Supporting Information

Assembly of 2D ionic layers by reaction of alkali halides with the organic electrophile 7,7,8,8-tetracyano-p-quinodimethane (TCNQ)

Christian Wäckerlin,[a] Cristian Iacovita,[b] Dorota Chylarecka,[a] Petra Fesser,[c] Thomas A. Jung*,[a] and Nirmalya Ballav*,[d]

[a] Laboratory for Micro- and Nanotechnology, Paul Scherrer Institute, 5232 Villigen, Switzerland.
E-mail: nballav@iiserpune.ac.in; thomas.jung@psi.ch; Fax: +41-56-310-2646; Tel: +41-56-310-4518
[b] Department of Physics, University of Basel, 4056 Basel, Switzerland
[c] Laboratory for Organic Chemistry, Department of Chemistry and Applied Biosciences, ETH Zürich, 8093 Zürich, Switzerland
[d] Indian Institute of Science Education and Research, Pune 411008, India

Addition of LiCl onto TCNQ/Au(111)

The STM image of the TCNQ+LiCl/Au(111) system (Fig. S1) exhibits a similar arrangement to TCNQ+NaCl/Au(111) system. XPS data for TCNQ+LiCl/Au(111) in submonolayer and multilayer regimes are shown in Fig. S2. In both, the NaCl and LiCl case, a significant decrease in N1s binding energy is observed after deposition of the ionic compound. Furthermore the C1s peak shape is modified consistently, as discussed in the main text for the TCNQ+NaCl/Au(111) sample.
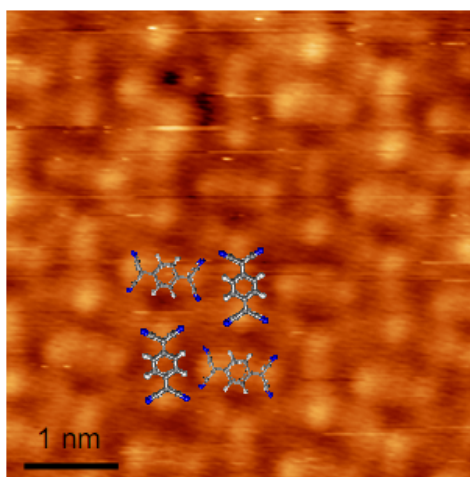
Figure S1: STM image of TCNQ molecules on Au(111) surface with subsequently evaporated LiCl.
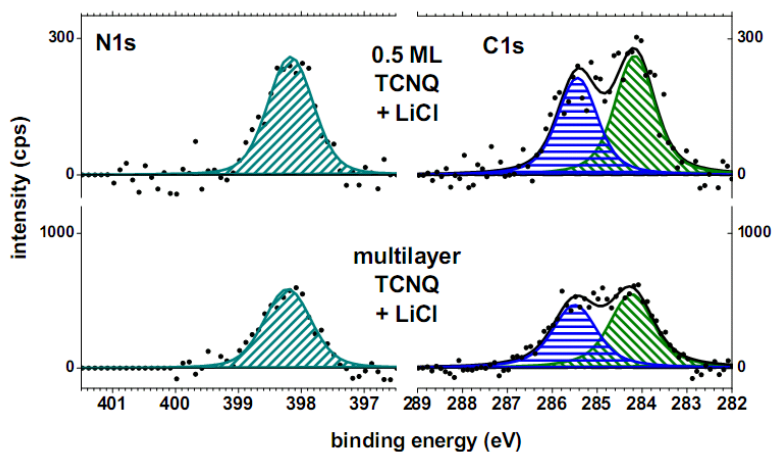
Figure S2: XPS data for TCNQ+LiCl/Au(111) in a submonolayer and multilayer regime.

Bias dependent STM of TCNQ+NaCl/Au(111)

Fig. S3 shows STM images of TCNQ+NaCl/Au(111) obtained at three different bias voltages. Intra-molecular resolution as shown in Fig. 1c was obtained with bias voltages close to -1.45 V.
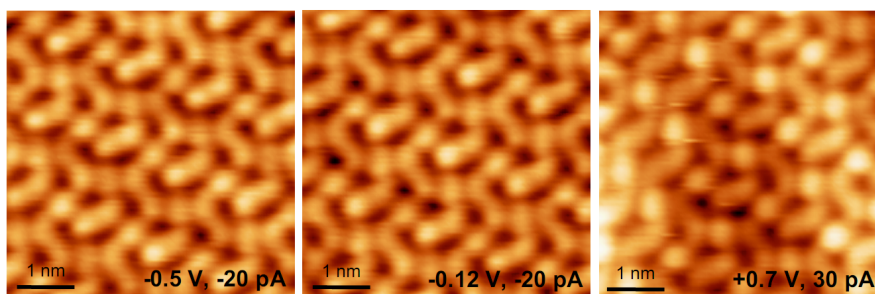
Figure S3: STM images of TCNQ+NaCl/Au(111) at different tunneling parameters

Dynamic vacancies in TCNQ/Ag(111)

Fig. S4 shows two subsequently taken STM images of TCNQ/Ag(111). By superposition of these two images the mobility of interstitial Ag can be visualized. Overlay data taken on the TCNQ/Ag(111) system displayed in Fig. 3. The numbers of vacancies are given in Tab. S1.
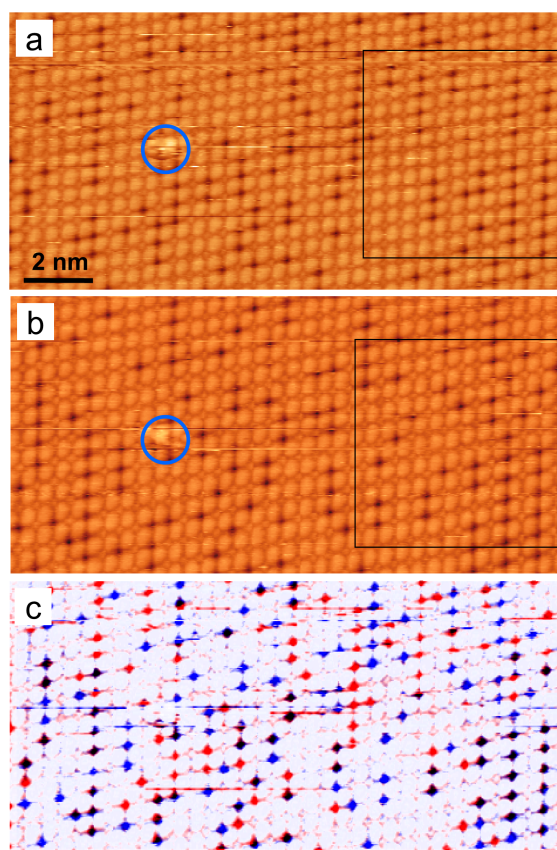
Figure S4: STM data of TNCQ/Ag(111). The two images a) and b) were recorded within 2 minutes. A
differential visualization of the vacancies is shown in c). Black dots correspond to vacancies observed in
both images, red dots indicate the vacancies appearing in the second image, while blue dots reveal the
vacancies visible in the first image and disappearing in the second image. A prominent defect is marked
(blue circle) to illustrate that the same sample area has been measured. The rectangular black frames denote
the section of the data chosen in preparation of Fig. 3 in the main text to support the frustrated dynamics of
the ionic layer.

	Number	Percentage
Total (vacant + full)	421	100 %
vacancies in a)	122	29.0 %
vacancies in b)	123	29.2 %
vacancies observed in both a) and b)	53	12.6 %

Table S1. Numbers of occupied and vacant sites in TCNQ/Ag(111) from Fig. 3

Experimental conditions

The experiments have been performed in ultra-high vacuum environment in a multi-chamber system with a base pressure in the order of 10^{-10} mbar. Au(111) and Ag(111) single crystals were cleaned by repeated sputtering / annealing cycles until no O1s and C1s peaks were observable in the XP spectrum. TCNQ and NaCl/LiCl (Sigma-Aldrich) were sublimed consecutively (first TCNQ and then NaCl) in a 1:2 molar ratio onto single crystals kept at room temperature. The deposition rate was monitored by a quartz crystal microbalance and the monolayer coverage was confirmed by XPS and STM. XPS has been measured using monochromatic Al Kα line. The full with half maximum of the Au4f$_{7/2}$ peak was 0.8 eV.

Valence spectra have been acquired using UV light generated by He I excitation (21.22 eV) and with an applied sample bias of ~-9 V. STM measurements have been performed at room temperature in constant current mode using electrochemically etched and in-situ sputtered tungsten tips. The respective tunneling parameters are given in Tab. S2.

Figure	Sample	Bias voltage (V)	Tunnel current (pA)
1a	TCNQ/Au(111)	-0.7	-10
1a (inset)	TCNQ/Au(111)	1.95	50
1b	TCNQ+NaCl/Au(111)	-1.3	-30
1c	TCNQ+NaCl/Au(111)	-1.45	-20
3; S4	TCNQ/Ag(111)	-0.5	-50
S1	TCNQ+LiCl/Au(111)	-0.9	-10
S3a	TCNQ+NaCl/Au(111)	-0.5	-20
S3b	TCNQ+NaCl/Au(111)	-0.12	-20
S3c	TCNQ+NaCl/Au(111)	0.7	30

Table S2 Tunneling parameters used in the generation of the STM images shown.

Conclusion

As discussed in the introduction, the complexity found in nature with its highly developed nanomachines demonstrates the possibilities and the prospects of molecular nanotechnology. In contrast to nature, the metal-organic complexes, shown here, are simple and well understood, the single-crystal surfaces are well defined and the used chemical stimuli are among the simplest ligands possible. On the basis of the above discussed example of heme b in hemoglobin it is not a surprise that a reasonable description of the ad-complexes magnetochemistry requires often (but not always) to include the substrate into considerations.[[2]]

This thesis deals with the questions i) how coordination chemistry can be used to control the magnetic properties of square-planar ad-complexes and ii) how the surface modifies the magnetochemistry of the ad-complexes. The on-surface magnetochemistry of the complexes is studied on ferromagnetic substrates which induce a magnetic moment into the molecular monolayer, thus the axial ligation acts on the induced magnetic moment which is a consequence of the spin-state of the ad-complexes. This arrangement also allows to study the influence of the axial ligation onto the exchange interaction with the ferromagnetic substrate. The element specific spectroscopies (XAS, XMCD and XPS) allow for a methodically interesting approach towards (on-surface) coordination chemistry. The spectroscopy methods are complemented by STM experiments which allow for the direct imaging of the ad-complexes and their axial ligands. The experimental results are complemented by DFT+U calculations.

This thesis shows that the magnetic moment in a monolayer of molecules can be controlled by the use of chemical stimuli.[[1–4]] We demonstrate that the axial ligation can *switch-off* [[1–3]] the magnetic moment in ferromagnetically and antiferromagnetically exchange-coupled ad-complexes. This can be achieved by i) using the spin-bearing NO ligand (S = 1/2) in combination

with the odd-spin CoTPP ad-complex (S = 1/2) as well as by ii) using the non-spin bearing NH_3 ligand (S = 0) in combination with the even-spin FePc ad-complex (S = 1). This demonstrates that the magnetic moment can be quenched by cancellation of the unpaired electrons (i) as well as by ligand-field effects (ii) inducing low-spin states. Using even-spin FeTPP (S = 1) and NO allows for the tuning of the magnetic moment.[[2, 3]] Furthermore, this thesis shows that a magnetic moment can be also induced by coordination-chemistry.[[4]] Many of the chemical reactions, presented here, are reversible, i.e. the initial state can be recovered by thermal annealing.

The coordination of a ligand on one side of a complex has usually consequences for the chemical bond with an other ligand on the other side of the complex (trans effect).[15, 23] It has been shown that this is also the case for the chemical bond with the surface (surface trans effect).[31] We show that, though this effect, apart from having consequences for the magnetic moment of the ad-complex, the axial ligation can also *modify the exchange interaction* with the ferromagnetic substrate (we propose the term *spin trans effect*).[[2]] Specifically, we found that i) the *strength*, as well as ii) the *sign of the exchange interaction* can be modified. This, as well as the modified magnetic moments found in the DFT+U calculations, is evidence that in order to understand the magnetic properties and the coordination chemistry at the organic – inorganic interface, one needs to include the substrate into the considerations.

Furthermore, we demonstrate that by using chemically directed self-assembly (as found in biological systems), two metal-organic molecules, with distinct magnetic centers (Fe and Mn), can be arranged into a supramolecular *chessboard-array* by mere co-evaporation.[[3]] With a chemical stimulus we were able to *selectively switch-off* one of the components in the chessboard-array. We directly imaged the ligand binding to the metal-organic complexes. Note that both, the chemically directed self-assembly as well as the magnetochemical control over the magnetic moments do scale very well with the number of involved molecules. As such, both approaches are clearly distinct from STM-based atom-by-atom manipulation used to fabricate and control magnetic nanostructures. Of course, the fabricated magnetic chessboard is only a simple structure, however it may allow for the study of the intermolecular exchange interaction (on a non-magnetic substrate) and can enable spin-polarized diffraction experiments. The demonstrated selective switching of the one-half of the magnetic chessboard-lattice is a straightforward way to control the magnetic unit-cell. Furthermore, since functional self-assembled nanomachines exist in biological systems,[8, 9] the possibility to use molecular self-assembly for the fabrication of very complex functional structures is already demonstrated.

It is evident that the chemical stimuli act as an input to control the magnetic properties of on-surface complexes. We are aware of the fact that the *chemical* stimuli used as *input* in these studies are distinct from physical stimuli (e.g. light or electric fields) as commonly used in solid-state devices for information processing. But the above examples from nature show that complex logic operations can be based on inputs via chemical stimuli.[10]

It would be exciting to study the on-surface magnetochemistry of metal-organic complexes by

a local probe like STM, i.e. by spin-polarized / inelastic tunneling.[45] At present, I am not aware of an STM study on the consequences of the surface trans effect onto the surface's magnetic properties. For example, the proposed spin-polarized interference pattern around a magnetic ad-atom / molecule [82, 83] should be related to the ad-complexes interfacial hybridization with the substrate. Since the axial ligation of the ad-complex modifies the substrate's electronic states by modification of the interaction between the ad-complex and the substrate, this may result in a modification of the spin-polarized interference pattern.

The results shown in this thesis may be useful in the context of organic spintronics, in particular at the organic – inorganic interface. They may find applications in magnetochemical sensors or as a means to control and fine tune the magnetic properties of ad-complexes in spintronic devices. We hope to contribute to the understanding of coordination-chemistry on the surface, specifically magnetochemistry on the surface. The studies demonstrate the successful use of XAS and XMCD as experimental methods to get a spectroscopic insight into the chemical reactions at surfaces and their impact on magnetic properties. By using STM as a tool to manipulate the axial ligands, the magnetic properties of individual ad-complexes could be controlled. Since the magnetochemical approach provides a straightforward way to control the magnetic quantum-state in a molecule, this may serve as an input for spintronic few-molecule devices or even devices exploiting the quantum nature of spin and its entanglement.

Bibliography

[1] E. HOWARD. Information Age. In *Wiley Encyclopedia of Computer Science and Engineering*. John Wiley & Sons, Hoboken, NJ (2009). ISBN 9780470050118.

[2] J. GLEICK. *The information: A history, A theory, A flood*. Vintage Books, New York (2011). ISBN 9781400096237.

[3] C. E. SHANNON and W. WEAVER. *The Mathematical Theory of Communication*. The University of Illinois Press, Urbana, IL (1949).

[4] D. BRAGA and G. HOROWITZ. High-Performance Organic Field-Effect Transistors. *Adv. Mater.*, **21**, 14-15, 1473–1486 (2009). DOI:10.1002/adma.200802733.

[5] R. JANSEN. Silicon spintronics. *Nat. Mater.*, **11**, 5, 400–408 (2012). DOI:10.1038/nmat3293.

[6] W. LU and C. M. LIEBER. Nanoelectronics from the bottom up. *Nat. Mater.*, **6**, 11, 841–850 (2007). DOI:10.1038/nmat2028.

[7] S. SANVITO. Molecular spintronics. *Chem. Soc. Rev.*, **40**, 6, 3336 (2011). DOI:10.1039/c1cs15047b.

[8] J. M. BERG, J. L. TYMOCZKO and L. STRYER. *Biochemistry*. W. H. Freeman, New York (2002). ISBN 978-0716749554.

[9] N. A. CAMPBELL, A. KRATOCHWIL, T. LAZAR and J. B. REECE. *Biologie*. Pearson Studium, München (2009). ISBN 9783827372871.

[10] S. M. DOUGLAS, I. BACHELET and G. M. CHURCH. A Logic-Gated Nanorobot for Targeted Transport of Molecular Payloads. *Science*, **335**, 6070, 831–834 (2012). DOI:10.1126/science.1214081.

[11] K. M. KADISH, K. M. SMITH and R. GUILARD. *The Porphyrin Handbook*. Academic Press (1999). ISBN 9780123932006.

[12] H. CHEN, M. IKEDA-SAITO and S. SHAIK. Nature of the Fe-O2 Bonding in Oxy-Myoglobin: Effect of the Protein. *J. Am. Chem. Soc.*, **130**, 44, 14778–14790 (2008). DOI:10.1021/ja805434m.

[13] W. R. SCHEIDT and C. A. REED. Spin-state/stereochemical relationships in iron porphyrins: implications for the hemoproteins. *Chem. Rev.*, **81**, 6, 543–555 (1981). DOI:10.1021/cr00046a002.

[14] A. SCHEYBAL, T. RAMSVIK, R. BERTSCHINGER, M. PUTERO, F. NOLTING and T. A. JUNG. Induced magnetic ordering in a molecular monolayer. *Chem. Phys. Lett.*, **411**, 1-3, 214–220 (2005). DOI:10.1016/j.cplett.2005.06.017.

[15] J. HUHEEY. *Inorganic chemistry: principles of structure and reactivity*. HarperCollins College Publishers, New York, 4th ed. edition (1993). ISBN 9780060429959.

[16] W. KAIM and B. SCHWEDERSKI. Non-innocent ligands in bioinorganic chemistry—An overview. *Coordin. Chem. Rev.*, **254**, 13-14, 1580–1588 (2010). DOI:10.1016/j.ccr.2010.01.009.

[17] T. Q. NGUYEN, M. C.-S. ESCAÑO and H. KASAI. Nitric Oxide Adsorption Effects on Metal Phthalocyanines. *J. Phys. Chem. B*, **114**, 31, 10017–10021 (2010). DOI:10.1021/jp1035426.

[18] H. WENDE, M. BERNIEN, J. LUO, C. SORG, N. PONPANDIAN, J. KURDE, J. MIGUEL, M. PIANTEK, X. XU, P. ECKHOLD, W. KUCH, K. BABERSCHKE, P. M. PANCHMATIA, B. SANYAL, P. M. OPPENEER and O. ERIKSSON. Substrate-induced magnetic ordering and switching of iron porphyrin molecules. *Nat. Mater.*, **6**, 7, 516–520 (2007). DOI:10.1038/nmat1932.

[19] M. BERNIEN, X. XU, J. MIGUEL, M. PIANTEK, PH. ECKHOLD, J. LUO, J. KURDE, W. KUCH, K. BABERSCHKE, H. WENDE and P. SRIVASTAVA. Fe-porphyrin monolayers on ferromagnetic substrates: Electronic structure and magnetic coupling strength. *Phys. Rev. B*, **76**, 21, 214406 (2007). DOI:10.1103/PhysRevB.76.214406.

[20] M. BERNIEN, J. MIGUEL, C. WEIS, MD. E. ALI, J. KURDE, B. KRUMME, P. M. PANCHMATIA, B. SANYAL, M. PIANTEK, P. SRIVASTAVA, K. BABERSCHKE, P. M. OPPENEER, O. ERIKSSON, W. KUCH and H. WENDE. Tailoring the Nature of Magnetic Coupling of Fe-Porphyrin Molecules to Ferromagnetic Substrates. *Phys. Rev. Lett.*, **102**, 4, 047202 (2009). DOI:10.1103/PhysRevLett.102.047202.

[21] D. CHYLARECKA, C. WÄCKERLIN, T. K. KIM, K. MÜLLER, F. NOLTING, A. KLEIBERT, N. BALLAV and T. A. JUNG. Self-Assembly and Superexchange Coupling of Magnetic Molecules on Oxygen-Reconstructed Ferromagnetic Thin Film. *J. Phys. Chem. Lett.*, **1**, 9, 1408–1413 (2010). DOI:10.1021/jz100253c.

[22] D. CHYLARECKA, T. K. KIM, K. TARAFDER, K. MÜLLER, K. GÖDEL, I. CZEKAJ, C. WÄCKERLIN, M. CINCHETTI, MD. E. ALI, C. PIAMONTEZE, F. SCHMITT, J.-P. WÜSTENBERG, C. ZIEGLER, F. NOLTING, M. AESCHLIMANN, P. M. OPPENEER, N. BALLAV and T. A. JUNG. Indirect Magnetic Coupling of Manganese Porphyrin to a Ferromagnetic Cobalt Substrate. *J. Phys. Chem. C*, **115**, 4, 1295–1301 (2011). DOI:10.1021/jp106822s.

[23] B. J. COE and S. J. GLENWRIGHT. Trans-effects in octahedral transition metal complexes. *Coordin. Chem. Rev.*, **203**, 1, 5–80 (2000). DOI:10.1016/S0010-8545(99)00184-8.

[24] H. HERTZ. Ueber einen Einfluss des ultravioletten Lichtes auf die electrische Entladung. *Ann. Phys.*, **267**, 8, 983–1000 (1887). DOI:10.1002/andp.18872670827.

[25] A. EINSTEIN. Über einen die Erzeugung und Verwandlung des Lichtes betreffenden heuristischen Gesichtspunkt. *Ann. Phys.*, **322**, 6, 132–148 (1905). DOI:10.1002/andp.19053220607.

[26] C. NORDLING, E. SOKOLOWSKI and K. SIEGBAHN. Precision Method for Obtaining Absolute Values of Atomic Binding Energies. *Phys. Rev.*, **105**, 5, 1676–1677 (1957). DOI:10.1103/PhysRev.105.1676.

[27] J. VICKERMAN. *Surface analysis : The principal techniques*. Wiley, Chichester U.K., 2nd ed. edition (2009). ISBN 9780470017630.

[28] C. FADLEY and D. SHIRLEY. Multiplet Splitting of Metal-Atom Electron Binding Energies. *Phys. Rev. A*, **2**, 4, 1109–1120 (1970). DOI:10.1103/PhysRevA.2.1109.

[29] T. LUKASCZYK, K. FLECHTNER, L.R. MERTE, N. JUX, F. MAIER, J.M. GOTTFRIED and H.-P. STEINRUCK. Interaction of Cobalt(II) Tetraarylporphyrins with a Ag(111) Surface Studied with Photoelectron Spectroscopy. *J. Phys. Chem. C*, **111**, 7, 3090–3098 (2007). DOI:10.1021/jp0652345.

[30] K. FLECHTNER, A. KRETSCHMANN, H.-P. STEINRÜCK and J. M. GOTTFRIED. NO-Induced Reversible Switching of the Electronic Interaction between a Porphyrin-Coordinated Cobalt Ion and a Silver Surface. *J. Am. Chem. Soc.*, **129**, 40, 12110–12111 (2007). DOI:10.1021/ja0756725.

[31] W. HIERINGER, K. FLECHTNER, A. KRETSCHMANN, K. SEUFERT, W. AUWÄRTER, JOHANNES V. BARTH, A. GÖRLING, H.-P. STEINRÜCK and J. M. GOTTFRIED. The

Surface Trans Effect: Influence of Axial Ligands on the Surface Chemical Bonds of Adsorbed Metalloporphyrins. *J. Am. Chem. Soc.*, **133**, 6206–6222 (2011). DOI:10.1021/ja1093502.

[32] H. ISHII, K. SUGIYAMA, E. ITO and K. SEKI. Energy Level Alignment and Interfacial Electronic Structures at Organic/Metal and Organic/Organic Interfaces. *Adv. Mater.*, **11**, 8, 605–625 (1999). DOI:10.1002/(SICI)1521-4095(199906)11:8<605::AID-ADMA605>3.0.CO;2-Q.

[33] J. BEARDEN and A. BURR. Reevaluation of X-Ray Atomic Energy Levels. *Rev. Mod. Phys.*, **39**, 1, 125–142 (1967). DOI:10.1103/RevModPhys.39.125.

[34] J. STÖHR. *NEXAFS spectroscopy*. Number 25 in Springer series in surface sciences. Springer, Berlin, 1st ed. corr. print edition (1996). ISBN 3540544224.

[35] J. STÖHR, K. BABERSCHKE, R. JAEGER, R. TREICHLER and S. BRENNAN. Orientation of Chemisorbed Molecules from Surface-Absorption Fine-Structure Measurements: CO and NO on Ni(100). *Phys. Rev. Lett.*, **47**, 5, 381–384 (1981). DOI:10.1103/PhysRevLett.47.381.

[36] G. VAN DER LAAN, B. THOLE, G. SAWATZKY, J. GOEDKOOP, J. FUGGLE, J.-M. ESTEVA, R. KARNATAK, J. REMEIKA and H. DABKOWSKA. Experimental proof of magnetic x-ray dichroism. *Phys. Rev. B*, **34**, 9, 6529–6531 (1986). DOI:10.1103/PhysRevB.34.6529.

[37] J. GOULON, C. GOULON-GINET, A. ROGALEV, V. GOTTE, C. MALGRANGE, C. BROUDER and C. R. NATOLI. X-ray natural circular dichroism in a uniaxial gyrotropic single crystal of LiIO3. *J. Chem. Phys.*, **108**, 15, 6394 (1998). DOI:10.1063/1.476046.

[38] G. SCHÜTZ, W. WAGNER, W. WILHELM, P. KIENLE, R. ZELLER, R. FRAHM and G. MATERLIK. Absorption of circularly polarized x rays in iron. *Phys. Rev. Lett.*, **58**, 7, 737–740 (1987). DOI:10.1103/PhysRevLett.58.737.

[39] J. STÖHR and H. C. SIEGMANN. *Magnetism: From Fundamentals to Nanoscale Dynamics*. Springer, Berlin, 1st ed. edition (2006). ISBN 9783540302827.

[40] C. DAVISSON and L. GERMER. Diffraction of Electrons by a Crystal of Nickel. *Phys. Rev.*, **30**, 6, 705–740 (1927). DOI:10.1103/PhysRev.30.705.

[41] K. OURA. *Surface science : An introduction*. Springer, Berlin (2003). ISBN 9783540005452.

[42] G. BINNIG, H. ROHRER, CH. GERBER and E. WEIBEL. Surface Studies by Scanning Tunneling Microscopy. *Phys. Rev. Lett.*, **49**, 1, 57–61 (1982). DOI:10.1103/PhysRevLett.49.57.

[43] C. CHEN. *Introduction to scanning tunneling microscopy*. Oxford University Press, Oxford, 2nd ed. edition (2008). ISBN 9780199211500.

[44] R. HOLM. The Electric Tunnel Effect across Thin Insulator Films in Contacts. *J. Appl. Phys.*, **22**, 5, 569 (1951). DOI:10.1063/1.1700008.

[45] K. VON BERGMANN and A. KUBETZKA. Magnetic Sensitive Scanning Tunneling Microscopy. In E. N. KAUFMANN (editor), *Characterization of Materials*. John Wiley & Sons, Inc., Hoboken, NJ, USA (2012). ISBN 0471266965, 9780471266969.

[46] A. CEULEMANS, W. OLDENHOF, C. GORLLER-WALRAND and L. G. VANQUICKEN-BORNE. Gouterman's "four-orbital" model and the MCD spectra of high-symmetry metalloporphyrins. *J. Am. Chem. Soc.*, **108**, 6, 1155–1163 (1986). DOI:10.1021/ja00266a007.

[47] B. B. WAYLAND and J. V. MINKIEWICZ. Reactions of nitric oxide with cobalt(II) tetraphenylporphyrin: a unique bis nitric oxide complex. *J. Chem. Soc. Chem. Comm.*, , 24, 1015 (1976). DOI:10.1039/c39760001015.

[48] R. SESSOLI, D. GATTESCHI, A. CANESCHI and M. A. NOVAK. Magnetic bistability in a metal-ion cluster. *Nature*, **365**, 6442, 141–143 (1993). DOI:10.1038/365141a0.

[49] M. MANNINI, F. PINEIDER, P. SAINCTAVIT, C. DANIELI, E. OTERO, C. SCIANCALE-PORE, A. M. TALARICO, M.-A. ARRIO, A. CORNIA, D. GATTESCHI and R. SESSOLI. Magnetic memory of a single-molecule quantum magnet wired to a gold surface. *Nat. Mater.*, **8**, 3, 194–197 (2009). DOI:10.1038/nmat2374.

[50] S. STEPANOW, A. MUGARZA, G. CEBALLOS, P. MORAS, J. C. CEZAR, C. CARBONE and P. GAMBARDELLA. Giant spin and orbital moment anisotropies of a Cu-phthalocyanine monolayer. *Phys. Rev. B*, **82**, 1, 014405 (2010). DOI:10.1103/PhysRevB.82.014405.

[51] C. IACOVITA, M. RASTEI, B. HEINRICH, T. BRUMME, J. KORTUS, L. LIMOT and J. BUCHER. Visualizing the Spin of Individual Cobalt-Phthalocyanine Molecules. *Phys. Rev. Lett.*, **101**, 11, 116602 (2008). DOI:10.1103/PhysRevLett.101.116602.

[52] P. GAMBARDELLA, S. STEPANOW, A. DMITRIEV, J. HONOLKA, F. M. F. DE GROOT, M. LINGENFELDER, S. S. GUPTA, D. D. SARMA, P. BENCOK, S. STANESCU, S. CLAIR, S. PONS, N. LIN, A.I P. SEITSONEN, H. BRUNE, J. V. BARTH and K. KERN. Supramolecular control of the magnetic anisotropy in two-dimensional high-spin Fe arrays at a metal interface. *Nat. Mater.*, **8**, 3, 189–193 (2009). DOI:10.1038/nmat2376.

[53] C. KITTEL. *Introduction to solid state physics*. Wiley, New York, 7th ed. edition (1996). ISBN 9780471111818.

[54] J. MIGUEL, C. F. HERMANNS, M. BERNIEN, A. KRÜGER and W. KUCH. Reversible Manipulation of the Magnetic Coupling of Single Molecular Spins in Fe-Porphyrins to a Ferromagnetic Substrate. *J. Phys. Chem. Lett.*, **2**, 12, 1455–1459 (2011). DOI:10.1021/jz200489y.

[55] K. FLECHTNER, A. KRETSCHMANN, L. R. BRADSHAW, M.-M. WALZ, H.-P. STEIN-RUCK and J. M. GOTTFRIED. Surface-Confined Two-Step Synthesis of the Complex (Ammine)(meso-tetraphenylporphyrinato)-zinc(II) on Ag(111). *J. Phys. Chem. C*, **111**, 16, 5821–5824 (2007). DOI:10.1021/jp071531d.

[56] C. ISVORANU, B. WANG, K. SCHULTE, E. ATAMAN, J. KNUDSEN, J. N. ANDERSEN, M. L. BOCQUET and J. SCHNADT. Tuning the spin state of iron phthalocyanine by ligand adsorption. *J. Phys.: Condens. Matter*, **22**, 47, 472002 (2010). DOI:10.1088/0953-8984/22/47/472002.

[57] B. B. WAYLAND, L. W. OLSON and Z. U. SIDDIQUI. Nitric oxide complexes of manganese and chromium tetraphenylporphyrin. *J. Am. Chem. Soc.*, **98**, 1, 94–98 (1976). DOI:10.1021/ja00417a016.

[58] J. V. BARTH. Molecular Architectonic on Metal Surfaces. *Annu. Rev. Phys. Chem.*, **58**, 1, 375–407 (2007). DOI:10.1146/annurev.physchem.56.092503.141259.

[59] K. W. HIPPS, L. SCUDIERO, D. E. BARLOW and M. P. COOKE. A Self-Organized 2-Dimensional Bifunctional Structure Formed by Supramolecular Design. *J. Am. Chem. Soc.*, **124**, 10, 2126–2127 (2002). DOI:10.1021/ja017561q.

[60] L. SCUDIERO, K. W. HIPPS and D. E. BARLOW. A Self-Organized Two-Dimensional Bimolecular Structure. *J. Phys. Chem. B*, **107**, 13, 2903–2909 (2003). DOI:10.1021/jp026875c.

[61] N. TSUKAHARA, K. NOTO, M. OHARA, S. SHIRAKI, N. TAKAGI, S. SHIN and M. KAWAI. Adsorption-Induced Switching of Magnetic Anisotropy in a Single Iron(II) Phthalocyanine Molecule on an Oxidized Cu(110) Surface. *Phys. Rev. Lett.*, **102**, 16, 167203 (2009). DOI:10.1103/PhysRevLett.102.167203.

[62] J. BREDE, N. ATODIRESEI, S. KUCK, P. LAZIĆ, V. CACIUC, Y. MORIKAWA, G. HOFF-MANN, S. BLÜGEL and R. WIESENDANGER. Spin- and Energy-Dependent Tunneling through a Single Molecule with Intramolecular Spatial Resolution. *Phys. Rev. Lett.*, **105**, 4, 047204 (2010). DOI:10.1103/PhysRevLett.105.047204.

[63] I. TORRENTE, K. FRANKE and J. PASCUAL. Structure and electronic configuration of tetracyanoquinodimethane layers on a Au(111) surface. *Int. J. Mass. Spectrom.*, **277**, 1-3, 269–273 (2008). DOI:10.1016/j.ijms.2008.07.013.

[64] T.C. TSENG, C. LIN, X. SHI, S. L. TAIT, X. LIU, U. STARKE, N. LIN, R. ZHANG, C. MINOT, M. A. VAN HOVE, J. I. CERDÁ and K. KERN. Two-dimensional metal-organic coordination networks of Mn-7,7,8,8-tetracyanoquinodimethane assembled on Cu(100): Structural, electronic, and magnetic properties. *Phys. Rev. B*, **80**, 15, 155458 (2009). DOI:10.1103/PhysRevB.80.155458.

[65] X. Q. Shi, C. Lin, C. Minot, T.-C. Tseng, S. L. Tait, N. Lin, R. Q. Zhang, K. Kern, J. Cerdá and M. A. Van Hove. Structural Analysis and Electronic Properties of Negatively Charged TCNQ: 2D Networks of (TCNQ)2 Mn Assembled on Cu(100). *J. Phys. Chem. C*, **114**, 40, 17197–17204 (2010). DOI:10.1021/jp104954w.

[66] T.C. Tseng, N. Abdurakhmanova, S. Stepanow and K. Kern. Hierarchical Assembly and Reticulation of Two-Dimensional Mn- and Ni–TCNQx (x = 1, 2, 4) Coordination Structures on a Metal Surface. *J. Phys. Chem. C*, (page 110502084400031) (2011). DOI:10.1021/jp2033643.

[67] N. Abdurakhmanova, A. Floris, T.-C. Tseng, A. Comisso, S. Stepanow, A. De Vita and K. Kern. Stereoselectivity and electrostatics in charge-transfer Mn- and Cs-TCNQ4 networks on Ag(100). *Nat. Commun.*, **3**, 940 (2012). DOI:10.1038/ncomms1942.

[68] J. M. Lindquist and J. C. Hemminger. High-resolution core level photoelectron spectra of solid TCNQ: determination of molecular orbital spatial distribution from localized shake-up features. *J. Phys. Chem.*, **92**, 6, 1394–1396 (1988). DOI:10.1021/j100317a005.

[69] J. M. Lindquist and J. C. Hemminger. High energy resolution x-ray photoelectron spectroscopy studies of tetracyanoquinodimethane charge transfer complexes with copper, nickel, and lithium. *Chem. Matr.*, **1**, 1, 72–78 (1989). DOI:10.1021/cm00001a017.

[70] W. D. Grobman, R. A. Pollak, D. E. Eastman, E. T. Maas and B. A. Scott. Valence Electronic Structure and Charge Transfer in Tetrathiofulvalinium Tetracyanoquinodimethane (TTF-TCNQ) from Photoemission Spectroscopy. *Phys. Rev. Lett.*, **32**, 10, 534 (1974). DOI:10.1103/PhysRevLett.32.534.

[71] P. Fesser, C. Iacovita, C. Wäckerlin, S. Vijayaraghavan, N. Ballav, K. Howes, J. P. Gisselbrecht, M. Crobu, C. Boudon, M. Stöhr, T. A. Jung and F. Diederich. Visualizing the Product of a Formal Cycloaddition of 7,7,8,8-Tetracyano-p-quinodimethane (TCNQ) to an Acetylene-Appended Porphyrin by Scanning Tunneling Microscopy on Au(111). *Chem. Eur. J.*, **17**, 19, 5246–5250 (2011). DOI:10.1002/chem.201100733.

[72] T. Hählen, C. Vanoni, C. Wäckerlin, T. A. Jung and S. Tsujino. Surface doping in pentacene thin-film transistors with few monolayer thick channels. *Appl. Phys. Lett.*, **101**, 3, 033305 (2012). DOI:10.1063/1.4737214.

[73] I. Fernández-Torrente, K. Franke and J. I. Pascual. Vibrational Kondo Effect in Pure Organic Charge-Transfer Assemblies. *Phys. Rev. Lett.*, **101**, 21 (2008). DOI:10.1103/PhysRevLett.101.217203.

[74] R. Jain, K. Kabir, J. B. Gilroy, K. A. R. Mitchell, K. Wong and R. G. Hicks. High-temperature metal–organic magnets. *Nature*, **445**, 7125, 291–294 (2007). DOI:10.1038/nature05439.

[75] N. Abdurakhmanova, T.-C. Tseng, A. Langner, C. S. Kley, V. Sessi, S. Stepanow and K. Kern. Superexchange-Mediated Ferromagnetic Coupling in Two-Dimensional Ni-TCNQ Networks on Metal Surfaces. *Phys. Rev. Lett.*, **110**, 2 (2013). DOI:10.1103/PhysRevLett.110.027202.

[76] D. S. Acker and W. R. Hertler. Substituted Quinodimethans. I. Preparation and Chemistry of 7,7,8,8-Tetracyanoquinodimethan. *J. Am. Chem. Soc.*, **84**, 17, 3370–3374 (1962). DOI:10.1021/ja00876a028.

[77] L. R. Melby, R. J. Harder, W. R. Hertler, W. Mahler, R. E. Benson and W. E. Mochel. Substituted Quinodimethans. II. Anion-radical Derivatives and Complexes of 7,7,8,8-Tetracyanoquinodimethan. *J. Am. Chem. Soc.*, **84**, 17, 3374–3387 (1962). DOI:10.1021/ja00876a029.

[78] J.-M. Lü, S. V. Rosokha, I. S. Neretin and J. K. Gimzewski. Quinones as Electron Acceptors. X-Ray Structures, Spectral (EPR, UV-vis) Characteristics and Electron-Transfer Reactivities of Their Reduced Anion Radicals as Separated vs Contact Ion Pairs. *J. Am. Chem. Soc.*, **128**, 51, 16708–16719 (2006). DOI:10.1021/ja066471o.

[79] S. Stepanow, R. Ohmann, F. Leroy, N. Lin, T. Strunskus, C. Wöll and K. Kern. Rational Design of Two-Dimensional Nanoscale Networks by Electrostatic Interactions at Surfaces. *ACS Nano*, **4**, 4, 1813–1820 (2010). DOI:10.1021/nn100303z.

[80] D. Skomski, S. Abb and S. L. Tait. Robust Surface Nano-Architecture by Alkali–Carboxylate Ionic Bonding. *J. Am. Chem. Soc.*, **134**, 34, 14165–14171 (2012). DOI:10.1021/ja3053128.

[81] D. Skomski and S. L. Tait. Ordered and Robust Ionic Surface Networks from Weakly Interacting Carboxyl Building Blocks. *J. Phys. Chem. C*, (page doi: 10.1021/jp400213a) (2013). DOI:10.1021/jp400213a.

[82] A. Stróżecka, A. Eiguren and J. I. Pascual. Quasiparticle Interference around a Magnetic Impurity on a Surface with Strong Spin-Orbit Coupling. *Phys. Rev. Lett.*, **107**, 18 (2011). DOI:10.1103/PhysRevLett.107.186805.

[83] S. Lounis, A. Bringer and S. Blügel. Magnetic Adatom Induced Skyrmion-Like Spin Texture in Surface Electron Waves. *Phys. Rev. Lett.*, **108**, 20 (2012). DOI:10.1103/PhysRevLett.108.207202.

Acknowledgments

Here, I would like to thank and acknowledge all the people who helped and supported me during my doctoral studies.

First of all, I want to thank my supervisor Thomas Jung for the possibility to work in his group and for the support he gave me during this time. I am grateful to Nirmalya Ballav for his supervision and for the many deep scientific discussions. I sincerely thank our outstanding technician Rolf Schelldorfer. Ultra-high vacuum experiments are a challenging task, because debugging them is time consuming. It is Rolf's simple, ingenious and rapidly build devices and his flexibility and high motivation to modify and fix them, which allowed for very productive experiments.

The beamtimes are clearly a group-effort. The significant complexity of the samples / experiments and the high rate of data-acquisition allowed / demanded a high effort in sample preparation and XMCD measurements. I would like to sincerely thank Nirmalya Ballav, Dorota Siewert, Kathrin Müller, Harald Rossmann, Cristian Iacovita, Tatjana Hählen, Jan Girovsky, Jan Nowakowski, Aneliia Shchyrba, Milos Baljozovic and Li Jingyi for their significant contributions. I gratefully acknowledge the SIM beamline staff: Frithjof Nolting, Armin Kleibert, Andrea Steger, Arantxa Fraile Rodriguez and Juri Honegger. Thank you for your 24/7 support in over 120 nights of beamtime.

A part of the STM experiments were performed at the Nanolab in Basel, I would like to thank Aneliia Shchyrba for her contributions as well as Sylwia Nowakowska, Jan Nowakowski, Toni Ivas, Marco Martina for help.

I sincerely thank Roland Steiner, Edith Meisel and Thomas Neiger, Soichiro Tsujino and Celestino Padeste. Simon Wenner is kindly acknowledged for the computer-rendered 3D computer graphics attached with publication [[2]]. Our chemistry collaborators, Michael Jaggi, Shi-Xia Liu and Silvio Decurtins, Petra Fesser and François Diederich are kindly acknowledged.

Curriculum vitae

Christian Wäckerlin

Born: November 30th 1983 in Siblingen, Switzerland
Nationality: Swiss
E-Mail: christian@waeckerlin.com

Education

2009 – 2013   PhD in Nanoscience, University of Basel Surface science, molecular nanoscience at the interdisciplinary interface between physics and chemistry. Investigations on the electronic and magnetic properties of square-planar metallo-organic coordination complexes on ferromagnetic surfaces and in particular the application of coordination chemistry on the surface. The focus is on how the axial ligand affects the spin of the molecules. Studies on those systems in ultra-high vacuum by a combination of local and non-local methods, namely scanning tunneling microscopy (STM), X-ray absorption and magnetic circular dichroism (XAS and XMCD), X-ray and ultra-violet photoelectron spectroscopy (XPS and UPS) and low energy electron diffraction (LEED). The experiments were performed at the Paul Scherrer Institute, the Swiss Light Source and at the University of Basel.

2007 – 2009   Master of Science, Nanoscience, University of Basel

- 3 month semester project in computational chemistry: *Ligand chemistry in truncated hemoglobin*, Prof. M. Meuwly
  Molecular dynamics simulations concerned with the diffusion of nitric oxide within the

truncated hemoglobin. The natural iron-porphyrin within the truncated hemoglobin in mycobacterium tuberculosis is responsible for the catalytic removal of nitric oxide.

- 3 month semester project in surface science: *Adhesion of TiN, AlN and TiAlN thin films on high speed steel*, Dr. Laurent Marot and Prof. P. Oelhafen
Growth of metal nitrides onto Si and steel substrates by reactive magnetron sputtering in high vacuum and characterization by X-ray and UV photoelectron spectroscopy, X-ray diffraction, scanning electron microscopy, nanoscratch/nanohardness tests.

- 6 month Master thesis in surface science: *Molecular electronics and molecular spintronics at interfaces*, Prof. T. A. Jung and Prof. P. Oelhafen
Investigations on paramagnetic transition metal complexes on oxygen-reconstructed, ferromagnetic surfaces and preliminary studies on the influence of nitric oxide onto such complexes. These complex samples were studied by X-ray and UV photoelectron spectroscopy, low energy electron diffraction, scanning tunneling microscopy and X-ray absorption spectroscopy / magnetic circular dichroism. The experiments were performed at the Paul Scherrer Institute and the Swiss Light Source.

2004 – 2007   Bachelor of Science, Major in Nanosciences, University of Basel

- 3rd generation of Nanoscience Students in Basel

1999 – 2003   Matura, Natural scientific profile, Kantonsschule Schaffhausen

- Programmed a web-shop as the matura-thesis

The following professors have contributed to my education: Nirmalya Ballav, Edwin Constable, Silvio Decurtins, Stefan Goedecker, Catherine Housecroft, Thomas Jung, Marcel Mayor, Frithjof Nolting, Markus Meuwly, Ernst Meyer, Peter Oelhafen, Christian Schönenberger.

Peer-reviewed Publications

1. D. CHYLARECKA, C. WÄCKERLIN, T. K. KIM, K. MÜLLER, F. NOLTING, A. KLEIBERT, N. BALLAV and T. A. JUNG. Self-Assembly and Superexchange Coupling of Magnetic Molecules on Oxygen-Reconstructed Ferromagnetic Thin Film. *J. Phys. Chem. Lett.*, **1**, 9, 1408–1413 (2010). DOI:10.1021/jz100253c.

2. C. WÄCKERLIN, D. CHYLARECKA, A. KLEIBERT, K. MÜLLER, C. IACOVITA, F. NOLTING, T. A. JUNG and N. BALLAV. Controlling spins in adsorbed molecules by a chemical switch. *Nat. Commun.*, **1**, 61 (2010). DOI:10.1038/ncomms1057.

3. D. Chylarecka, T. K. Kim, K. Tarafder, K. Müller, K. Gödel, I. Czekaj, C. Wäckerlin, M. Cinchetti, Md. E. Ali, C. Piamonteze, F. Schmitt, J.-P. Wüstenberg, C. Ziegler, F. Nolting, M. Aeschlimann, P. M. Oppeneer, N. Ballav and T. A. Jung. Indirect Magnetic Coupling of Manganese Porphyrin to a Ferromagnetic Cobalt Substrate. *J. Phys. Chem. C*, **115**, 4, 1295–1301 (2011). DOI:10.1021/jp106822s.

4. P. Fesser, C. Iacovita, C. Wäckerlin, S. Vijayaraghavan, N. Ballav, K. Howes, J. P. Gisselbrecht, M. Crobu, C. Boudon, M. Stöhr, T. A. Jung and F. Diederich. Visualizing the Product of a Formal Cycloaddition of 7,7,8,8-Tetracyano-p-quinodimethane (TCNQ) to an Acetylene-Appended Porphyrin by Scanning Tunneling Microscopy on Au(111). *Chem. Eur. J.*, **17**, 19, 5246–5250 (2011). DOI:10.1002/chem.201100733.

5. C. Wäckerlin, C. Iacovita, D. Chylarecka, P. Fesser, T. A. Jung and N. Ballav. Assembly of 2D ionic layers by reaction of alkali halides with the organic electrophile 7,7,8,8-tetracyano-p-quinodimethane (TCNQ). *Chem. Commun.*, **47**, 32, 9146 (2011). DOI:10.1039/c1cc12519b.

6. T. Hählen, C. Vanoni, C. Wäckerlin, T. A. Jung and S. Tsujino. Surface doping in pentacene thin-film transistors with few monolayer thick channels. *Appl. Phys. Lett.*, **101**, 3, 033305 (2012). DOI:10.1063/1.4737214.

7. C. Wäckerlin, K. Tarafder, D. Siewert, J. Girovsky, T. Hählen, C. Iacovita, A. Kleibert, F. Nolting, T. A. Jung, P. M. Oppeneer and N. Ballav. On-surface coordination chemistry of planar molecular spin systems: novel magnetochemical effects induced by axial ligands. *Chem. Sci.*, **3**, 3154–3160 (2012). DOI:10.1039/c2sc20828h.

8. L. Marot, T. de los Arcos, A. Bünzli, C. Wäckerlin, R. Steiner, P. Oelhafen, E. Meyer, D. Mathys, P. Spätig and G. Covarel. Nanocomposite of carbon nanotube embedded in a (Ti,Al)N coated film. *Surf. Coat. Tech.*, **212**, 223–228 (2012). DOI:10.1016/j.surfcoat.2012.09.053.

9. N. Moridi, C. Wäckerlin, V. Rullaud, R. Schelldorfer, T. A. Jung and P. Shahgaldian. Langmuir–Blodgett monolayer stabilization using supramolecular clips. *Chem. Commun.*, **49**, 4, 367 (2013). DOI:10.1039/c2cc35976f.

10. C. Wäckerlin, J. Nowakowski, S.-X. Liu, M. Jaggi, D. Siewert, J. Girovsky, A. Shchyrba, T. Hählen, A. Kleibert, P. M. Oppeneer, F. Nolting, S. Decurtins, T. A. Jung and N. Ballav. Two-Dimensional Supramolecular Electron Spin Arrays. *Adv. Mater.*, **25**, 17, 2404–2408 (2013). DOI:10.1002/adma.201204274.

11. J. Nowakowski, C. Wäckerlin, J. Girovsky, D. Siewert, T. A. Jung and N. Ballav. Porphyrin metalation providing an example of a redox reaction facilitated by a surface reconstruction. *Chem. Commun.*, **49**, 2347–2349 (2013). DOI:10.1039/c3cc39134e.

12. C. Wäckerlin, T. Kartick, J. Girovsky, J. Nowakowski, T. Hählen, A. Shchyrba, D. Siewert, A. Kleibert, F. Nolting, P. M. Oppeneer, T. A. Jung and N. Ballav. Ammonia Coordination Introducing a Magnetic Moment in On-Surface Low-Spin Porphyrin. *Angew. Chem. Int. Ed.*, **52**, 4568–4571 (2013). DOI:10.1002/anie.201208028.

The image on page iv displays STM data of the supramolecular chessboard-array self-assembled from Fe and Mn containing molecular phthalocyanine building-blocks. Note the different contrast in the center of the molecules due to the Fe and Mn ions.
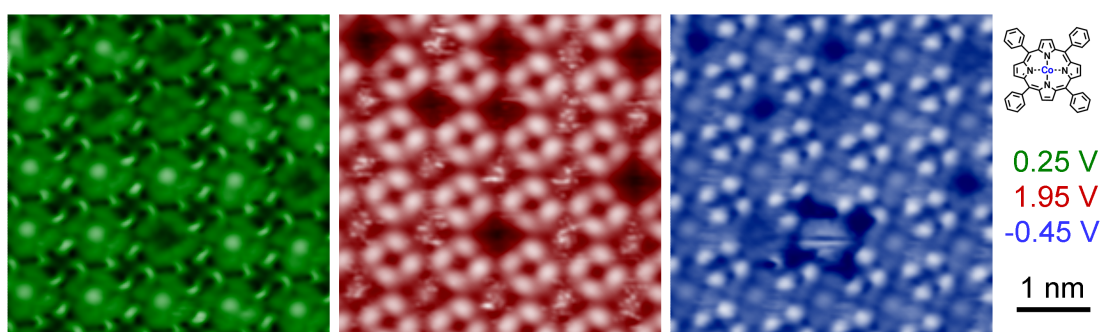
The images on this page display room-temperature STM data of a self-assembled monolayer of Co tetraphenyl-porphyrins decorated with nitric oxide (NO) ligands. The green, red and blue images show the same area, but different electronic states are probed. The missing molecule helps to identify the exact position of the molecules (blue image). The NO-coordinated molecules are imaged with bright protrusions (green image).